

## PDF hosted at the Radboud Repository of the Radboud University Nijmegen

The following full text is an author's version which may differ from the publisher's version.

For additional information about this publication click this link.

<http://hdl.handle.net/2066/76514>

Please be advised that this information was generated on 2017-12-06 and may be subject to change.

# Symmetry in (inter)action

Een wetenschappelijke proeve op het  
gebied van de Sociale Wetenschappen

## **Proefschrift**

ter verkrijging van de graad van doctor  
aan de Radboud Universiteit Nijmegen  
op gezag van de rector magnificus **prof. mr. S. C. J. J. Kortmann**,  
volgens besluit van het college van decanen  
in het openbaar te verdedigen op **donderdag 18 februari 2010**  
om **15.30 uur** precies

door

**Matthias Sebastian Treder**

geboren op 31 maart 1979

te Lauenburg

## Promotores

Prof. dr. Charles M. M. de Weert

Prof. dr. Ruud G. J. Meulenbroek

## Manuscriptcommissie

Prof. dr. Herbert J. Schriefers

Prof. dr. Stephen Palmer (University of California, Berkeley)

Dr. Raymond van Ee (Helmholtz Institute, Utrecht)

---

## Preface

---

This thesis comprises six chapters presenting original work in psychological research on human symmetry perception. Chapter 1 gives a comprehensive introduction to the field and was compiled in May/June 2009. Chapters 2, 3, and 4 present experimental work conducted in collaboration with my supervisor Dr. Peter van der Helm, who is an expert in the field for more than 20 years. Owing to his mathematical background, his own research focuses on theoretical aspects of human perception of visual regularities. Our empirical investigations spanned the years 2004–2008, but collaboration on publications continues up to date. The joint work yielded three manuscripts, with Peter van der Helm being first author in one of them. Two of the manuscripts have been published and one is currently under revision (status december 2009). To Chapter 2, Dr. Gert van der Vloed, a former PhD student of Peter van der Helm, contributed his valuable expertise in the field. He is currently working at Eindhoven University of Technology and doing research in human-technology interaction. Chapter 5 is the product of a collaboration with one of my promoters, Prof. dr. Ruud Meulenbroek, who is an expert on motion and motor-planning with a scientific record of more than 20 years. The collaboration on the interaction between symmetry processing and motion processing started in summer 2008 and culminated in a manuscript in early 2009. The paper is now in press. Chapter 6 discusses the contribution of this thesis to the field of symmetry perception and was compiled in May/June 2009.



---

# Contents

---

<b>1</b>	<b>Introduction</b>	<b>1</b>
1.1	General Introduction . . . . .	3
1.2	Reflections about symmetry . . . . .	4
1.3	Methodology . . . . .	7
1.4	Characteristics of symmetry perception . . . . .	16
1.5	Models of symmetry perception . . . . .	27
1.6	Outline of the thesis . . . . .	36
<b>2</b>	<b>Interactions between symmetries</b>	<b>39</b>
2.1	Introduction . . . . .	41
2.2	Correlation rectangles . . . . .	45
2.3	Relative orientation of symmetry axes . . . . .	52
2.4	General discussion . . . . .	62
2.5	Appendix A: One-fold symmetry detection model . . . . .	69
2.6	Appendix B: Artificial neural network dynamics . . . . .	71
<b>3</b>	<b>Detection of (anti)symmetry and (anti)repetition</b>	<b>73</b>
3.1	Introduction . . . . .	75
3.2	Experiment 1 . . . . .	79
3.3	Experiment 2 . . . . .	87
3.4	General discussion . . . . .	91
<b>4</b>	<b>Symmetry and repetition in cyclopean vision</b>	<b>101</b>
4.1	Introduction . . . . .	103
4.2	Experiments 1a and 1b . . . . .	107
4.3	Experiments 2a and 2b . . . . .	114
4.4	General discussion . . . . .	117
4.5	Conclusion . . . . .	125

<b>5</b>	<b>Integration of structure-from-motion and symmetry</b>	<b>127</b>
5.1	Introduction . . . . .	129
5.2	Experiment 1 . . . . .	133
5.3	Experiment 2 . . . . .	143
5.4	Experiment 3 . . . . .	149
5.5	General discussion . . . . .	153
<b>6</b>	<b>Discussion</b>	<b>159</b>
6.1	Status quo . . . . .	161
6.2	Notes on empirical research . . . . .	163
6.3	Notes on theoretical research . . . . .	169
6.4	Prospect . . . . .	171
	<b>Bibliography</b>	<b>173</b>
	<b>Samenvatting</b>	<b>189</b>
	<b>Summary</b>	<b>191</b>
	<b>Zusammenfassung</b>	<b>193</b>
	<b>Dankwoord</b>	<b>195</b>
	<b>Publications</b>	<b>197</b>
	<b>Curriculum vitae</b>	<b>199</b>

# CHAPTER **1**

---

Introduction

---





## 1.1 General Introduction

Perceptual organization refers to the mental construction of visual objects by means of grouping and segmentation of stimulus parts. This thesis is devoted to the investigation of one of the integral components of perceptual organization, namely mirror-symmetry processing (henceforth symmetry processing). In early views on perceptual organization, symmetry processing was construed as one out of a set of encapsulated modules processing particular features of the visual input. Not only has the rigid partitioning of visual perception into independent streams of processing been progressively softened (e.g., Kourtzi et al., 2008), there is even evidence for the penetration of visual processing by other modalities; for instance, inputs from the vestibular system have been shown to affect the perception of orientation (Howard, 1982).

In spite of the acknowledged interactivity of the visual system and the long tradition of symmetry research (starting with Mach, 1886), most studies on symmetry processing adhere to a reductionist style. This means that experiments often feature artificial symmetric stimuli that are bare of other, potentially obtrusive features. It is true that this is the method-of-choice to disclose the basic mechanisms governing symmetry processing.

The aim of this thesis, however, is to characterize the *role* of symmetry processing in perceptual organization. Since interactions in the visual system are known to be non-linear, a study of the input-output relations of an isolated process may not be sufficient to understand how symmetry processing behaves in a richer visual environment that is defined along multiple feature dimensions. To overcome this limitation, the reductionist approach is not abandoned, but, throughout the chapters, stimulus complexity is gradually increased and symmetry is put in competition with other principles of perceptual organization.

Chapter 2 paves the way by investigating the interaction between component symmetries in a multiple symmetry. It is shown that, contrary to ideas in the literature, the relative orientation of the symmetry axes in a multiple symmetry is important, not the additional structural relationships it gives rise to.

Chapter 3 sharpens what qualifies as a visual symmetry (i.e., a symmetry

the visual system is sensitive to) and what does not. It is shown that symmetry has been used as an umbrella term to also include structures that do not play a role in perceptual organization.

Chapter 4 puts symmetry processing into competition with another determinant of perceptual organization, stereoprocessing. It is shown that symmetry processing can shift from a retinotopic to a stereoscopic frame of reference. Symmetry can be readily perceived in stereoscopic space, but only if stereoscopic information is compatible with the perceptual structure of symmetry.

Chapter 5 sets symmetry in motion. It is demonstrated that sinusoidal motion of dots in a 2D symmetric pattern yields a multistable percept that can switch between symmetry-based and motion-based percepts, suggesting an ongoing interaction between these two kinds of visual processing.

Naturally, these studies do not come out of the blue. A significant body of empirical and theoretical findings has accumulated within the last decades. The studies presented in this thesis are embedded in and motivated by this past research. Therefore, the rest of this chapter is devoted to a comprehensive introduction into the methodology of symmetry and its empirical and theoretical aspects. Its length notwithstanding, this introduction is not meant to be exhaustive. In the face of 150 years of symmetry research, a review is necessarily selective.

## **1.2 Reflections about symmetry**

Symmetry seems to pervade nature at all spatial scales that have been subject to human investigation, whether the microcosm of string theory and the structure of crystals, or the gigantic architecture of galaxies. Not surprisingly, then, the concept of symmetry can be encountered in scientific disciplines as diverse as social sciences, physics, chemistry, and even philosophy of science (e.g., Rosen, 2009). The exact definition, however, varies considerably with the area of application. As van der Vloed et al. (2005) pointed out, many of the symmetries in nature are beyond the reach of our visual system. Some can be visualized with appropriate magnification (e.g., microscopes and telescopes), while others are even hard to



**Figure 1.1.** Charlottenburg Palace in Berlin, Germany. All components of the palace, including the street lamps in front of the estate, are located symmetrically with respect to its central line.

imagine. Therefore, the notion of symmetry employed in this thesis builds on the phenomenological experience of visual symmetry in daily life. The shorthand symmetry refers to what has been denoted as mirror-symmetry, bilateral symmetry or reflectional symmetry. For a symmetric object, there is at least one symmetry axis (or one symmetry plane in 3D) that splits the object into two identical but mirror-inverted halves. There is a striking preponderance of such objects in our urban habitat. Whether a cup of coffee, a car, a mobile phone, or the computer screen, there is hardly any man-made object that does not feature at least one axis of symmetry. For a part, this can be attributed to human anatomy, because a symmetric body can often interact more efficiently with another object if the counterpart is also symmetric (e.g., a bicycle or a chair). The use of symmetry, however, goes beyond mere functionality. This is witnessed by the fact that symmetry is omnipresent in art, craft, and architecture, where symmetrical compositions are used by virtue of the fact that they are aesthetically pleasing to the observer (see also Palmer, 1991; Palmer et al., 2008). An example is given in Figure 1.1.

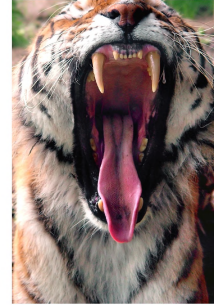
Not only the artificial environment abounds with symmetry. In nature, living beings predominantly belong to the group of bilateria, that is, bilaterally symmetric animals (Figure 1.2). Living beings can be prey or predator, or – in the case of humans – friend or fiend. On the one hand, this seems



(a) Stenopus Hispidus



(b) Capuchin monkey



(c) Siberian tiger

**Figure 1.2.** Animals from the group of bilateria, exhibiting vertical symmetry.

to suggest that sensitivity to symmetry might foster the detection of an animal in front of an (allegedly asymmetric) background. On the other hand, the high degree of symmetry encountered in some plants (e.g., flowers) or, roughly, the trunk of a tree, relativizes its distinctiveness for distinguishing animals from other objects.

On a more subtle level, symmetry also seems to play a role in social behaviour. It has been suggested as a marker of genetic quality and developmental stability and it has also been associated with judgments of physical attractiveness (Grammer & Thornhill, 1994; Grammer et al., 2003, 2005; Møller & Thornhill, 1998). At least regarding facial attractiveness, however, symmetry does not appear to be the only relevant factor. Scheib et al. (1999) showed that symmetric faces are judged as more attractive than less symmetric faces even if symmetry cues are removed by showing only one half of the face; the authors identified other factors, such as cheek-bone prominence, that are positively correlated with the degree of symmetry. This covariance of multiple physical attributes with symmetry makes it difficult to disentangle the separate contributions of each visual feature.

As the foregoing suggests, whether or not sensitivity to symmetry evolved as a specific result of evolutionary pressure is still a matter of debate. In contrast, there is little debate about the fact that symmetry usually signifies single objects; in other words, it is usually not a visual feature spanning multiple objects. It is true that 3D symmetric objects are hardly ever

seen head-on, which is the only case in which their projection would yield a perfect 2D symmetry. Nevertheless, some structural properties of symmetry are retained under perspective projection and there is evidence that symmetry in perspective can be detected by human observers (van der Vloed et al., 2005). The fact that retinal symmetry can serve as a powerful object cue during image segmentation and grouping suggests that symmetry detection is a basic component of perceptual organization that is applied to any visual input. This idea fits well the observation that sensitivity to it is encountered in various other animals, for instance pigeons (Delius & Nowak, 1982), bees (Benard et al., 2006; Giurfa et al., 1996), and dolphins (von Ferson et al., 1992), and it is endorsed by the fact that symmetry appears strong even in abstract, meaningless stimuli based on random noise (see Figure 1.3).

The fact that the visual system is tuned to extract symmetry from any visual stimulus allowed for the use of abstract stimuli in symmetry research. Abstraction from natural stimuli is important to disable potentially interfering effects from semantic processing. Furthermore, it allows for the control of other features that can play a role in perceptual organization, such as color, size, and orientation. Throughout the years, methodological standards in symmetry research emerged. Since most empirical work presented in this thesis draws on these standards, it is expedient to introduce them next.

## **1.3 Methodology**

In symmetry research, a small battery of standard procedures and a set of standard stimulus types has been established. Conforming to these standards is practical not only because they are theoretically and empirically founded, but also because it ensures comparability across different studies.

### **1.3.1 Procedure**

Often, experiments on symmetry processing involve a symmetry detection task, whereby symmetric and non-symmetric (random) stimuli are pre-

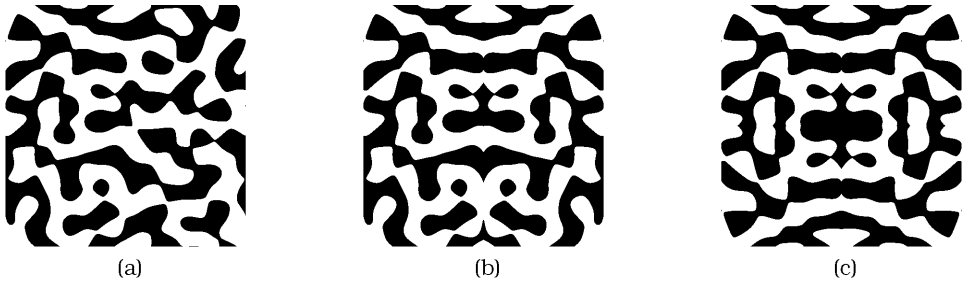


**Figure 1.3.** The emergence of symmetry in meaningless patterns. (a) A random blob pattern consisting of black and white blobs. (b) If the left half of that pattern is reflected about the vertical midline, the percept becomes perceptually organized, yielding a salient 1-fold vertical symmetry. (c) The organization can be further strengthened by adding another axis of symmetry. To create this pattern, the upper left quadrant of the random pattern in (a) was taken, reflected about the vertical midline, and the result was reflected about the horizontal midline, yielding a perfect 2-fold symmetry.

sented under short presentation times, usually in the order of 80–250 ms. In the yes/no paradigm, stimuli are successively presented in random order. After each presentation, the participant has to indicate whether the previous stimulus was symmetric or random. In a variant of this paradigm, reaction times (i.e., the time between the onset of the stimulus and a correct button press) are measured in order to quantify performance. Usually then, stimuli are again presented one after the other, but they remain on the screen until a button is pressed.

In the two-intervals forced-choice (2IFC) paradigm, participants are presented two stimuli in each trial, one symmetric and one random. The symmetric stimulus can appear either in the first interval or in the second interval, and the participant's task is to indicate in which interval the symmetry was presented.

A drawback of these paradigms is that they suffer from different sources of bias which can contaminate 'raw' measures of performance such as percent correct. To be more clear, the yes/no paradigm suffers from criterion bias which means that some participants are more apt to press 'symmetry present' and others are more apt to press 'symmetry absent'; even more critically, participants might adapt their criterion to particular experimental conditions. Although the 2IFC paradigm does not suffer from criterion bias, it is not completely bias-free either; participants may have a prefer-

ence for choosing the first or the second interval.

To obtain a relatively bias-free measure of detection performance, many studies rely on the sensitivity index  $d'$  which is rooted in signal detection theory (Swets, 1964; see also Wickens, 2002). Signal detection theory (SDT) allows to discern between the bias  $\beta$ , which indicates how much a participant is biased towards one of the possible responses, and sensitivity  $d'$ , which indicates how well a symmetric stimulus can be discriminated from a random stimulus. Roughly stated, SDT conceptualizes the visual system as a noisy sensor. The psychological response of the system to a stimulus at any instant is determined by signal magnitude plus the current magnitude of internal noise. SDT implies that the perceived magnitude of symmetry can vary across trials even when it does not change physically and, moreover, that symmetry can be perceived even if it was absent. Translated into terms of SDT, then, the task of a participant in the yes/no paradigm boils down to choosing whether the percept was generated by the noise distribution or the signal+noise distribution.

In some situations (see, e.g., Chapter 3),  $d'$  cannot be straightforwardly computed because the experimental paradigm requires more than two stimulus classes. Often, reaction-time measures are employed in these cases. Using reaction times, one has to take into account that participants apply a speed-accuracy trade-off. This trade-off implies that some participants decrease their reaction time by accepting a higher error rate. To check whether a speed-accuracy trade-off contaminates the data, reaction times are usually analyzed along with accuracy in a particular experimental condition.

### 1.3.2 Stimuli

The principal component of any experiment on symmetry, and at the same time its bottleneck, is the symmetric stimulus. A clear-cut experimental question can only come to fruition if it can be accommodated by an appropriate stimulus manipulation. The stimuli recruited in most symmetry experiments fall into three classes, as illustrated in Figure 1.4.

The first class comprises dot patterns, which have found extensive use in symmetry research (e.g., Barlow & Reeves, 1979; Joung et al., 2000; Nucci



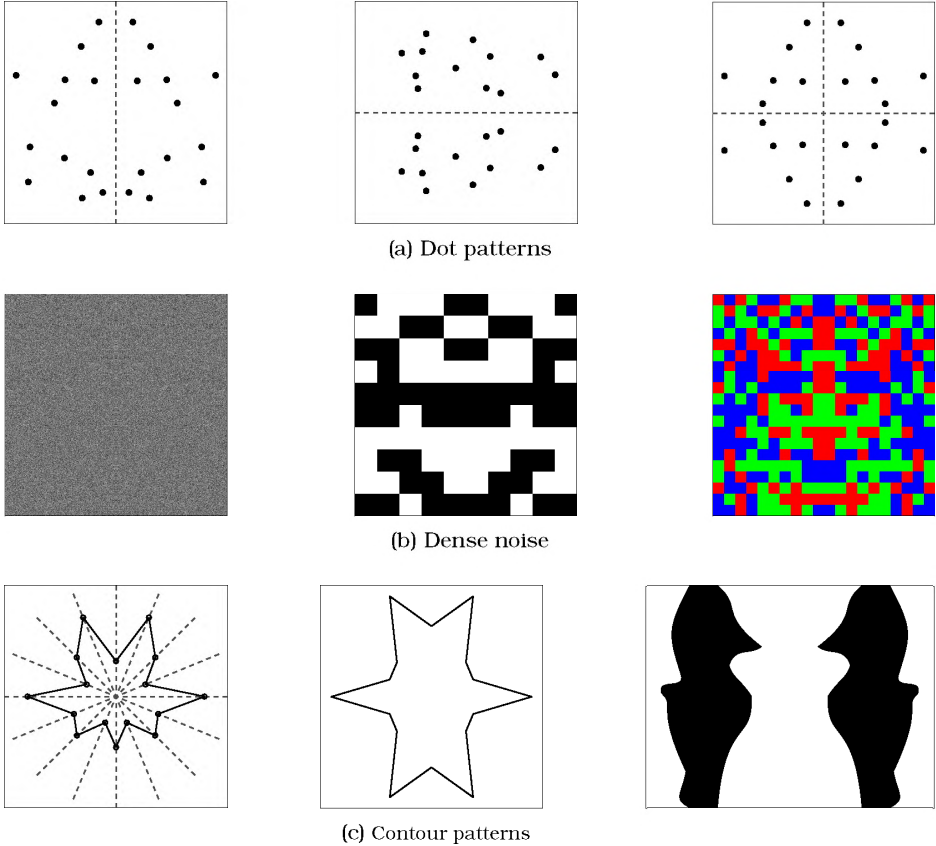


**Figure 1.4.** Three standard classes of symmetric stimuli. (a) Dot patterns consist of dots that have been randomly placed on a uniform background and then reflected about one or more axes. Dashed lines indicate the symmetry axes. Left: Vertical symmetry. Middle: Horizontal symmetry. Right: Two-fold symmetry with a horizontal and a vertical symmetry axis. (b) Dense noise consists of a matrix of rectangular checks. Left: Pixel noise drawn from a Gaussian distribution. Middle: Random luminances drawn from a uniform distribution and thresholded to black and white. Right: Checks of  $20 \times 20$  px<sup>2</sup> partitioned into roughly equal amounts of red, green, and blue patches. (c) Contour patterns are figures enclosed by a symmetric contour. Left: A polygon (solid black line), created by placing dots on radial axes (dashed lines) and connecting them by straight lines. Middle: A polygon with two symmetry axes created in the same way. Right: Two filled symmetric objects whose contours are defined by quadratic Bézier curves.

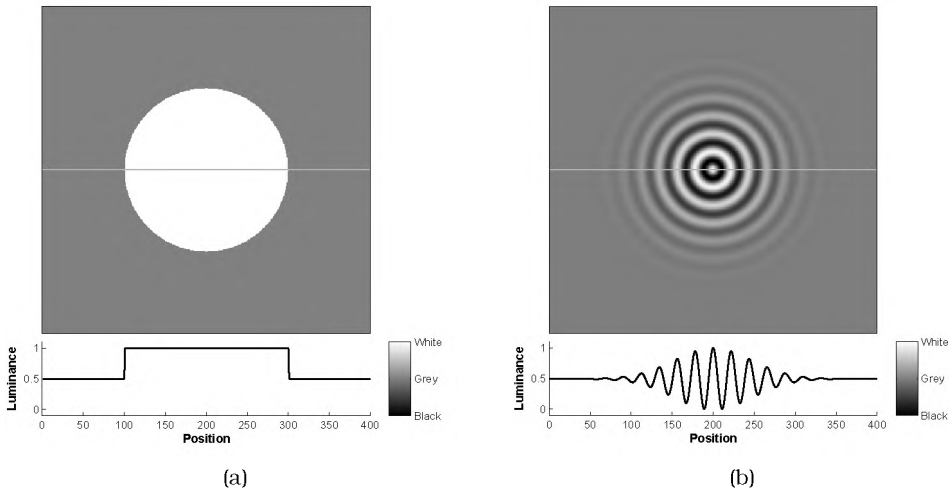


**Figure 1.5.** Luminance profile of an enlarged hard-edge dot (a) and a radial sinusoid windowed by a Gaussian function (b). The gray line in each image represents a horizontal slice, with the luminance function corresponding to that slice is given in the panel underneath. The dot is broadband because it contains power at all spatial frequencies. The radial sinusoid, in contrast, is bandlimited.

& Wagemans, 2007; Troscianko, 1987; Wagemans et al., 1991; Wenderoth, 1995, 1996, 1997; Wenderoth & Welsh, 1998b; Zhang & Gerbino, 1992). In dot patterns, a moderate number of dots (usually <100) is randomly distributed on a uniform background. Reflection of dots about one or more symmetry axes yields a symmetric stimulus (Figure 1.4a). Dot patterns are sparse patterns because the area in the image taken in by the background is usually substantially larger than the area occupied by the dots.

The second stimulus class comprises checkerboard-like patterns with checks whose size can vary from that of individual pixels to large rectangular blocks (Figure 1.4b). The most important difference between dense noise and dot patterns is that there is a clear figure-ground organization in dot patterns but not in dense noise. It is true that in a binary pattern (Figure 1.4b middle) one might still conceive of white as the foreground and black as the background (or vice versa), but in stimuli with multiple gray levels (Figure 1.4b left) such a distinction is not viable. In dot patterns, symmetry can be distinguished from random patterns by the positioning

of the constituting dots. In contrast, in dense noise, elements are laid out in a matrix, which in a sense implies that they are always symmetric with respect to each other. Here, it is the luminance or color of each check rather than position per se which signals symmetry. This stimulus difference can possibly explain why reversing contrast polarity of symmetry pairs heavily interferes with symmetry detection in dense noise (Mancini et al., 2005) but not in dot patterns (Wenderoth, 1996).

A third class of stimuli that has been used in symmetry research is contour patterns (Figure 1.4c), that is, figures wherein the symmetry is given by the figure outline. Symmetric contours do not have to be closed or join to a single figure to elicit a salient percept (Bertamini et al., 1997; Corbalis & Roldan, 1974; Friedenbergr & Bertamini, 2000).

These standard stimuli underwent many modifications to make them suitable for particular experimental questions. Maybe the most notable modifications stem from research on the role of spatial filters in symmetry processing. The spatial filtering approach to visual processing is inspired by the fact that many visual neurons act like spatial filters. That is, within their receptive field, they are tuned to only pick up luminance variations within a limited frequency band and within a limited orientation band. A great deal of work has been devoted to answering the question whether spatial filtering plays a role in symmetry perception. A severe obstacle to spatial filtering research with standard stimuli is that they are spatially broadband. This is illustrated in Figure 1.5. To circumvent this problem, spatial filtering has been applied to the three stimulus classes, resulting in stimuli in which the slope of the power spectrum, the spatial frequency content and the orientation content can be selectively filtered. Examples are depicted in Figure 1.6. These kind of stimuli have also found wide application in symmetry research (e.g., Dakin & Herbert, 1998; Julesz & Chang, 1979; Rainville & Kingdom, 1999, 2000, 2002; Saarinen & Levi, 2000; Wilkinson et al., 1998; Wilson & Wilkinson, 2002 ).

Many studies on symmetry are parametric experiments wherein the amount of symmetry is used as a continuous independent variable. Therefore, almost as important as the stimulus self is the degree to which it allows to manipulate the amount of symmetry. As illustrated in Figure 1.7a–d, a number of different noise manipulations have been introduced to dot stim-

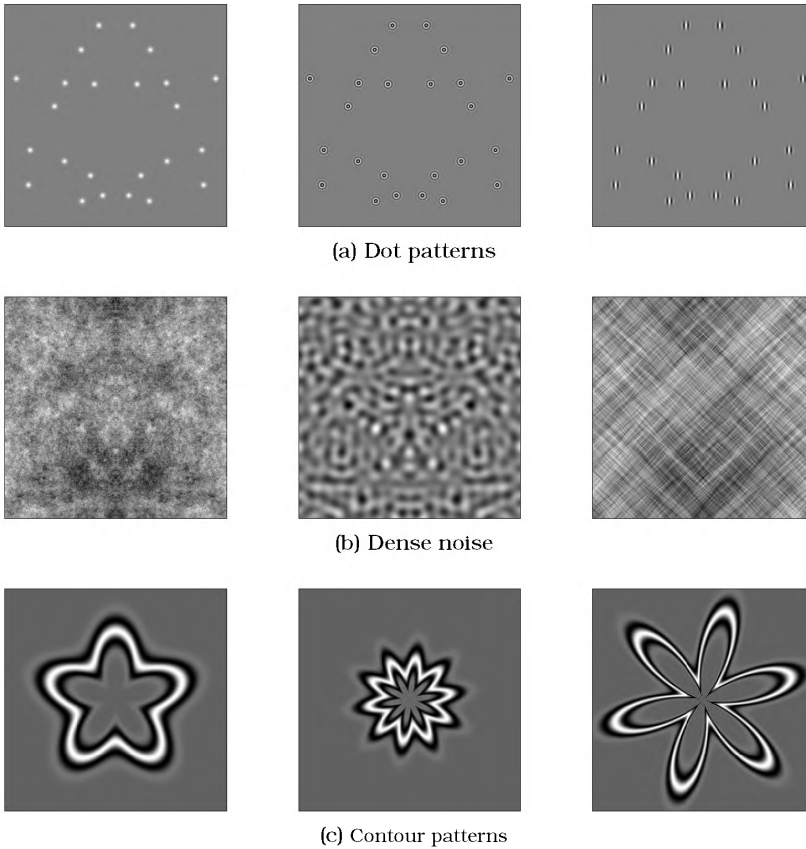


**Figure 1.6.** Spatial frequency filtered versions of the three classes of stimuli introduced in Figure 1.4. (a) Bandlimited dot patterns. All patterns are based on the 1-fold symmetry in Figure 1.4a, but the luminance function of the dots has been changed. Left: Dots with a Gaussian envelope, attenuating high spatial frequencies. Middle: Radial sinusoids tapered by Gaussian functions, making the spatial frequency content of the dots narrow-band. Right: Gabor functions, that is, vertically oriented sinusoids tapered by Gaussian functions, limiting both spatial frequency and orientation content. (b) Filtered dense noise. All examples are based on the same Gaussian pixel noise pattern, but they have been filtered in different ways. Left: The spectral slope of the broadband noise has been changed from flat to  $1/f^2$ , which means that power falls off with the square of frequency, attenuating high spatial frequencies. This slope is similar to the spectral slopes encountered in natural images. Middle: The result of filtering with a one-octave wide (10–20 cycles per image) idealized isotropic bandpass filter. Right: The noise has been given a  $1/f^2$  spectral slope and, additionally, all orientation content except for orientations within  $10^\circ$  of the left and right diagonals has been rejected. (c) Radial frequency (RF) contour stimuli introduced by Wilkinson et al. (1998). RF stimuli are circular contours with a bandlimited luminance profile. The patterns are defined by sinusoids in polar coordinates. The three images show examples with different parameters for mean radius, radial modulation amplitude, and radial frequency (see reference for details). RF stimuli were generated using the RFPattern MATLAB function by Aaron Clarke.

uli. Probably the most often utilized manipulation is random noise (Figure 1.7), whereby the dot pattern is interspersed with randomly positioned dots. In these stimuli, it is straightforward to quantify signal-to-noise noise as the number of symmetric dots divided by the total number of dots. In different variant, spatial jitter (Figure 1.7b), a vector of particular length is added to all dots, whereby the angle is randomized for each dot. The amount of distortion is controlled via the magnitude of the jitter vector. In nature, distortions of symmetry usually comprise misalignments of otherwise symmetric counterparts. This makes spatial jitter a better model of natural distortions of symmetry than random noise.

To introduce noise in a more controlled fashion, mathematical transformations have also been applied to dot patterns. For instance, affine transformations are linear transformations followed by translations, using the function  $f(x) = A \cdot x + t$ , where  $A$  is a transformation matrix,  $x$  represents the original coordinates of a given point, and  $t$  is the translation vector. An affine transformation that was used by Wagemans et al. (1993) to investigate the role of geometric relationships between dot pairs is skewing or shearing (Figure 1.7c).

In dense noise, phase jitter is a way to control the amount of symmetry. With phase jitter, a random offset is added to the phase components in the Fourier transform. The magnitude of the random angle determines the degree of distortion of the symmetry. As Figure 1.7ef shows, symmetry can be gradually degraded with phase jitter. For contour stimuli, a similar phase-offset technique has been applied to radial frequency patterns (Wilkinson et al., 1998; Wilson & Wilkinson, 2002). No standard has been established for polygons, with one of the difficulties being that it is not straightforward to find a continuous measure for the distortion of symmetry in these patterns (although, see Zabrodsky & Algom, 1994 for a possible approach).

Many characteristics of symmetry perception have been discovered using the stimulus types introduced in this section. The next section gives an overview of the findings.

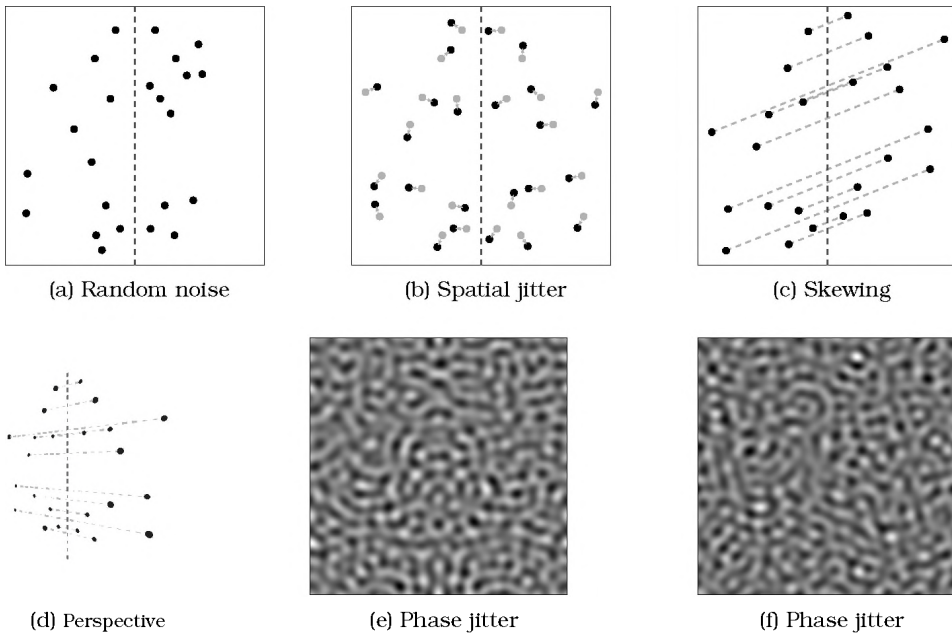


**Figure 1.7.** Noise manipulations. Dot stimuli (a–d) are based on the perfect symmetry depicted in Figure 1.4. The symmetry axis is shown as a vertical dashed line. (a) Random noise in dot stimuli. One third of the symmetry pairs (8 dots) has been removed and replaced by random dots. (b) Starting from the perfect symmetry (gray dots), each dot has been moved by 14 px (arrows) to a new position (black dots). The black dots form a jittered symmetry. (c) After skewing, the virtual lines (indicated by the dashed lines) connecting symmetry pairs are not orthogonal with respect to the symmetry axis. However, in contrast to the random noise and spatial jitter manipulations, the virtual lines are still midpoint collinear and parallel with respect to each other, so that some geometric properties of perfect symmetry are preserved. (d) In perspective distortion, virtual lines point towards a vanishing point and, hence, are neither parallel nor midpoint collinear. (e) A bandlimited noise pattern like introduced in Figure 1.6b middle, with a random phase offset of up to  $100^\circ$ . Symmetry is distorted but still perceivable. (f) The same pattern with a random phase offset of up to  $140^\circ$ . The symmetry percept has almost disappeared.

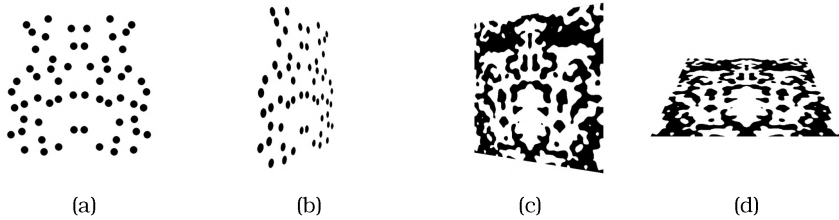


**Figure 1.8.** Stimuli used by van der Vloed et al. (2005) in their study on symmetry and repetition in perspective, kindly provided by the first author. (a) Frontoparallel dot pattern. (b) The same dot pattern rotated about the vertical midline (y-axis). The retinal symmetry is distorted because the virtual lines connecting dot pairs are neither midpoint collinear nor parallel. (c) Blob pattern (thresholded Gaussian noise) rotated about the vertical midline. (d) Blob pattern rotated about the horizontal midline (x-axis). In this pattern, both midpoint collinearity and orientational uniformity of the virtual lines connecting symmetry pairs is preserved. In accordance with the 2D properties of the symmetric projection, the authors found that rotations about the y-axis hamper detection but rotations about the x-axis do not.

## 1.4 Characteristics of symmetry perception

Empirical research on symmetry has a tradition that dates back to the nineteenth century (Mach, 1886). Since then, considerable progress has been made on different fields of symmetry perception. Since these fields partly developed in parallel, it is convenient to discuss them one by one.

### 1.4.1 Modus operandi

Does symmetry processing operate on 2D symmetries in the retinal image or on 3D symmetries of objects in depth? On the one hand, perfect retinal symmetries do not occur very often in nature. On the other hand, as pointed out before, 3D symmetric objects virtually always give rise to a 2D symmetric projection, albeit distorted in depth. Compelling support for the idea that symmetry processing operates retinally stems from van der Vloed et al. (2005), who reported that symmetry detection is feasible for various veridical views of planar symmetries slanted in depth, but that there is a deterioration of detection performance that is well-predicted from the deterioration of symmetry in the retinal image. Essentially, symmetry processing was not obstructed by perspective when a frontoparallel symmetry was rotated about the horizontal midline (x-axis) but it was severely ob-

structed following rotations about the vertical midline (y-axis). This is in accordance with the fact that retinal symmetry stays intact after rotations about the x-axis but not after rotations about the y-axis. However, the fact that symmetry operates on the retinal image does not preclude that it plays a role in 3D object reconstruction. I will expand on this below.

### **1.4.2 Spatial and temporal efficiency**

Although symmetry is perceived best if its projection is that of a perfect symmetry, consisting of mirror-positioned elements viewed head-on, it remains detectable under all of the noise manipulations and for all of the stimuli introduced in Section 1.3.2. The salience (i.e., detectability) of symmetry degrades gracefully with the amount of noise, whether interspersed random dots, spatial or phase jitter, or geometric transformations (e.g., Barlow & Reeves, 1979; Dakin & Herbert, 1998; Jenkins, 1983; van der Vloed et al., 2005). At the same time, small deviations from perfect symmetry are easily picked up (Barlow & Reeves, 1979). This combination of robustness and sensitivity to perturbations suggests that the amount of symmetry is rather accurately represented in the visual system. This is corroborated by Csathó et al. (2004), who suggested that the salience of symmetry is a rather straightforward function of signal-to-noise ratio. In the face of this evidence, symmetry detection seems qualified to face the distortions encountered in natural symmetries, whether caused by perspective, occlusion, or asymmetries in the object itself, and to play an integral role in perceptual organization. In line with this putative role, symmetry detection has been shown to be very quick. A number of studies demonstrated symmetry detection under presentation times of 100 ms or less (Wagemans, 1995), and there is recent evidence that symmetry in dot patterns can be detected with a presentation time as low as 13 ms (Niimi et al., 2005).

### **1.4.3 The role of cognition**

A lot of symmetry research in the 80's and 90's was dedicated to fleshing out to what extent symmetry detection is a 'hardwired' process that is en-



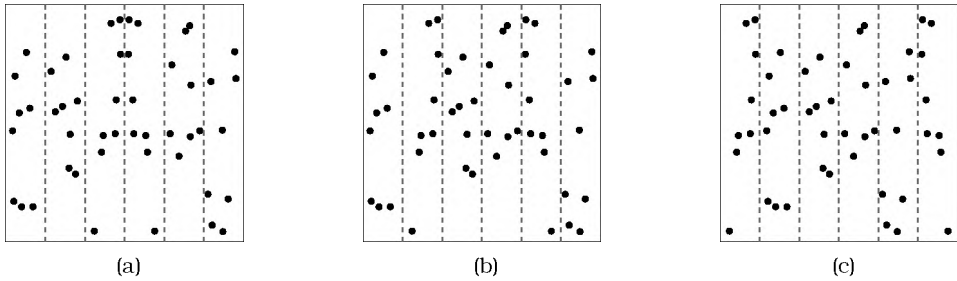


**Figure 1.9.** Position effects of symmetry information in a dot pattern. The pattern is split into three symmetric pairs of vertical stripes, with one pair containing symmetrically positioned dots and the other two pairs containing random dots. (a) Symmetry is centered around the symmetry axis and is perceived well. (b) Symmetry is confined to the second and fifth stripe. Saliency is markedly lower. (c) Symmetry is confined to the outermost stripes. It is slightly better detectable than in the previous case.

capsulated from higher-level cognition, and to what extent it is penetrated by cognition, involving focused attention and search strategies. Pashler (1990) and Wenderoth & Welsh (1998a) demonstrated that knowledge affects symmetry processing: If the experiment features different orientations of the symmetry axis and the orientation is cued prior to the trial, a valid cue leads to an increase and an invalid cue leads to a decrease of detection rate, relative to a neutral cue. Furthermore, Wenderoth & Welsh (1998b) showed that task parameters changing the expectancy of the participant affect performance. In particular, the saliency of vertical symmetry was drastically reduced when the majority of the trials featured oblique or near-oblique symmetry axes, which indicates the involvement of voluntary shifts of spatial attention.

On the other hand, there is manifold evidence that the computation of symmetry is 'hardwired' and performed preattentively. For instance, in the experiments by Pashler (1990) and Wenderoth & Welsh (1998a), cuing of the symmetry axis did not obliterate anisotropies in the processing of symmetries of different orientations (see below). Symmetry was also shown to affect performance when it is not relevant to the task. For instance, visual search was shown to speed up when the spatial arrangement of the distracters is symmetric compared to random (Wolfe & Friedman-Hill, 1992). In a clinical study, figure-ground segregation was investigated in a

patient who suffered from hemispatial neglect; following right-hemisphere damage, the patient was unable to deploy attention to the left half of the visual field, although he was not blind on that side (Driver et al., 1992). Interestingly, in stimuli with an ambiguous figure-ground organization, he perceived the symmetric parts of the stimulus as figure (just as healthy observers do), although he did not display conscious experience of the symmetry. Furthermore, Bertamini et al. (1997) and Koning & Wagemans (2009) showed that in a task where participants have to judge whether the facing contours of two objects are repeated or reflected, the outer task-irrelevant contours also affect performance if they are symmetric.

Taken together, evidence seems to favor the reconciling view that symmetry detection is an automatic process and that some, but not all, of its aspects can be modulated by higher-level cognition (e.g., prior information and expectancy), probably by means of selective attention.

#### **1.4.4 Orientation and location of symmetry axes**

Symmetry processing is anisotropic with regard to the orientation of the symmetry axis. This was first noted by Mach (1886) and since then has been confirmed in further experiments (e.g., Palmer & Hemenway, 1978; Wenderoth, 1997). Despite some incongruity across different studies, the general picture seems to be that there is a gradient of sensitivities to different axis orientations, with the vertical axis orientation yielding the most salient symmetry, followed by horizontal, then left/right oblique, and finally all other axis orientations (Barlow & Reeves, 1979; Wenderoth, 1994).

Not only the orientation of the symmetry axis, also its location in the visual field seems to be relevant. Although foveation of the symmetry axis is not a prerequisite for symmetry detection, the efficiency of symmetry detection drops considerably with axis eccentricity (Saarinen, 1988). Sally & Gurnsey (2001) found that symmetry detection performance can be equated across eccentricities if stimuli are scaled with a factor  $F = 1 + E/E_2$ , where  $E$  is eccentricity and  $E_2$ , lying in the range of  $0.88^\circ$  to  $1.38^\circ$ , is the eccentricity at which stimulus size is doubled.

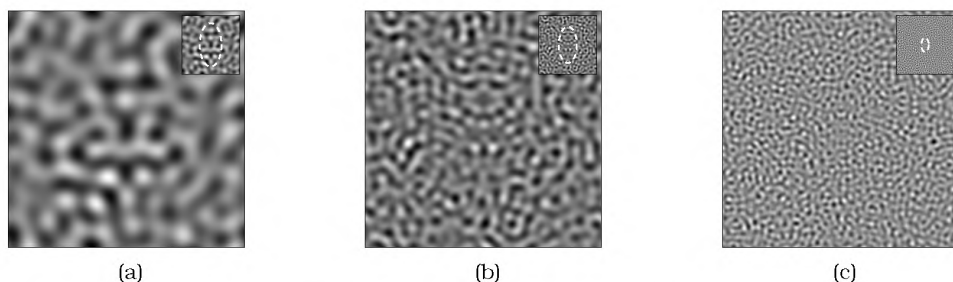


**Figure 1.10.** Filtered Gaussian noise stimuli, similar to the stimuli used in an experiment on the symmetry integration region by Dakin & Herbert (1998). Spatial frequency content in each sample stimulus is restricted to a one-octave passband, expressed in cycles per image (cpi). Each stimulus contains a central, elliptic patch of symmetry, indicated by the dashed ellipses in the insets. Stimuli feature three different spatial frequency passbands, namely 5–10 cpi (a), 10–20 cpi (b), and 20–40 cpi (c).

### 1.4.5 Multiple symmetry

There is also consensus that the salience of symmetry generally increases with the number of symmetry axes (e.g., Palmer & Hemenway, 1978; van der Vloed et al., 2005; Wagemans et al., 1991; Wenderoth, 1997; Wenderoth & Welsh, 1998b). Partly, this can be attributed to a probabilistic increase of chance in finding a symmetry axis. However, some researchers proposed that, in multiple symmetry, additional mechanisms come into play. In particular, it has been suggested that multiple symmetry gives rise to additional structural relationships, and that these relationships can be detected by the visual system, thereby enhancing symmetry detection (Palmer & Hemenway, 1978; Wagemans et al., 1991, 1993). Whether this or other characteristics of multiple symmetry (such as the relative orientation of the symmetry axes) play a role in symmetry detection is addressed in Chapter 2.

### 1.4.6 Information integration and scale invariance

Tapiovaara (1990) investigated discrimination of symmetry from noise for dense displays with different numbers of elements. The author noted an initial increase of performance with the number of elements and a saturation at a modest number. This suggests that only a limited amount of

symmetry information is integrated during symmetry processing. In fact, as Barlow & Reeves (1979) showed, there seems to be a differential weighting of symmetry information depending on its distance to the symmetry axis. A crucial role has been ascribed to the area about the symmetry axis. If a dot pattern is split into three pairs of vertical stripes (on either side of the symmetry axis) and symmetry is confined to one of the pairs, it is best perceived if the symmetry is located close to the axis (Figure 1.9). This suggests that proximity to the symmetry axis is an important factor in symmetry detection. However, Barlow & Reeves also found that symmetry is detected better when it is confined to the outermost stripes rather than when it is confined to the intermediate stripes. The latter effect is probably due to a symmetric 'subjective contour' which arises when one connects the outermost dots by straight lines. Indeed, Wenderoth (1995) showed that, if one masks the pattern outline of dot stimuli by embedding them in surrounding random dots, the detectability of symmetry is reduced by a fixed amount for all axis orientations. Similarly, if one introduces a gap between the two symmetry halves, symmetry detection deteriorates with increasing gap size (Corbalis & Roldan, 1974). However, if one compensates for the deterioration of symmetry processing by scaling up stimulus size proportionally with eccentricity, detection performance is fairly constant (Tyler & Hardage, 1996).

This issue of information integration was more rigorously investigated by Jenkins (1982) using dynamic random dot patterns. The stimuli consisted of strips of symmetry surrounded by noise. By varying the width of the symmetric strips, Jenkins showed that the area of effective symmetry information uptake is limited to a  $1.1^\circ$  strip about the symmetry axis. Since the width of the strip was independent of stimulus size, Jenkins considered it to be spatially fixed. The latter conclusion was disproved by Dakin & Herbert (1998). They used bandpass filtered Gaussian noise patterns similar to the examples in Figure 1.15. Their stimuli consisted of a central symmetric region embedded in noise of the same spatial frequency. Using phase jitter, the degree of symmetry was varied to obtain psychophysical thresholds. Furthermore, the size of the elliptical patch was varied along the x and y dimensions to find the maximum extent of the region wherein symmetry information is being processed. They found that the region is

elongated along the symmetry axis with an aspect ratio of approximately 2:1 and, furthermore, that it scales inversely with spatial frequency. This is schematically indicated by the dashed ellipses in Figure 1.15. In particular, the extent of the spatial region scales such that it encompasses a constant number of cycles.

This conclusion was somewhat refined in further research. Using stimuli with limited information content, Rainville & Kingdom (2000) showed that the symmetry integration region is flexible, with aspect ratio varying from 20:1 and 2:1 as a function of orientation content. In a follow-up experiment, Rainville & Kingdom (2002) investigated whether it is really spatial frequency as such that is decisive to the extent of the symmetry integration region or rather one of the covarying factors numerosity (number of elements), element density (number of elements per unit area), or display size. Interestingly, they found that the symmetry integration regions scales with density only. In other words, the amount of information picked up from a stimulus is constant, showing that symmetry detection is scale invariant. In the kind of symmetry detection task used by the authors, information uptake seems to be limited to about 18 elements.

### **1.4.7 Symmetry as a one-object cue**

Given its preponderance in real-world objects, symmetry has long been conceived of as a cue for the presence of an object, in contrast to repetition (i.e., repeated rather than reflected halves) which has been conceived of as a cue for the presence of multiple objects. Empirical evidence for this idea stems from Corbalis & Roldan (1974), who used symmetric and repeated patterns with joint and disjoint pattern halves. They showed that symmetry is better detected if its halves form one object than when they form two objects, and vice versa for repetition. This is consistent with Baylis & Driver (1994) and Bertamini et al. (1997), who showed that symmetric contours are detected better when they are part of one object rather than part of two objects, and again the opposite holds for repetition. Koning & Wagemans (2009) replicated these findings for 3D surfaces slanted in depth, showing that perfect 2D symmetry is not necessary for these effects to occur.

### **1.4.8 Recovery of 3D structure from symmetry**

Symmetry is a non-accidental property of images. In other words, it is unlikely that a symmetric image results from a particular view of an asymmetric object. In the computer vision literature, image-symmetry has been appreciated as a powerful tool for more than 20 years. It has been used as a structural constraint to reduce the degrees of freedom in solving the inverse problem (i.e., recovery of 3D shape from a 2D view) for objects presented in slanted views, both under orthogonal projection, that is, affine transformations (e.g., Cham & Cipolla, 1994), and perspective projection (e.g., Glachet et al., 1993). Furthermore, Zabrodsky & Weinshall (1997) demonstrated that implementing a 3D symmetry constraint generally enhances the performance of reconstruction algorithms such as structure-from-motion algorithms. Recently, Li et al. (2009) introduced a shape recovery model in which the constraint of symmetry makes the use of other depth cues superfluous.

Curiously, except for research on object representation and object recognition (e.g., Marr & Nishihara, 1978; Vetter et al., 1994), empirical research in human symmetry perception treated this topic rather stepmotherly (but see Kontsevich, 1996, who suggested that symmetry aids human 3D perception by providing additional virtual views of an object). It is true that Wagemans provided substantial work on skewed symmetry (Wagemans et al., 1991, 1992, 1993; Wagemans, 1995). However, his experiments were aimed towards establishing the importance of certain higher-order structures in symmetry detection rather than its role in depth perception. Hence, Wagemans et al. (1992) closed the issue by concluding that skewing seriously disrupts automatic processing of symmetry. Moreover, he employed affine transformations which are not veridical views for close-up objects. As reported above, van der Vloed et al. (2005) used veridical perspective views of symmetric stimuli but their research was aimed to investigate whether symmetry is detected from the retinal image or some form of transformed image normalized for perspective distortion.

This left open the question as to whether or not symmetry processing is directly involved in the computation of the orientation of objects in depth. To be more clear, perspective does not simply distort symmetry in a ran-

dom way as noise would do (see Figure 1.7). Rather, the virtual lines connecting symmetry pairs undergo lawful geometric transformations that could, in principle, be picked up by the visual system and serve as a depth cue. Recently, this issue came back into the focus of symmetry research. Niimi & Yokosawa (2008) used a depth-matching task for pairs of three-dimensional everyday objects, for different viewing angles. Results suggest that participants used symmetry, among other cues, to determine object orientation. Saunders & Backus (2006) suggested that the convergence of virtual lines indeed plays a role in depth perception, but their stimuli were confounded. They used dot matrices which, in addition to symmetry, also featured repetition and good continuation. Consequently, at present, it is still unclear in how far symmetry contributes to depth perception, if at all.

### **1.4.9 Neural implementation**

While the functional properties of symmetry perception are, to a certain extent, well-articulated, its neural basis is still poorly understood. There is some evidence for the recruitment of binocular visual neurons during symmetry processing. Although Erkelens & van Ee (2007) suggested that observers use a monocular vantage point when judging 3D symmetry, Julesz (1960, 1966) showed that symmetry can be both defined and destroyed by binocular disparity. Similarly, Wenderoth (2000) demonstrated that two random dot patterns presented to different eyes can be perceived as symmetric if their superposition yields a symmetry; in contrast, two monocular symmetries are perceived as random if their superposition does not yield a symmetry. A reconciling view stems from van der Zwan et al. (1998) who suggested that both V1 and extrastriate areas, and both monocular and binocular cells are involved in symmetry processing. Using symmetric dot stimuli, they showed that symmetry axes elicit the same tilt-aftereffects as usually observed with oriented lines. Based on these results, the authors proposed that similar mechanisms might underlie the encoding of orientation and the encoding of symmetry. This accords with studies that demonstrated the simultaneous processing of symmetry at different spatial scales and for different orientation content (using stimuli restricted in spatial-frequency and/or orientation content, see Figure 1.6), suggesting

that simple cortical filters such as those found in V1 could subserve symmetry detection (Dakin & Herbert, 1998; Dakin & Watt, 1994; Julesz & Chang, 1979; Rainville & Kingdom, 1999, 2000, 2002).

The neural foundations of symmetry processing were more directly assessed in neurofunctional studies employing electrophysiological and hemodynamic indices. Wilkinson & Halligan (2002) had participants engage in a Landmark task wherein participants have to judge whether or not the parts of a transected line are of equal length. They showed that presence versus absence of symmetry is correlated to activity in right anterior cingulate gyrus, which is involved in the deploying of attention. However, no symmetry-specific activation was found in earlier cortical areas. For symmetric dot patterns, Tyler et al. (2005) found predominant symmetry-specific activity in dorsolateral occipital, and none in earlier cortical areas either. This picture was refined in a follow-up experiment, where Sasaki et al. (2005) reported a more widespread network including V3A, V4d/v, V7, and the lateral occipital complex (LOC). The response of these areas was largely indifferent to changes in stimulus type (i.e., dot patterns and curved line patterns) and stimulus size. A control experiment revealed that these activations were partly modulated by attention, but symmetry-specific activity was found even when participants involved in a probe-detection task to which the structure of the stimulus was not relevant. This is in line with the the idea that symmetry detection is an automatic mechanism that applies to any visual input. The authors also showed that the magnitude of activation in areas V3A, V4d/v, V7, and LOC was correlated with the perceptual salience of the percept. In other words, activation was higher for 4-fold symmetry than for 2-fold or 1-fold symmetry, higher for perfect than for noisy symmetry, and higher for vertical than for horizontal symmetry.

This picture sketched by the fMRI studies is complemented by electrophysiological studies on the temporal dynamics of symmetry processing. In line with the idea that primary visual areas do not contribute significantly to symmetry detection, symmetric stimuli were shown to modulate only later components of the event-related potential (ERP). For instance, Höfel & Jacobsen (2007) exposed participants to abstract geometric patterns that were symmetric or non-symmetric and had them judge either



the beauty or the symmetry of the stimulus. In the symmetry judgment task, the ERP showed a late sustained negativity, roughly in the 500–1000 ms post-stimulus period, for posterior electrode sites. A similar negativity was obtained in a precursor to that study (Jacobsen & Höfel, 2003). Norcia et al. (2002) presented quick alternations (500 ms stimulus-to-stimulus time) of 2-fold symmetric and random dot patterns and found, similar to the previous study, a divergence of the ERPs in form of a sustained negativity for symmetric patterns. However, this time, ERPs diverged from about 200 ms post-stimulus, which is substantially earlier than in the previous study. Compatible results were reported in a study using symmetric checker stimuli (Oka et al., 2007).

Concluding, neurofunctional studies rather unequivocally pinpoint higher-tier visual areas as the locus of symmetry processing. On the one hand, this seems reasonable. Since symmetry is a global stimulus property, information needs to be integrated across large distances. Visual areas such as LOC, containing neurons with large receptive fields, seem to accommodate the adequate neural tissue for such global computations. On the other hand, there seems to be a discrepancy with parts of the psychophysical literature, which suggests that symmetry detection is critically supported by low-level filtering processes.

These seemingly contradictory views can be reconciled if one takes into account the possibility that, as conjectured by Dakin & Watt (1994), spatial filters involved in symmetry detection could be general-purpose filtering mechanisms recruited by many processes during perceptual organization. This indicates that one should not discount the role of early visual areas such as V1 prematurely, because EEG and fMRI analyses rely critically on differential activation (i.e., differences in activity elicited by symmetric stimuli and control stimuli), so they may be insensitive to a significant amount of 'pre-processing' of symmetries that is performed in primary visual areas.

Actually, such a critical two-stage architecture is implicitly or explicitly implemented in some spatial filtering accounts. These accounts conceptualize an initial, basic filtering stage serving as a kind of pre-processing module, followed by a symmetry operator that extracts the amount of symmetry from the output of that module. To give an example, Dakin & Watt's

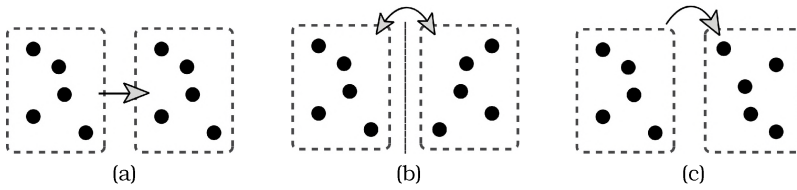


**Figure 1.11.** The transformational approach conceptualizes different types of symmetries associated with different invariance transformations. Symmetry halves get a block structure, as indicated by the dashed boxes. (a) Translational symmetry, obtained by translation along the  $x$ - or  $y$ -axis. (b) Reflection symmetry, obtained by 3D rotation around the vertical dashed line (indicating the symmetry axis). (c) Rotational symmetry, obtained by a rotation of  $180^\circ$ .

(1994) model comprises such a two-stage architecture. In an initial filtering stage, the visual input is convolved with an oriented filter. A similar operation could be subserved by simple cells in primary visual cortex which are selective both for orientation and spatial frequency. Subsequently, thresholding yields a number of blobs that tend to accumulate the symmetry axes in the image. A blob-alignment measure is then applied to estimate the amount of symmetry present. In contrast to the initial filtering stage, which involves local filtering operations, the blob alignment stage requires the integration of information about larger portions of the visual field, a function that could, at least in theory, be subserved by neural structures such as LOC featuring neurons with large receptive fields. This model will be introduced in more detail in the next section.

## 1.5 Models of symmetry perception

Over the years, a number of models of symmetry detection have been developed. Some are specialist, modeling a particular characteristic of symmetry perception, while others are more comprehensive (or at least they claim so). Since a short overview is necessarily incomplete, only those models with a relatively broad scope are considered. Furthermore, in an attempt to make the selection of models that are reviewed as representative as possible, different classes of models will be covered. Generally, one can distinguish four classes of symmetry detection models. Repre-

representational models of symmetry detection define the structures and relationships between stimulus parts underlying the perception of symmetry. Process models specify the operations to be carried out on raw visual input in order to enable the representation of symmetry. Neural models try to specify the neural architecture underlying the computation of symmetry. Finally, there is a class of hybrid models that share characteristics with both process models and neural models. These are spatial filtering models, which draw upon spatial mechanisms reminiscent of the spatial filtering operations that are known to be carried out in visual cortex. So, in fact, spatial filtering models are process models, but processes are specified in a fashion that is suggested to be neurally plausible.

### 1.5.1 Representational models

The most influential representational models on the perception of symmetry (and also other regularities) have been the transformational approach (TA) and the holographic approach (HA). Wrapped as a one-liner, the central tenet of TA can be said to be invariance under motion. In vision research, TA was promoted by Garner (1974) and Palmer (1983) and it conceives symmetries as a number of linear geometric transformations. The set of operations includes translation, rotation, and reflection, and it gives rise to a number of different symmetries. Although TA was originally coined to describe 3D structures, it readily generalizes to 2D patterns, as illustrated in Figure 1.11. The TA owes its elegance to its mathematical roots, in which the formation of symmetry is broken down into a number of geometric operations. By this, TA provided a common framework encompassing the kinds of geometric relationships the human visual system seems to be sensitive to.

In contrast to TA's invariance under motion, the rivaling holographic approach (HA), introduced by van der Helm & Leeuwenberg (1996, 1999, 2004), postulates invariance under growth. That is, in a regularity, each substructure should exhibit the same kind of regularity. This principle is known as holography and it can be exemplified by flowers, for instance, who preserve their symmetry when they grow. According to HA, another constraint a regularity should adhere to in order to qualify as a visual

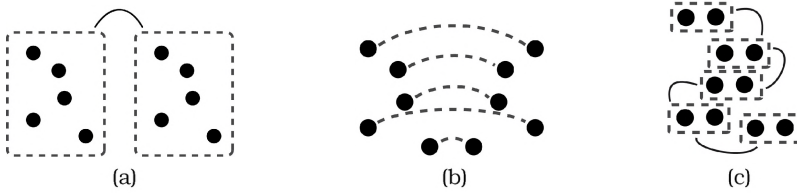


**Figure 1.12.** The holographic approach postulates invariance under growth. In other words, each substructure of a regularity is composed of that same regularity. This implies different structures for the regularities. (a) Repetition is characterized by relationships between repeats. A repetition grows by the addition of repeats. As a result, as in the transformational approach, repetition has a block-structure. (b) Symmetry is characterized by relationships between symmetric elements and symmetry grows pair-by-pair. Consequently, symmetry has a point-structure. (c) Glass patterns are characterized by relationships between equal pairs of elements (dipoles). As a result, Glass patterns have a dipole structure.

regularity is transparency. Crudely stated, transparency implies that patterns containing multiple regularities should be described by a unique hierarchical organization in which each component regularity is separately accessible. Application of the two mathematical constraints holography and transparency yielded three kinds of regularities, repetition (which corresponds to Palmer's translational symmetry), symmetry, and alternation (Figure 1.12). The latter regularity, alternation, gives rise to the class of Glass patterns to which the visual system has been shown to be sensitive to (Glass, 1969).

TA and HA do not differ so much in the kind regularities they postulate. Both accounts capture regularities that are perceptually relevant. They differ mainly in the way they conceive of the structure of these regularities. Most relevant to this thesis, HA gives symmetry a point structure rather than a block structure, as TA does. Furthermore, by means of the holographic goodness model, HA makes quantitative predictions concerning the goodness (i.e., detectability) of a regularity. This quantification boils down to the simple formula  $W = E/n$ , where  $W$  is the weight of evidence, that is, the amount of evidence for the presence of a regularity. In symmetry,  $E$  refers to the number of symmetry pairs, while  $n$  is the total number of elements. Consequently,  $W$  is bracketed between zero (no symmetry) and 0.5 (perfect symmetry). Among other predictions, holographic goodness predicts a graceful degradation of the goodness of symmetry with

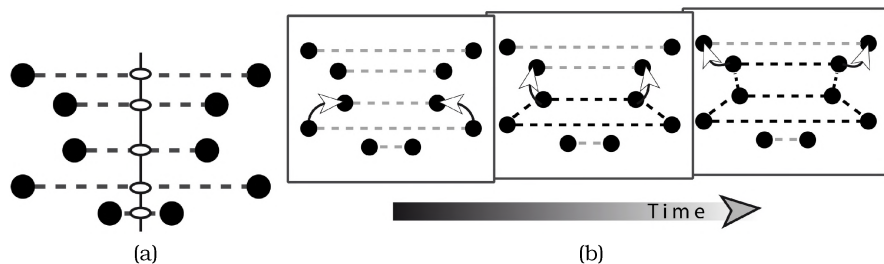


**Figure 1.13.** Illustration of Jenkins' (1983) first-order model and the bootstrapping approach of Wagemans et al. (1993). (a) If the symmetry pairs in a perfect symmetry are connected by virtual lines (dashed horizontal lines), two features arise. First of all, orientational uniformity, which means that the virtual lines are parallel with respect to each other. Second, midpoint collinearity (white ellipses), which means that the midpoints of virtual lines lie on a straight line coinciding with the symmetry axis (vertical line). (b) Wagemans et al. (1993) expanded Jenkins' first-order structures to also include higher-order structures, formed by joined pairs of virtual lines into correlation quadrangles. In the bootstrapping process, virtual lines are successively added, as indicated by the arrows, to existing higher-order structures (black dashed lines) until the whole stimulus is parsed.

noise, which is supported by virtually all literature on symmetry detection (e.g., Barlow & Reeves, 1979; Csathó et al., 2004; Dakin & Herbert, 1998). For a more detailed discussion on the commonalities and differences between TA and HA, refer to van der Helm & Leeuwenberg (1996, 1999) and van der Helm (2000).

## 1.5.2 Process models

In contrast to representational models, which describe the static relationships between stimulus parts in symmetry and other regularities, process models address the dynamics of the mechanism extracting symmetry from visual input. Numerous process models have been proposed in the literature, but a few of them stick out.

Among these is Jenkins' (1983) component processes model. Jenkins noted that, when symmetry pairs are connected by virtual lines, these lines are both of a uniform orientation and they are midpoint collinear. This is illustrated in Figure 1.13a. Jenkins conjectured that the visual system is sensitive to these first-order structures and uses them as anchors for symmetry detection. His detection model comprises three component pro-

cesses, one detecting the orientational uniformity of virtual lines, one fusing most salient point-pairs into a salient feature, and another estimating the symmetry in this feature.

Wagemans et al. (1993) pointed out that these first-order structures are insufficient for an apprehension of symmetry detection. In particular, using affine transformations, they showed that symmetry detection deteriorates in skewed symmetry even though orientational uniformity and mid-point collinearity are preserved (compare Figure 1.7c). This led them to propose the importance of higher-order structures formed by joining symmetry pairs into so-called correlation quadrangles. Wagemans et al. proposed that symmetry detection employs a bootstrapping process to form these higher-order structures by successively joining virtual lines, as illustrated in Figure 1.13b.

The bootstrapping approach paved the way for holographic bootstrapping, which essentially comes down to a marriage between mechanisms postulated by Wagemans (1995) and Wagemans et al. (1992, 1993) with principles proclaimed in the holographic approach (Section 1.5.1). In contrast to the bootstrapping model, which treated detection of symmetry, repetition, and Glass patterns in basically the same way, holographic bootstrapping is most notable for its distinction between the detection of a symmetry and the detection of a repetition. In particular, it captures the fact that the detection of repetition is comparatively slower than the detection of symmetry. It postulates that symmetry detection employs a parallel process, whereby each virtual line in a higher-order structure serves as the starting point for bootstrapping, whereas the detection of repetition employs a serial process, joining only one translation-pair per iteration step. For more details on holographic bootstrapping, refer to van der Helm & Leeuwenberg (1999).

The next two process models bear on the remarkable resistance of symmetry detection to spatial jitter (see Figure 1.7b). Based on this observation, Barlow & Reeves (1979) concluded that the visual system does not perform a rigid point-to-point matching but rather operates within a certain tolerance area. According to the model, the visual system mimics an operation that boils down to tiling the stimulus into a number of equisized rectangles corresponding to the size of this tolerance area, counting the

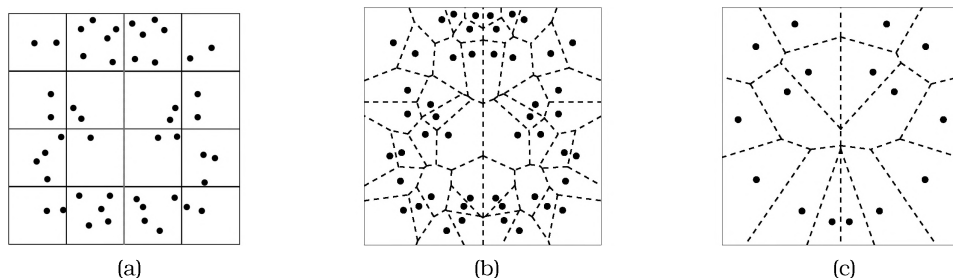


**Figure 1.14.** Illustration of Barlow & Reeves' (1979) and Dry's (2008) process models. (a) Sketch of the model by Barlow & Reeves (1979) applied to a jittered dot pattern. The pattern is tiled into a number of rectangular cells (here, 4x4 squares). The model acts by counting the number of elements within each square and comparing dot frequencies for symmetrically positioned cells. Despite the jitter, there is a perfect match in dot frequencies for most symmetric pairs of cells. In the third row, however, there is a mismatch, with the first two cells containing 4 dots and 1 dot, respectively, and their symmetric counterparts containing 3 dots and 2 dots. Consequently, there is a slight deterioration of symmetry compared to perfect symmetry. (b) Dry's model abandons the somewhat artificial rectangular tiling of the stimulus. Rather, each dot is placed in its Voronoi cell (see text for details), whose boundaries are indicated by dashed lines. (c) If the number of dots is decreased, the size of the Voronoi cells increases. This demonstrates that the model's jitter tolerance scales with element density.

number of elements within this area and comparing it to the number in the corresponding symmetry half. This is illustrated in Figure 1.14a.

A recent model on symmetry detection, although based on a different rationale, constitutes in some respect a refinement of Barlow & Reeves' account. Dry's (2008) utilizes Voronoi tessellation to render spatial relationships between the dots. Each dot is placed in a cell of variable size, whereby the cell's border circumscribes the area that is closest to the dot in the cell (Figure 1.14b). Similar to Barlow & Reeves' account, symmetry detection is performed by superimposing one half of the pattern with the reflected Voronoi tessellation of the other half and then assessing the number of dots falling into each cell. In a perfect symmetry, there would be a perfect match. Interestingly, the Voronoi model explicitly predicts scale invariance (see Figure 1.14c), a property of symmetry perception that was verified by Rainville & Kingdom (2002).

Note that the rationale underlying these two models is very different. The Voronoi model draws on evidence that the visual system is indeed performing operations mimicking Voronoi tessellation. In contrast, Barlow

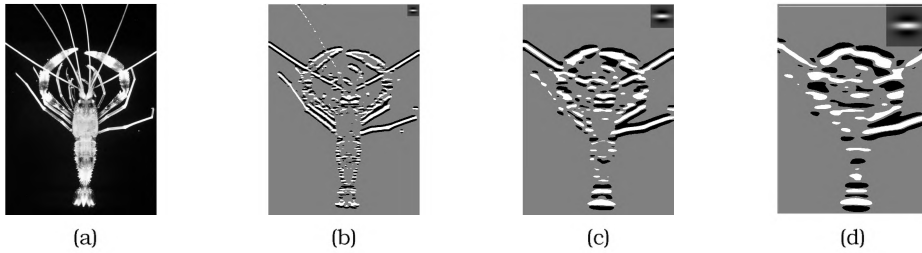


**Figure 1.15.** Application of Dakin & Watt's filtering model to a grayscale version of the *Stenopus Hispidus* introduced in Figure 1.2a. (a) Grayscale version of the original image. (b) Image filtered with a relatively fine-scale filter selective for horizontal orientations. The resulting image is obtained by thresholding the output to a ternary image. The according filter is shown in the top right corner. At this scale, the filter is responsive mainly to the fine-scale details of the figure, not the symmetry. (c) Filtering at a slightly coarser scale. Upon visual inspection, the blobs at the lower tip of the animal and blobs at the head are roughly aligned about the symmetry axis. (d) Filtering with a coarse filter. Again, the lower half of the animal displays some degree of blob alignment.

& Reeves' account relies on symmetry analysis at a lower spatial scale than the scale of individual dots. In this sense, it is related to spatial filtering accounts and, hence, bridges the gap to the next class of models.

### 1.5.3 Spatial filtering models

The 90's were the advent of spatial filtering models in symmetry perception. These models capitalize on the fact that the visual system performs something like a localized Fourier analysis of visual input (e.g., Graham, 1989; Valois, 1977; Valois et al., 1974, 1985; ?). Spatial filtering models recruit mechanisms sensitive to spatial frequency, orientation, and spatial phase. Consequently, frequency domain transforms and convolution with a bank of filters selective for spatial scale, phase, and/or orientation, are frequently utilized tools. Many models adopt a filter-rectify-filter regime, whereby an initial filtering operation is followed by a nonlinearity (e.g., a squaring operation), and then the output is subjected to a second linear or nonlinear operation.

One such two-stage model was introduced by Dakin & Watt (1994). In the first stage, the input image is convolved with an oriented filter responsive to particular spatial frequencies. The resulting output is then thresh-



olded to a ternary image (Figure 1.15bcd). Values lower than one standard deviation off the mean are depicted in black, values higher than one standard deviation are white, and the values in between are gray. Thus, the filtering operation yields a number of black and white blobs. In the second stage, a blob alignment procedure is applied that measures how well the centroids of the blob align about a putative symmetry axis. Upon visual inspection of the examples in Figure 1.15, blob alignment about the central vertical symmetry axis is obvious in only the lower half of the animal for rather coarse filters (1.15cd).

More complex two-stage models were presented by Kovesi (1997, 1999) and Osorio (1996). Both authors realized that, if an image is decomposed into its frequency components, phase information is instructive regarding the location of a local symmetry axis. In particular, three types of stimulus features, namely edges, lines, and symmetry axes, are characterized by phase congruency, as follows. Edges are defined by sharp luminance transitions, so that corresponding spatial harmonics can be characterized by sine waves in  $0^\circ$  or  $180^\circ$  phase. Lines feature luminance maxima or minima with spatial harmonics congruently in  $90^\circ$  (cosine) or  $270^\circ$  phase. Although there is no specific intensity change at symmetry axes, spatial harmonics are a mixture of  $90^\circ$  and  $270^\circ$  phase. To squeeze out symmetry information from an input image, both authors used quadrature-pair filters (two filters, one in sine phase and one in cosine phase) to obtain measures of symmetry and asymmetry. After this first filtering stage, signals were squared. Osorio (1996) separately added up energy from even-symmetric and odd-symmetric filters. Points were marked as lying on a symmetry axis when the sum obtained from the even-symmetric filters was at a maximum and the sum obtained from odd-symmetric filters was close to zero. Kovesi (1997) combined even- and odd-symmetric filter outputs by determining the absolute difference between the outputs for each spatial scale and then calculating a weighted mean normalized by the total energy. Note that these models compute only local symmetry. Information is not integrated across a larger area to find the global symmetry axis, as done by Dakin & Watt (1994).

Global computation of the symmetry axis is achieved in a three-stage model presented in Gurnsey et al. (1998). In the first stage, the image is

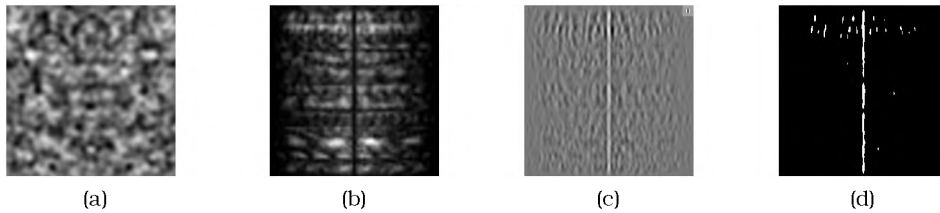


**Figure 1.16.** Application of the model by Gurnsey et al.. (a) First stage. Pixel symmetry corrupted with pixel noise is convolved with a Gaussian kernel to enhance low spatial frequencies. (b) Second stage. A global differencing operation is performed in search for a vertical symmetry axis. A black trough appears at its position. (c) Third stage. The symmetry axis is explicitly detected by convolution with a vertical filter (small inset at the right top). (d) Just for visualization purposes, the image in (c) was thresholded to illustrate that filter output is indeed highest at the symmetry axis.

convolved with a Gaussian kernel to get a smoothed image. Then, a global differencing operation is performed, wherein the squared difference in luminance between symmetrically positioned pixels is calculated for each column in the image. In the third stage, the output of the differencing operation is convolved with a vertical filter to explicitly detect the symmetry axis. These stages are documented in Figure 1.16 for a sample stimulus.

Note that this overview is not exhaustive. Other capable models have been proposed in the literature, such as a two-stage model by Rainville & Kingdom (2002), which applies quadrature-pair filters first to luminances and then to filter output. The model is theoretically sound and implements the complex process of density invariance.

### 1.5.4 Neural models

At present, there is no full-fledged neural model of symmetry detection. For one, this is due to the still patchy knowledge about the implementation of symmetry perception in the brain. Second, at some point, even functional models have to surrender in view of the versatility of the symmetry detection system. Despite the lack of facts, there were some ideas about how symmetry processing might be implemented. In early approaches, the superiority of vertical symmetry spawned theories suggesting that symmetry processing is accounted for by the symmetric architecture of the visual cortex (e.g., Mach, 1886; Julesz, 1971). Recently, a similar scheme

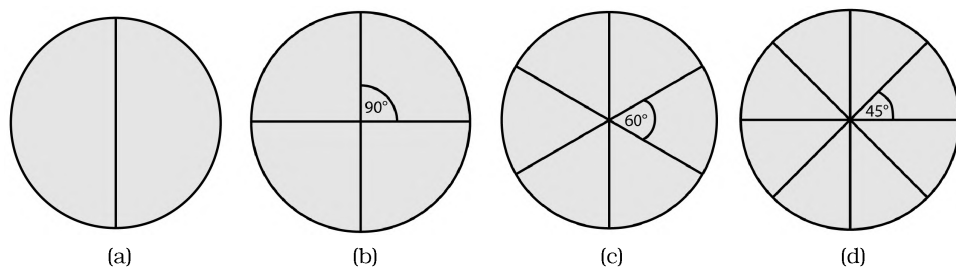


**Figure 1.17.** A schematic sketch of the symmetry axes in 1-fold (a), 2-fold (b), 3-fold (c), and 4-fold (d) symmetry. Evidently, the angle between the symmetry axes, that is, relative orientation, changes with the number of symmetry axes.

was proposed, whereby the corpus callosum was speculated to establish long-range connections between cortical filters (Saarinen & Levi, 2000). Both views can be regarded as obsolete, because virtually all experimental results militate against a rigid architecture involving interhemispheric point-to-point computations. In particular, as reviewed above, the fact that symmetry can be detected under various axis orientations, for different eccentricities, and the fact that the salience of symmetry increases when symmetry axes are added suggests a more flexible underlying substrate.

## 1.6 Outline of the thesis

As the review of the literature suggests, research today can look back on a considerable body of knowledge on symmetry processing. The many advances notwithstanding, the field of symmetry processing is far from being fully charted. This thesis focuses on a complex topic that has not received as much attention as the fundamental research into symmetry perception, namely the interaction between multiple perceptual processes.

Chapter 2 sets the stage by investigating the interaction between two component symmetries in a multiple symmetry. In multiple symmetry, there is a number of stimulus characteristics that are tied to the number of symmetry axes in perfect symmetry. For instance, as depicted in Figure 1.17, in perfect symmetry, the angle between the symmetry axes, that is, relative orientation, decreases with the number of symmetry axes. Another

point is that multiple symmetry gives rise to additional structural relationships between stimulus elements. For instance, there are dot pairs in a 1-fold symmetry (i.e., a symmetry with one symmetry axis) but dot quartets in a 2-fold symmetry. These two factors were investigated by using different noise manipulations to decouple the number of symmetry axes from relative orientation and from the availability of additional structural relationships.

Chapter 3 investigates the interaction between the processing of symmetry and repetition and the processing of contours. It serves to sharpen the definition of what is to be considered a symmetry and a repetition the visual system is sensitive to and what not. In Figure 1.18, the difference between regularity (i.e., symmetry and repetition) and antiregularity (i.e., antisymmetry and antirepetition) is described. In the literature (Baylis & Driver, 1995; Bertamini et al., 1997; Koning & Wagemans, 2009), this distinction has not been honored which led to a jumble of seemingly contradictory results.

Chapter 4 investigates the interaction between the processing of symmetry and repetition and processing of stereoscopic depth cues (stereoprocessing). Using shutter glasses, different information can be presented to the left and the right eye of observers. We used this technique to spread symmetry and repetition information across two depth planes in different ways, as illustrated in Figure 1.19 for symmetry. We conjectured that these manipulations should have different effects on symmetry and repetition provided their assumptive role in perception. To trace the interaction

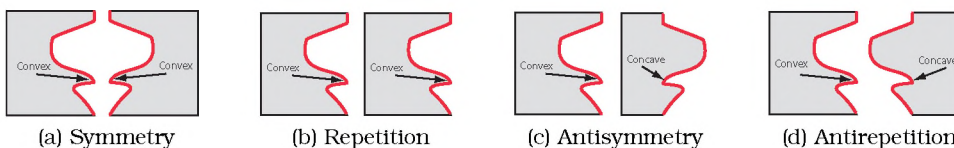


**Figure 1.18.** Schematic overview of the four types of stimuli used in the experiments in Chapter 3. Each stimulus consists of two shapes (gray) and two reflected or repeated contours (indicated here by red color) have to be matched. On basis of whether there is a match in contour polarity (i.e., convexities match with convexities, concavities match with concavities) or a mismatch in contour polarity, we define the resulting structure as regularity (symmetry and repetition) or antiregularity (antisymmetry and antirepetition). The arrows point at examples for matched and mismatched contour polarity.

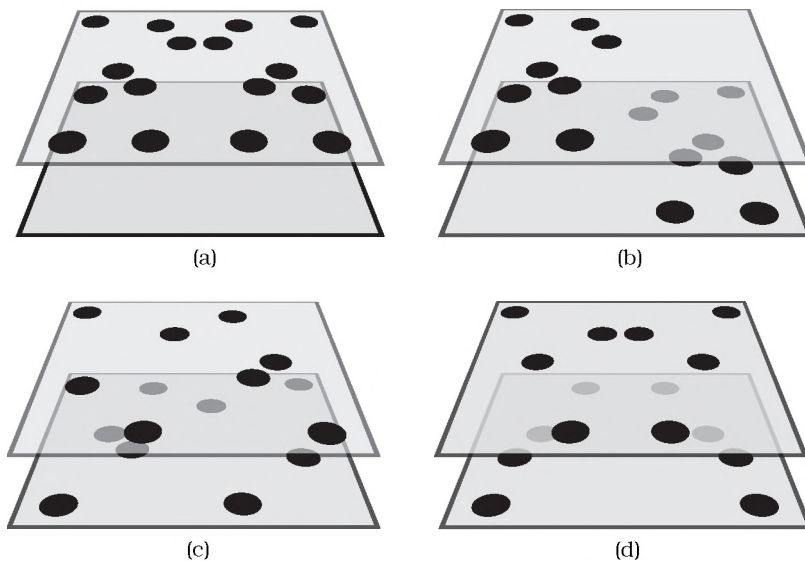


**Figure 1.19.** Schematic overview of the stereoscopic manipulations in Chapter 4 for symmetric stimuli. Each panel shows a view of two depth planes which, for illustrative purposes, have been tilted backwards. (a) Baseline stimulus. A perfect symmetry is shown on the first (upper) depth plane, with no information in the other depth plane. (b) Starting from the same pattern, symmetry information is spread across two depth planes such that each symmetry half resides on a different depth plane. (c) Starting from the pattern in (a), symmetry is spread across two depth planes such that the pattern on each individual plane looks random. (d) Starting from the pattern in (a), symmetry is spread across two depth planes such that symmetric relationships are preserved within depth planes.

between symmetry and repetition processing and stereoprocessing across time, we varied the length of the presentation time of each stimulus.

Chapter 5 investigates the interaction between symmetry processing and motion processing. Displays consisting of elements that move periodically according to a sinusoidal velocity function have been shown to elicit a strong percept of 3D form, a phenomenon entitled structure-from-motion or kinetic depth effect. In this chapter, we focus on how structure-from-motion is affected if 2D symmetry information is introduced to the stimulus.

In the final discussion chapter of this thesis we will summarize the main findings and sketch future lines of research that remain to be explored.

## CHAPTER 2

---

Interactions between the constituent single  
symmetries in multiple symmetry

---



The detectability of multiple symmetry is known to depend on the number of constituent single symmetries, but it is unclear whether and, if so, how these symmetries interact. Therefore, in six experiments on imperfect 2-fold symmetry, the role of the relative orientation of symmetry axes was investigated. The results suggest (a) that symmetry detection is not only facilitated in case of orthogonal axes but also impeded in case of nonorthogonal axes, and (b) that both effects are due to the relative orientation of the axes itself rather than to so-called correlation rectangles whose presence or absence depends on the relative orientation of the axes. Both effects are proposed to be accounted for by the neural mechanism of surround inhibition.

## 2.1 Introduction

Detection of mirror symmetry (henceforth, symmetry) is believed to be an integral part of the perceptual organization process that is applied to any visual input. A large body of empirical studies shows that human symmetry detection is quick, versatile, and resistant to noise and spatial jitter (for overviews, see Tyler, 1996; van der Helm & Leeuwenberg, 1996, 2004; Wagemans, 1995). Furthermore, symmetry processing was shown to interact with other factors in perceptual organization (e.g., stereoprocessing; Treder & van der Helm, 2007). Most empirical studies on symmetry perception focused on 1-fold symmetry alone, some included repetition and Glass patterns, but only few focused on multiple symmetry. Yet, insight in all these visual regularities is necessary to build general theories of perceptual organization. The aim of this study, therefore, is to provide more insight into the mechanisms underlying multiple symmetry perception.

To this end, we investigated whether the symmetries in 2-fold symmetry interact, and we modeled the interactions we found in a neurophysiologically plausible way. Although this study focuses on 2-fold symmetry, the scope of this study extends to multiple symmetry with any number of sym-



metry axes. This is illustrated by indicating how our research question was triggered by the few existing studies on multiple symmetry.

Most research on multiple symmetry involved 2-fold and 4-fold symmetry, that is, curiously, not 3-fold symmetry. For 1-fold, 2-fold, and 4-fold symmetry, data show consistently that salience increases with the number of symmetry axes (e.g., Nucci & Wagemans, 2007; Palmer & Hemenway, 1978; Wagemans et al., 1991; Wenderoth, 1997). To explain this, one needs hardly more than the idea that the probability of detecting a symmetry axis increases with the number of symmetry axes (cf. Corbalis & Roldan, 1974; Palmer & Hemenway, 1978). But what about 3-fold symmetry which, in contrast to 2-fold and 4-fold symmetry, has only nonorthogonal symmetry axes?

The only three empirical studies we know on 3-fold symmetry are indecisive on this point. Hamada & Ishihara's (1988) data suggest that 3-fold symmetry behaves like 3-fold rotational symmetry (i.e., with three local mirror symmetries but without global mirror symmetries). Furthermore, for  $n$ -fold symmetry with  $n=1,2,3,4$ , van der Vloed (2005) found that salience increases linearly with  $n$ , but Wenderoth & Welsh (1998b) found that 3-fold symmetry is not more salient than 2-fold symmetry and rather tends to be less salient. Models of 1-fold symmetry perception that have been claimed to extend to multiple symmetry also disagree on this point – this is discussed next.

First, in the so-called transformational approach (Palmer, 1983), a 1-fold symmetry is characterized by a  $180^\circ$  3-D rotation about the symmetry axis. Likewise, an  $n$ -fold symmetry is characterized by  $n$  such 3-D rotations plus  $n$  2-D rotations of  $360/n$  degrees in the image plane. This suggests that the salience of multiple symmetry, including 3-fold symmetry, simply increases with the number of symmetry axes.

Second, the so-called holographic approach (van der Helm & Leeuwenberg, 1991, 1996, 1999, 2004) builds on the idea that symmetry allows for efficient stimulus representations (e.g., Leeuwenberg, 1969, 1971). In terms of symbol strings, this may be illustrated by the compression of the symmetrical string *abcdeffedcba* into the symmetry code  $S[(a)(b)(c)(d)(e)(f)]$ . Likewise, the double symmetry in the string *abccbaabccba* can be represented by a hierarchical combination of two symmetries. That is, the string

can be encoded into the code  $S[(a)(b)(c)(c)(b)(a)]$  which can be encoded further to yield the code  $S[S[(a)((b))((c))]]$ . Hence, this code captures all symmetry by combining two separate 1-fold symmetries, which suggests that both symmetries add to the total salience. For the triple symmetry in the string *abbaabbaabba*, however, this coding approach implies that, after having captured the global symmetry in the code  $S[(a)(b)(b)(a)(a)(b)]$ , only one local symmetry can be captured yielding either  $S[S[(a)((b))]]$   $(a)(b)$  or  $S[(a)(b) S[(b)((a))]]$ . Notice that these codes are more complex than the one above for the double symmetry.

Translated to 2-D multiple symmetries, the foregoing implies that the two extra symmetries in 3-fold symmetry are predicted to add less to the total salience than the single extra symmetry in 2-fold symmetry does (van der Helm & Leeuwenberg, 1996). The applied coding principles suggest that this is due to the relative orientation of the symmetry axes. That is, in case of 3-fold symmetry, the applied coding principles imply that capturing one of the two extra symmetries disables the other, or in other words, they suggest that nonorthogonal symmetries impede each other.

Third, in contrast to the holographic approach, the so-called bootstrap approach (Wagemans et al., 1991, 1993) suggests facilitation in case of orthogonal symmetry axes (i.e., not impediment in case of nonorthogonal axes). This may be explicated as follows. In 1-fold symmetry, two symmetrically corresponding points can be connected by a virtual line, and such virtual lines can in turn be joined to form virtual trapezoids. Distortion of these so-called lower and higher order structures has been shown to impair symmetry detection (Jenkins, 1983; Sawada & Pizlo, 2008; Wagemans et al., 1991, 1993; van der Vloed et al., 2005). Notice that the normals to the parallel virtual lines in a virtual trapezoid indicate in which two directions the propagation process may continue, that is, in which directions subsequent propagation steps should search for additional symmetry pairs (see Figure 2.1a). In 2-fold symmetry, however, some trapezoids are rectangles. These quartetwise correlations indicate four propagation directions and imply that twice as many symmetry pairs can be added during each subsequent propagation step (see Figure 2.1b). The correlation rectangles are therefore proposed to facilitate 2-fold symmetry detection. Such correlation rectangles do not occur in 3-fold symmetry which therefore cannot

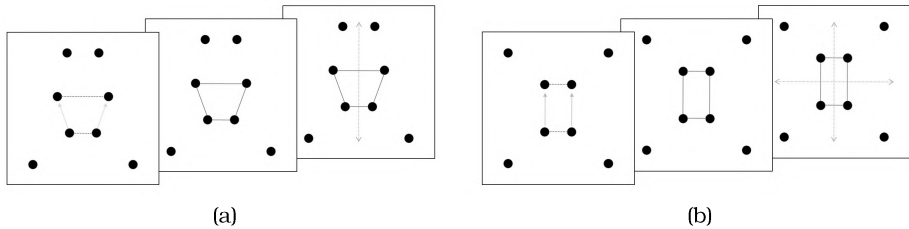


**Figure 2.1.** Symmetry detection by way of bootstrapping in 1-fold and 2-fold symmetry. (a) In 1-fold symmetry, symmetry pairs yield virtual lines (dashed lines) which join to form a correlation trapezoid (solid lines). These pairwise correlations suggest one propagation axis (up/down) along which additional symmetry pairs should be searched for during subsequent propagation steps. (b) In 2-fold symmetry, two virtual lines (dashed lines) join to form a correlation rectangle (solid lines). These quartetwise correlations suggest two propagation axes (up/down and right/left). This allows for the addition of twice as many symmetry pairs in each subsequent propagation step.

benefit from their facilitatory effect.

Notice that, in Marr's (1982) terms, the three just-discussed approaches to multiple symmetry perception are approaches at the computational and algorithmic levels of description. In the General Discussion, we complement this type of approach by including the implementational level of description, that is, by casting the just-discussed facilitation and impediment in terms of excitatory and inhibitory neural mechanisms. In any case, the foregoing shows that the existing literature contains various views on interactions between the constituent symmetries in multiple symmetry. To investigate these interactions in more detail, we conducted two triples of experiments on imperfect 2-fold symmetry.

Imperfect multiple symmetries do abound in nature and art (e.g., in flowers and band patterns), and our study does seem relevant to biology and art science, but the main reason we considered imperfect multiple symmetry is that we aimed at investigating properties of the human visual system. One of *the* methods to this end is to probe the detectability of symmetry in the presence of noise. Importantly, in the case of multiple symmetry, it allows for a decoupling of the number of symmetry axes, correlation rectangles, and relative axis orientation – factors which cannot be decoupled in perfect multiple symmetry because, in perfect multiple symmetry, one factor dictates the others.

In the first triple of experiments, we focused on the idea that correlation rectangles, which occur only in case of orthogonal symmetry axes, facilitate 2-fold symmetry detection. This idea is plausible enough to be taken seriously, but it had never been tested. In the second triple of experiments, we used only symmetries without correlation rectangles to investigate the more general characteristic of the relative orientation of symmetry axes.

## 2.2 Correlation rectangles

In experiments 1a, 1b, and 1c, we examined whether correlation rectangles indeed have the facilitating effect on 2-fold symmetry detection as proposed in the bootstrap approach. To prevent that an effect of correlation rectangles is contaminated with effects of the number of symmetry axes or of relative axis orientation, we kept the latter factors constant. To this end, we focused on imperfect 2-fold symmetries which, by means of various noise manipulations, had 50% noise about each symmetry axis. Because the experimental setup was largely identical across the three experiments, we outline the general method below.

### 2.2.1 General method

#### 2.2.1.1 Participants

Twenty-one undergraduate students participated in experiment 1a, 19 other undergraduate students participated in experiment 1b, and 37 undergraduate students participated in experiment 1c. Two of latter had participated in one of the previous experiments more than one month before. All participants had normal or corrected-to-normal vision and received course credits or money for their participation.

#### 2.2.1.2 Stimuli

Each stimulus comprised 80 nonoverlapping bandpass elements. The luminance profile of an element was given by the radial Gaussian function

$$l(d) = 0.5 + 0.5 \cdot e^{-\frac{d^2}{2\sigma^2}}$$

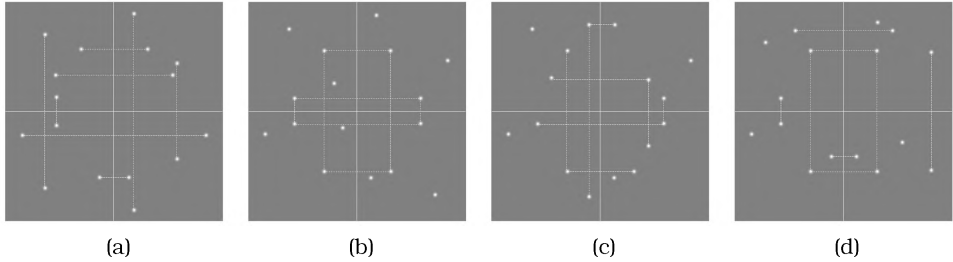


**Figure 2.2.** Schematic overview of the 2-fold symmetry stimulus manipulations in experiments 1a, 1b, and 1c. For simplicity, each display shows only 16 elements (the actual stimuli contained 80 elements). The solid lines indicate the symmetry axes and the dashed lines indicate symmetry pairs (these lines were not present in the actual stimuli). For details on the stimuli, see the general method. (a) No-rectangles condition. (b) Rectangles condition. (c) L-condition. (d) 25%-rectangles condition.

where  $d \in [0; 16]$  is the distance in pixels from the center of the window, and  $\sigma = \sqrt{10}$ . The stimuli were constructed such that they formed various 2-fold symmetries featuring a vertical and a horizontal symmetry axis. Additionally, in all three experiments, we used 1-fold symmetries as baseline trials and random patterns as catch trials.

More specifically, in experiment 1a, we tested the effect of correlation rectangles by comparing the detectability of 2-fold symmetries in the so-called no-rectangles and rectangles conditions (see Figure 2.2a and Figure 2.2b). In the no-rectangles condition, symmetries did not feature correlation rectangles; to this end, 50% of the elements were placed symmetrically about the horizontal axis alone, and the other 50% were placed symmetrically about the vertical axis alone. In the rectangles condition, symmetries featured correlation rectangles; to this end, 50% of the elements were placed as quartets (i.e., elements were symmetrical about both axes) and the other 50% were randomly distributed so that they constituted global noise (i.e., elements which are symmetric about neither axis). Hence, to each symmetry axis in each condition, 50% of the elements constituted symmetry pairs and the other 50% of the elements constituted noise.

In experiment 1b, to test the effect the global noise may have had in the rectangles condition, we replaced the rectangles condition by the so-called L condition (see Figure 2.2c). In the L condition, 75% of the elements were part of L-triplets produced by first placing a symmetrical dot quartet (e.g.,

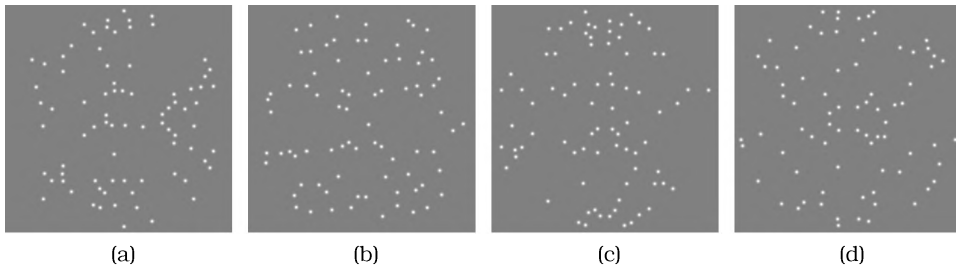


**Figure 2.3.** Examples of the 2-fold symmetry stimuli used in experiments 1a, 1b, and 1c. All stimuli featured 50% noise about each symmetry axis. For further details about the stimulus manipulations, see the general method. (a) No-rectangles condition (experiments 1a and 1b). (b) Rectangles condition (experiment 1a). (c) L condition (experiments 1b and 1c). (d) 25%-rectangles condition (experiment 1c).

four dots which are symmetrical about both axes) and then removing one dot from the dot quartet so that the remaining three dots form a virtual “L” instead of a rectangle. The other 25% of the elements constituted global noise. Consequently, neither the no-rectangles condition nor the L condition featured correlation rectangles. Furthermore, both kinds of 2-fold symmetries contained 50% noise about either symmetry axis, but they differed in the proportion of global noise, namely, 0% in the no-rectangles condition and 25% in the L-condition.

In experiment 1c, we further tested the above-mentioned factors by comparing the L condition and the so-called 25%-rectangles condition (see Figure 2.2d). In the 25%-rectangles condition, 25% of the elements were placed in symmetrical dot quartets (i.e., elements were symmetrical about both axes), 25% were symmetrical about the horizontal symmetry axis only, 25% were symmetrical about the vertical symmetry axis only, and 25% constituted global noise. Hence, these two conditions were matched in terms of the amount of global noise (25%) and the amount of noise for each symmetry axis (50%). However, the L condition featured no correlation rectangles, whereas in the 25%-rectangles condition, 25% of the elements were part of correlation rectangles.

Example stimuli for all 2-fold symmetry conditions are given in Figure 2.3. Furthermore, in the baseline condition, we used 1-fold symmetries in which 40 elements were positioned symmetrically about an axis (vertical

or horizontal) while the remaining 40 elements were distributed randomly. In the catch trial condition, we used random stimuli in which all elements were randomly distributed. All stimuli were circular and subtended about 16° visual angle. Absolute axis orientations were horizontal and vertical. The background of the display was set to mean luminance (16.64  $cd/m^2$ ). Using Matlab, a unique set of stimuli was generated for each participant.

### 2.2.1.3 Procedure

Participants were seated 60 cm in front of an 19 in. monitor with a 100 Hz refresh rate and a resolution of 1280 × 1024 pixels. A chinrest was used to restrict head movements. Participants performed a two-alternatives forced choice (2AFC) task in which a symmetrical stimulus (either a 1-fold or a 2-fold symmetry) and a random stimulus were presented in subsequent intervals in a random order. Participants had to indicate which of the two intervals featured symmetry. Responses were recorded using a button box.

Prior to each experiment, each participant completed a practice block of 60 trials with feedback given after each trial. Each interval was preceded by a central fixation dot presented for 500 ms. During the intervals, stimuli were flashed for 120 ms. The number of experimental trials totalled 4 [symmetry conditions] × 120 [measurements] = 480. The experiments were self-paced.

## 2.2.2 Experiment 1a

In this experiment, we contrasted 2-fold symmetries in which correlation rectangles are present (the rectangles condition) to 2-fold symmetries in which correlation rectangles are absent (the no-rectangles condition). The rationale was that, if correlation rectangles facilitate 2-fold symmetry detection (as proposed in the bootstrap approach), then the former should be more salient than the latter.

### 2.2.2.1 Results

For each subject and each subcondition, the discriminability measure  $d'$  was calculated on the basis of the correct scores on trials wherein the sym-

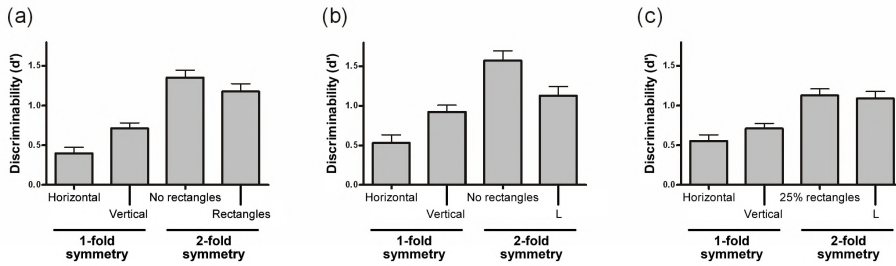


**Figure 2.4.** Results of experiments 1a, 1b, and 1c. Error bars represent 1 SEM. In all experiments, vertical symmetry is more salient than horizontal symmetry, and 2-fold symmetry is more salient than 1-fold symmetry. (a) Results of experiment 1a. Performance is worse in the rectangles condition than in the no-rectangles condition. (b) Results of experiment 1b. Performance is better in the L condition than in the no-rectangles condition. Because there are no correlation rectangles in both conditions, this difference can be attributed to the global noise which is present in the L condition but not in the no-rectangles condition. (c) Results of experiment 1c. For a fixed amount of global noise, performance in the L condition does not differ from performance in the 25%-rectangles condition.

metry was presented in one interval and the error scores on trials wherein the symmetry was presented in the other interval (e.g., Swets, 1964; Wickens, 2002). Subsequently,  $d'$  values were compared using paired-samples  $t$ -tests. Vertical 1-fold symmetry was more salient than horizontal 1-fold symmetry,  $t(20) = 3.540$ ,  $p < .01$ , and less salient than 2-fold symmetry – both with and without correlation rectangles,  $t(20) = 8.066$ ,  $p < .001$ , and  $t(20) = 10.613$ ,  $p < .001$ , respectively. Furthermore,  $d'$  on 2-fold symmetry tended to be lower in the rectangles condition than in the no-rectangles condition, but this effect was not significant ( $p = .084$ ). The results are depicted in Figure 2.4a.

### 2.2.2.2 Discussion

In contrast to what the bootstrap approach predicts, we did not find that symmetries with correlation rectangles are better detectable than symmetries without. This suggests that correlation rectangles do not play a role in symmetry detection. Note, however, that in the no-rectangles condition, every element was symmetrical about one of the axes, whereas in the rectangles condition, 50% of the elements constituted global noise (i.e., elements which are symmetrical about neither symmetry axis). Because, in



principle, a negative effect of global noise could have overshadowed a positive effect of correlation rectangles, we conducted two control experiments to estimate the magnitude of both effects separately.

### 2.2.3 Experiment 1b

In this experiment, we probed the effect of global noise when correlation rectangles are absent. To this end, we contrasted the no-rectangles condition to the L condition. Neither condition features correlation rectangles, but the no-rectangles condition does not feature global noise whereas the L condition does (i.e., 25% of the elements form global noise).

#### 2.2.3.1 Results

We again found that vertical 1-fold symmetry was more salient than horizontal 1-fold symmetry,  $t(18) = 3.470$ ,  $p < .01$ , and less salient than 2-fold symmetry – both in the no-rectangles condition and in the L condition,  $t(18) = 7.731$ ,  $p < .001$ , and  $t(18) = 2.128$ ,  $p < .05$ , respectively. Furthermore,  $d'$  on 2-fold symmetry was significantly lower in the L condition than in the no-rectangles condition,  $t(18) = 5.218$ ,  $p < .001$ . The results are depicted in Figure 2.4b.

#### 2.2.3.2 Discussion

We found that performance is lower in the L condition than in the no-rectangles condition. Since these conditions differ only in the amount of global noise, we may conclude that global noise hampers symmetry detection more than noise about the axes separately. This implies that, in experiment 1a, a negative effect of global noise may indeed have overshadowed a positive effect of correlation rectangles. To control for the effect of global noise, we conducted the following experiment.

### 2.2.4 Experiment 1c

In this experiment, we probed the effect of correlation rectangles, if any, when the amount of global noise is fixed. To this end, we contrasted the L

condition and the 25%-rectangles condition. Both conditions feature 25% global noise, but the L condition does not feature correlation rectangles whereas the 25%-rectangles condition does (i.e., 25% of the elements form correlation rectangles). To uncover an effect of correlation rectangles even if it is small, the number of participants was considerably larger than in the previous experiments.

#### 2.2.4.1 Results

One participant was excluded from the analysis because the overall  $d'$  was negative. This time, we did not find that vertical 1-fold symmetry is more salient than horizontal 1-fold symmetry ( $p = .063$ ), but this was mainly due to two participants who apparently focused their attention on the horizontal axis: they performed better for horizontal symmetry than in all other symmetry conditions (removal of these two participants would have yielded  $p = .004$ , with little effect on the other statistical comparisons). Furthermore, vertical 1-fold symmetry was again less salient than 2-fold symmetry – both in the 25%-rectangles condition and in the L condition,  $t(35) = 5.993$ ,  $p < .001$ , and  $t(35) = 5.478$ ,  $p < .001$ , respectively. Crucially, we did not find a difference between the 25%-rectangles condition and the L condition ( $p = .502$ ). The results are depicted in Figure 2.4c.

#### 2.2.4.2 Discussion

In spite of the large number of participants, we did not find a difference between 2-fold symmetries with correlation rectangles and 2-fold symmetries without. This suggests that the negative tendency in experiment 1a was solely due to global noise, and it strengthens our conclusion that correlation rectangles do not play a role in symmetry detection.

Apart from the empirical evidence, there are also theoretical grounds to assume that correlation rectangles add little. Relatively local correlation trapezoids may occur anywhere along either axis, but relatively local correlation rectangles can occur only at the intersection of both axes. The detection process probably uses such relatively local structures as anchors to propagate from, so that the limited presence of relatively local corre-

lation rectangles automatically limits the potential impact of correlation rectangles in general.

All in all, the foregoing suggests that the allegedly special status of orthogonal symmetry axes is not due to correlation rectangles, that is, correlation rectangles do not seem to facilitate 2-fold symmetry detection. The question then is whether orthogonal symmetry axes have a special status at all. This is examined further in the next triplet of experiments, in which we turn to a more general characteristic of multiple symmetry, namely, the relative orientation of the symmetry axes.

## 2.3 Relative orientation of symmetry axes

In experiments 2a, 2b, and 2c, we investigated whether the relative orientation of symmetry axes affects symmetry processing. To get a clear picture of this, the effect of relative orientation has to be isolated from an effect of the number of symmetry axes and, to be sure, also from a potential effect of correlation rectangles. To this end, we combined two different perfect 1-fold symmetries in various relative orientations – in particular, orthogonal (90° relative orientation) and nonorthogonal (45°/135° relative orientation, i.e., one angle between the axes is 45° and the other angle is 135°). Furthermore, because the salience of single and multiple symmetry is known to vary with absolute orientation (Wenderoth & Welsh, 1998b), we used absolute axis orientations of +22.5° and -22.5° with respect to the vertical and the horizontal, yielding four roughly equisalient symmetry axis orientations. As we report next, the three experiments differed regarding stimulus type and regarding the way the 1-fold symmetries were combined.

### 2.3.1 Experiment 2a

In this experiment, we used dot stimuli and we composed 2-fold symmetries by superimposing two different perfect 1-fold symmetries in different relative orientations. This yields 2-fold symmetries without correlation rectangles, and with 50% noise about each axis.

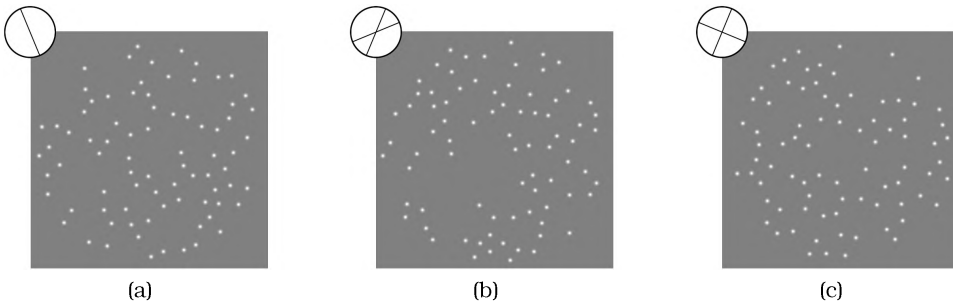


**Figure 2.5.** Examples of the stimuli used in experiment 2a. In the insets, the absolute orientations of the symmetry axes are indicated by straight lines. (a) One-fold symmetry. (b) Nonorthogonal 2-fold symmetry with a relative axis orientation of  $45^\circ/135^\circ$ . (c) Orthogonal 2-fold symmetry with a relative axis orientation of  $90^\circ$ .

### 2.3.1.1 Participants

Twenty-two undergraduate students participated in the experiment. None of them had participated in any of the previous experiments. All had normal or corrected-to-normal vision and received course credits or money for their participation.

### 2.3.1.2 Stimuli

To create 2-fold symmetries, we superimposed two perfect but different 1-fold symmetries of 40 elements each in either orthogonal ( $90^\circ$ ) or nonorthogonal ( $45^\circ/135^\circ$ ) relative orientation. To have approximately equisalient symmetry axes across all conditions, we used absolute axis orientations of  $+22.5^\circ$  and  $-22.5^\circ$  with respect to the vertical and the horizontal.

By way of baseline, we created 1-fold symmetries, in which 40 elements were positioned symmetrically about an axis at one of the four designated absolute orientations while 40 further elements were distributed randomly. By way of catch trials, we constructed random stimuli in which all elements were distributed randomly. Using Matlab, a unique set of stimuli was generated for each participant. Examples are given in Figure 2.5.

### 2.3.1.3 Procedure

As before, and using the same apparatus and settings, participants performed a 2AFC task in which a symmetrical stimulus and a random stimulus were presented in subsequent intervals in a random order. Participants had to indicate which of the two intervals featured symmetry. Responses were recorded using a button box. Prior to the experiment, each participant completed a practice block of 60 trials with feedback given after each trial. Each interval was preceded by a central fixation dot presented for 500 ms. During the intervals, stimuli were flashed for 200 ms. This is longer than in the previous experiments, but increasing the presentation time was necessary to maintain a comparable level of performance, since symmetries with symmetry axes off the four cardinal orientations (vertical, horizontal, left/right oblique) are more difficult to detect. The number of experimental trials totalled 3 [symmetry conditions]  $\times$  4 [axis orientations]  $\times$  50 [measurements] = 600. The experiment was self-paced.

### 2.3.1.4 Results

For the 1-fold symmetries, we did not find a difference in salience between the absolute axis orientations. Therefore, for each condition, we pooled across the absolute axis orientations. Subsequently,  $d'$  values obtained for 1-fold, nonorthogonal, and orthogonal symmetry were compared using paired-samples  $t$ -tests. Nonorthogonal symmetry tended to be more salient than 1-fold symmetry, but this was not significant ( $p = .065$ ). Orthogonal symmetry, however, was significantly more salient than 1-fold symmetry,  $t(21) = 3.694$ ,  $p < .01$ . Crucially, orthogonal symmetry was significantly more salient than nonorthogonal symmetry,  $t(21) = 2.525$ ,  $p < .05$ . The results are depicted in Figure 2.8a.

### 2.3.1.5 Discussion

The results show that 2-fold symmetry is more salient when the axes are orthogonal than when the axes are nonorthogonal. Notice that this effect goes against the bootstrap approach which attributes a positive effect of orthogonality solely to correlation rectangles which, here, were absent.

Apparently, the relative orientation of symmetry axes is an independent factor affecting multiple symmetry perception. To investigate whether the now found effect generalizes across stimulus types, we conducted the next experiment.

### 2.3.2 Experiment 2b

In this experiment, we used dense displays, and we composed 2-fold symmetries by superimposing, again in different relative orientations, two perfect 1-fold symmetries that were confined to different spatial frequency bands. This yields noisy 2-fold symmetries, and the two different luminance distributions ensure the absence of correlation rectangles.

#### 2.3.2.1 Participants

Sixteen undergraduate students participated in the experiment. None of them had participated in any of the previous experiments. All had normal or corrected-to-normal vision and received course credits or money for their participation.

#### 2.3.2.2 Stimuli

All stimuli were constructed by superimposing two images filtered in the spatial frequency (SF) domain (similar filtering techniques were employed by, e.g., Dakin & Herbert, 1998; Julesz & Chang, 1979; Rainville & Kingdom, 1999, 2000). Each image was generated starting from randomly distributed Gaussian luminance ( $\mu=0$ ,  $\sigma=0.125$ ). To obtain a 1-fold symmetrical image, an image half was filled with random luminance and reflected about the vertical. Using Fourier transformation, each image was transformed from the spatial domain into the SF domain. Each Fourier-transformed image then was filtered using an idealized isotropic bandpass filter with a bandwidth of one octave. The filter ( $H$ ) was defined in the SF domain by

$$H = \begin{cases} 1 & \text{if } f_{low} \leq f \leq f_{high} \\ 0 & \text{otherwise} \end{cases}$$

where  $f_{low}$  and  $f_{high}$  were lower and upper cut-off frequencies, respectively. To generate a relatively low SF image, we selected a one-octave band with lower and higher cut-off frequencies of 0.31 cpd (cycles per degree) and 0.62 cpd, respectively. To generate a relatively high SF image, we selected a one-octave band with lower and higher cut-off frequencies of 1.26 cpd and 2.52 cpd, respectively. This implies that the one-octave bands were separated by a gap of also one octave. To create a stimulus, low-SF and high-SF images were transformed back into the spatial domain by means of inverse Fourier transformation. The resulting images were rotated to the desired orientations and then superimposed by averaging their luminances at each pixel position. The resulting intensity distribution was shifted to mean luminance and normalized to 25% root-mean-square contrast.

As in experiment 2a, we used absolute axis orientations of  $+22.5^\circ$  and  $-22.5^\circ$  with respect to the vertical and the horizontal. The 2-fold symmetries were created by combining a near-vertical symmetry in one SF band with a near-horizontal symmetry in the other SF band, with a relative orientation of  $90^\circ$  in the orthogonal condition and  $45^\circ/135^\circ$  in the nonorthogonal condition. By way of two baseline conditions, we constructed stimuli with 1-fold symmetry in either the high-SF band or the low-SF band; in both cases, the complementary SF band contained noise. Catch trials featured stimuli in which both SF bands contained noise. All stimuli were circular with a diameter of about  $10.6^\circ$  of visual angle against a black background. Using Matlab, a unique set of stimuli was generated for each participant. Figure 2.6 gives examples of the stimuli.

### 2.3.2.3 Procedure

We used the same apparatus as in the previous experiments. Participants performed a signal detection (yes/no) task. In each trial, a symmetrical or random pattern was presented and participants had to indicate whether the pattern was symmetrical (irrespective of the number of symmetry axes

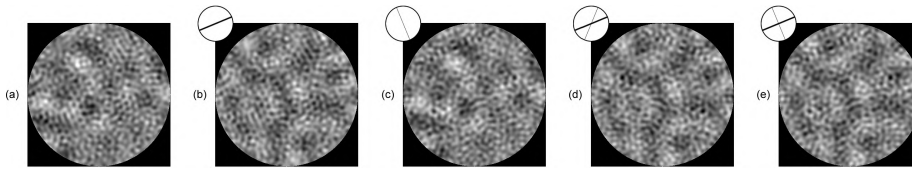


**Figure 2.6.** Examples of the stimuli used in experiment 2b. In the insets, the absolute orientations of the symmetry axes are indicated by straight lines; thick lines refer to the low-SF band and thin lines refer to the high-SF band. (a) Random pattern. (b) One-fold symmetry in the low-SF band. (c) One-fold symmetry in the high-SF band. (d) Two-fold nonorthogonal symmetry. (e) Two-fold orthogonal symmetry. For illustrative purposes, the low-SF and high-SF symmetries in (b) and (c) are the same as the ones that were combined in (d) and (e), respectively. Thus, the only difference between the nonorthogonal symmetry in (d) and the orthogonal symmetry in (e) is the relative orientation between the component symmetry axes.

that might be present) or random. Responses were recorded using a standard keyboard.

The experiment was preceded by 120 practice trials with feedback given after each trial. Each trial started with a central fixation cross presented for 500 ms. Subsequently, the stimulus was presented for 250 ms. Following the response and an inter-trial interval of 100 ms, the next trial commenced automatically. The number of trials totalled 2 [symmetrical/random]  $\times$  4 [symmetry conditions]  $\times$  4 [axis orientations]  $\times$  20 [measurements] = 640. Breaks were given each time after 128 trials.

### 2.3.2.4 Results

Based on the correct scores for symmetrical targets (hits) and error scores for random targets (false alarms),  $d'$  was calculated and was used as a dependent variable in a series of paired-samples  $t$ -tests. Note that, although a yes/no paradigm was used here and 2AFC paradigm was used in the previous experiments, signal detection theory shows a linear relationship between  $d'$  values obtained in these two ways (Wickens, 2002). This allows for a qualitative comparison of effects across experiments, irrespective of the method used.

For the 1-fold symmetries, we did not find a difference in salience between the absolute axis orientations. Therefore, for each condition, we



pooled the absolute axis orientations. In line with Julesz & Chang (1979), we found that the salience of low-SF 1-fold symmetry was higher than the salience of high-SF 1-fold symmetry,  $t(15) = 2.826$ ,  $p < .05$ . Furthermore,  $d'$  for 2-fold symmetry with nonorthogonal axes was higher than  $d'$  for both high-SF 1-fold symmetry,  $t(15) = 4.925$ ,  $p < .001$ , and low-SF 1-fold symmetry,  $t(15) = 2.467$ ,  $p < .05$ . Similarly,  $d'$  for 2-fold symmetry with orthogonal axes was higher than  $d'$  for both high-SF 1-fold symmetry,  $t(15) = 9.542$ ,  $p < .001$ , and low-SF 1-fold symmetry,  $t(15) = 5.85$ ,  $p < .001$ . Crucially, orthogonal symmetry was again more salient than nonorthogonal symmetry,  $t(15) = 5.034$ ,  $p < .001$ . The results are depicted in Figure 2.8b.

### 2.3.2.5 Discussion

Also for this stimulus type, we found that 2-fold symmetry is more salient when the axes are orthogonal than when the axes are nonorthogonal. This demonstrates the robustness of this effect and suggests that it is not a stimulus-dependent artifact but, rather, a general characteristic of symmetry perception. An implication of these results is that the single symmetries constituting multiple symmetry apparently engage in an orientation-dependent interaction. To shed more light on the underlying mechanism, we conducted the following priming experiment in which we investigated the interaction between 1-fold symmetries separated in the time domain (i.e., rather than in the spatial frequency domain).

### 2.3.3 Experiment 2c

The effect revealed in the previous two experiments suggests the involvement of orientation-selective processes in multiple symmetry perception. It is unclear, however, whether this effect stems from the mutual facilitation of orthogonal symmetry axes, or from the mutual impediment of nonorthogonal symmetry axes, or from both. To investigate this, we used a paradigm wherein two symmetries were presented in succession, the first one serving as prime and the second one serving as target. The rationale was that, if orthogonal axes facilitate each other, the detection of a symmetry should be enhanced when it is preceded by an orthogonal prime (i.e.,

a prime whose symmetry axis is orthogonal to the symmetry axis of the target). Likewise, if nonorthogonal axes impede each other, the detection of a symmetry should be hampered when it is preceded by a nonorthogonal prime.

### **2.3.3.1 Participants**

Nineteen undergraduate students participated in the experiment. None of them had participated in the other experiments. All had normal or corrected-to-normal vision and received course credits or money for their participation.

### **2.3.3.2 Stimuli**

Stimuli consisted of spatially filtered Gaussian noise. They resembled the stimuli used in the previous experiment, but they consisted of only a single SF band instead of two. First, the Gaussian noise was transformed into the SF domain using Fourier transformation. An idealized isotropic bandpass filter, defined as in experiment 2b, with lower and higher cut-off frequencies of 1.29 cpd (cycles per degree) and 2.59 cpd, respectively, was used to retain only one octave of spatial frequencies. After inverse Fourier transformation into the spatial domain, the resulting intensity distribution was shifted to mean luminance and normalized to 25% root-mean-square contrast. We again used absolute axis orientations of  $+22.5^\circ$  and  $-22.5^\circ$  with respect to the vertical and the horizontal.

We created 1-fold symmetrical primes and targets, and we created primes and targets containing randomly distributed Gaussian noise. The random targets were used in catch trials, and the random primes were included to establish a baseline against which the priming effect of the symmetrical primes could be measured. All stimuli were circular with a diameter of about  $10^\circ$  of visual angle on a black background. Using Matlab, a unique set of stimuli was generated for each participant.

### 2.3.3.3 Procedure

We used the same apparatus and parameters as before, except for the following. In each trial, a prime (1-fold symmetrical or random) was presented, followed by a target (1-fold symmetrical or random). Participants performed a signal detection (yes/no) task, that is, they had to indicate whether the target was symmetrical or random.

Apart from the random prime condition, there were three symmetrical prime conditions. The crucial conditions were the nonorthogonal condition, in which the relative orientation of the symmetry axes in prime and target was 45°/135°, and the orthogonal condition, in which it was 90°. We also included the 'same' condition, in which the symmetry axes in prime and target had the same orientation. In all conditions, both the prime and the target were masked using a checkerboard pattern. Masking was necessary to remove apparent-motion artifacts which, during pilot experiments, were found to arise particularly when both prime and target were symmetric.

The experiment was preceded by 50 practice trials. Each trial started with a central fixation cross presented for 500 ms. Subsequently, the prime was presented for 500 ms. We chose for a long presentation time to ensure that the participant really detected the symmetry in the prime. The prime was immediately followed by a checkerboard pattern presented for 50 ms and a blank screen lasting for 150 ms. Then, the target was presented for 200 ms, followed by another mask presented for 50 ms. Following the response and an inter-trial interval of 100 ms, the next trial commenced automatically. The time-course of a trial is depicted in Figure 2.7. The number of trials totalled 2 [symmetrical/random prime] x 4 [prime orientations] x 2 [symmetrical/random target] x 4 [target orientations] x 10 [measurements] = 640. Breaks were given each time after 128 trials.

### 2.3.3.4 Results

Again, based on the correct scores for symmetrical targets (hits) and error scores for random targets (false alarms),  $d'$  was calculated. As a measure of the priming effect, we used  $\Delta d'$ , calculated by subtracting  $d'$  on random primes from  $d'$  on symmetrical primes. This measure indicates how much

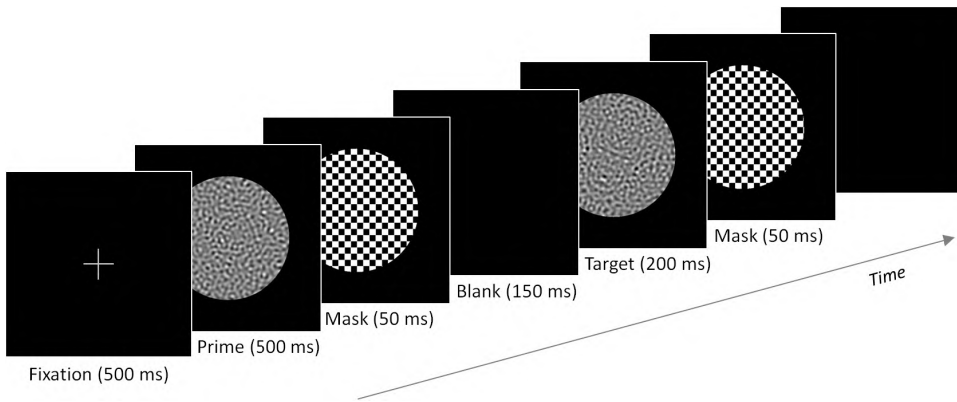


**Figure 2.7.** The time course of a trial in priming experiment 2c. See the procedure of experiment 2c for details.

a symmetric prime facilitates (positive  $\Delta d'$ ) or impedes (negative  $\Delta d'$ ) symmetry detection relative to a random prime. One-sample  $t$ -tests were used to analyze  $\Delta d'$ . In the 'same' condition,  $\Delta d'$  tended to be positive, but this was not significant ( $p = .093$ ). In the orthogonal condition, there was a significant positive priming effect,  $t(18) = 3.326$ ,  $p < .01$ . The latter two conditions did not differ significantly from each other ( $p = .529$ ). Finally, there was significant negative priming effect in the nonorthogonal condition,  $t(18) = 2.631$ ,  $p < .05$ . The results are depicted in Figure 2.8c.

### 2.3.3.5 Discussion

The results reveal a positive priming effect in case prime and target have orthogonal symmetry axes as well as a negative priming effect in case they have nonorthogonal symmetry axes. We also ran a control experiment using a thin (1 px) line as a prime instead of a symmetric pattern. In this control experiment, we found no priming effects in the orthogonal and nonorthogonal conditions, which suggests that the above-mentioned priming effects are indeed inherent to symmetry processing. This, in turn, suggests that the results obtained in the previous two experiments are due to an orientation-dependent interaction between symmetry axes, with both a

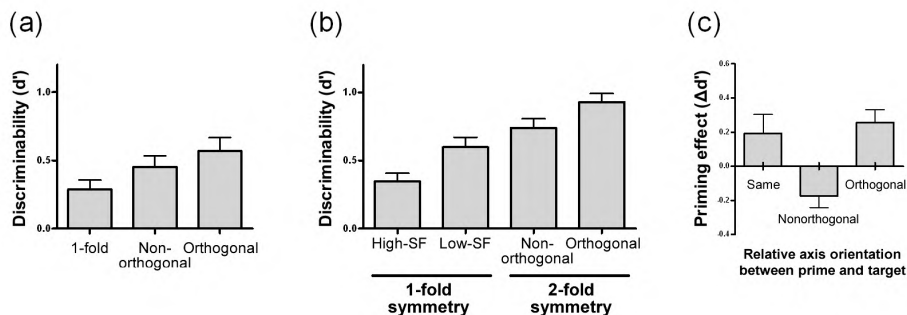


**Figure 2.8.** Results of experiments 2a, 2b, and 2c. Error bars represent 1 SEM. (a) Results of experiment 2a. Nonorthogonal 2-fold symmetry is more salient than 1-fold symmetry but, crucially, less salient than orthogonal 2-fold symmetry. (b) Results of experiment 2b. Low-SF 1-fold symmetry is more salient than high-SF 1-fold symmetry and less salient than both nonorthogonal and orthogonal 2-fold symmetry. Most importantly, orthogonal 2-fold symmetry is more salient than nonorthogonal 2-fold symmetry. (c) Priming effects obtained in experiment 2c. The priming effect was defined by  $\Delta d'$ , calculated by subtracting  $d'$  on random primes from  $d'$  on 1-fold symmetrical primes. The priming effect was not significant, positive, and negative, when the symmetry axes in prime and target had the same orientation, orthogonal orientations, and nonorthogonal orientations, respectively.

mutual facilitation of orthogonal symmetry axes and a mutual impediment of nonorthogonal symmetry axes. As we elaborate in the next section, both effects can be accounted for by a mechanism based on surround inhibition.

## 2.4 General discussion

In experiments 1a, 1b, and 1c, we found no evidence that 2-fold symmetry with correlation rectangles is better detectable than 2-fold symmetry without. Regarding Wagemans et al.; Wagemans et al.'s (1991, 1993) bootstrap model, this does not challenge its primary assumption that correlation trapezoids are the anchors for the detection of symmetry about an axis, but it casts doubts on its secondary assumption that correlation rectangles facilitate the detection of multiple symmetries containing orthogonal symmetry axes.

In experiments 2a, 2b, and 2c, we investigated whether the relative orientation between symmetry axes affects symmetry detection. We found that orthogonal symmetry is consistently more salient than nonorthogonal

symmetry, even when correlation rectangles are absent. In experiment 2c, we also found that detection of a target symmetry is both facilitated by an orthogonal symmetry prime and impeded by a nonorthogonal symmetry prime. As for the computational and algorithmic models outlined in the Introduction, these results do not seem to be consistent with the transformational and bootstrap approaches. That is, the transformational approach predicts no interaction between axes, while the bootstrap approach predicts facilitation in case of orthogonal axes due to a questionable factor (i.e., due to correlation rectangles which we found to be effectless and which, here, were absent). Our results do seem consistent, however, with the holographic approach even though, as we discussed in the Introduction, it predicts only an impeding effect in case of nonorthogonal axes. That is, as we discuss next at the implementational level of description, a neural mechanism that is responsible for inhibition in case of nonorthogonal axes suffices to also yield facilitation in case of orthogonal axes.

Neurally, orientation-dependent interactions between orientation-selective neurons are ubiquitous. It is true that visual neurons are usually involved in the processing of luminance edges, not symmetry axes, but Lee et al. (1998) found a late enhancement of responses in V1 cells of rhesus monkeys when receptive fields were centered at a symmetry axis. Furthermore, symmetrical dot patterns and luminance contours were shown to elicit similar visually evoked potentials if the luminance contours and the symmetry axes are co-oriented (Beh & Latimer, 1997). Moreover, symmetry axes in dot patterns elicit tilt aftereffects comparable to those of lines (Joung et al., 2000; Joung & Latimer, 2003; van der Zwan et al., 1998). In line with this evidence, Gurnsey et al. (1998) suggested that, within the visual system, symmetry axes form subjective contours which are processed in a similar way as luminance contours (see also Sally & Gurnsey, 2001).

The exact link between symmetry processing and orientation processing is still unclear, but our data call for a hopefully fruitful speculation about how known properties of the neural processing of orientation might be related to the interaction between single symmetries in multiple symmetry. To this end, we first go into more detail on orientation selectivity and on spatial filtering models of 1-fold symmetry detection which build on it.

### 2.4.1 Orientation selectivity and spatial filtering

Orientation selectivity is a characteristic of many cortical cells such as simple and complex cells in V1 (Blakemore & Campbell, 1969; Bredfeldt & Ringach, 2002; Valois & Valois, 1988; Hubel & Wiesel, 1968; Shapley et al., 2003), and it also has been shown to persist in post-V1 areas (Vanduffel et al., 2002b). The prevalence of orientation selectivity suggests that it has an important functional role throughout the visual cortex.

Building on this, spatial filtering (SF) models of 1-fold symmetry detection recruit frequency filtering and orientation filtering mechanisms. Most models follow a filter-rectify-filter regime, with the first stage usually being the convolution of the input image by bandpass-filters, followed by a nonlinear operation (e.g., a squaring operation), and then an operation which serves to explicitly detect the symmetry axis or estimate the amount of symmetry (Dakin & Watt, 1994; Gurnsey et al., 1998; Osorio, 1996; Rainville & Kingdom, 1999, 2002). For instance, Gurnsey et al. (1998) presented a model wherein the input image is first convolved with a Gaussian kernel. Then, a nonlinear differencing operation is performed, whereby the squared difference in luminance between symmetrically positioned pixels is calculated for each column in the image. Finally, the output of the differencing operation is convolved with a vertical filter to explicitly detect the symmetry axis. Furthermore, Dakin & Watt (1994) presented a model wherein the input image is first convolved with an elongated difference-of-Gaussians filter. In a second step, a thresholding nonlinear operation yields a number of blobs, which happen to occur predominantly about the symmetry axis in dense stimuli. Finally, the degree of co-alignment between these blobs is taken as a measure of the amount of symmetry. Dakin & Watt's (1994) model is depicted schematically in the shaded box in Figure 2.9.

Because, thus far, SF models addressed only 1-fold symmetry detection, they had no need to implement the fact that a significant number of orientation-sensitive neurons display a bipolar response, also known as surround inhibition, whereby the excitatory peak is flanked by inhibitory troughs (e.g., Gur et al., 2005; Ringach et al., 1997; Shapley et al., 2003). As we argue next, however, the inclusion of surround inhibition allows for

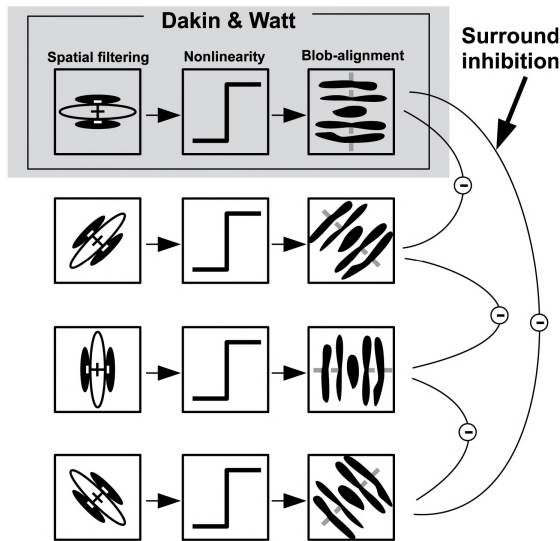


**Figure 2.9.** Extension of Dakin & Watt's (1994) spatial filtering model to include surround inhibition. The shaded box shows the original model (see text and Appendix A for details). The extended model is obtained by concatenating filters for various orientations and then applying inhibitory connections to pairs of filters that are sensitive to nonorthogonal orientations (in this case, 45°/135°).

a plausible extension of these models to multiple symmetry.

## 2.4.2 Implementing surround inhibition

As we show here, adding surround inhibition to existing SF models allows for the accommodation of the interaction effects reported in this paper. This is demonstrated for Dakin & Watt's (1994) model, but the same principle could be applied just as well to Gurnsey et al.'s (1998) and Rainville & Kingdom's (2002) models. Figure 2.9 sketches the extension of Dakin & Watt's (1994) model to multiple symmetry by means of surround inhibition.

To obtain quantitative data, we applied the extended model to the same Gaussian noise stimuli as used in experiment 2b, that is, random stimuli, 1-fold symmetries, and 2-fold symmetries. We used two different spatial frequencies and, for simplicity, four different orientations. Dakin & Watt's symmetry measure was then calculated for each spatial frequency



and each orientation separately, yielding eight symmetry values. Details on the implementation of Dakin & Watt's model are given in Appendix A.

To simulate surround inhibition, the symmetry outputs for each spatial frequency and each orientation were used as activations in a standard interactive activation and competition (IAC) network. An IAC network is an artificial neural network (ANN) consisting of units that are characterized by specific levels of activation and that can have excitatory or inhibitory connections. By way of mutual excitation and inhibition, the levels of activation of the units vary until a state of equilibrium is reached. Since our aim was to give a functional implementation of surround inhibition in symmetry detection, our network featured inhibitory connections for pairs of units representing nonorthogonal symmetry-axis orientations. The strength of the inhibition was given by the inhibition parameter  $\lambda$ . To not make an arbitrary choice regarding this parameter, we included it as an independent variable in the analysis. More details on the ANN are given in Appendix B.

As a rough estimate of how well the model classifies symmetries and random patterns, we calculated signal-to-noise ratios for each class of stimuli and each level of  $\lambda$ . According to its standard definition, we define the signal-to-noise ratio in symmetrical stimuli by

$$\xi_{symmetry} = \frac{\sum signal}{\sum signal + \sum noise}$$

where the term signal refers to the output of the filter that was tuned for the spatial frequency and orientation of the symmetry that was present in the stimulus. Consequently, in 1-fold symmetries, one of the eight filters in our implementation provided the signal, and in 2-fold symmetries, two filters provided the signal. The output of the other filters was considered noise.

Figure 2.10 depicts, for each class of stimuli, the resulting signal-to-noise ratio as a function of the inhibition parameter  $\lambda$ . The graphs reveal two remarkable consequences of surround inhibition. First, for the 1-fold symmetries and for orthogonal symmetry, the signal-to-noise ratio improves with increasing  $\lambda$ . Second, for nonorthogonal symmetry, it also improves initially but then deteriorates for high values of  $\lambda$ . This suggests that our

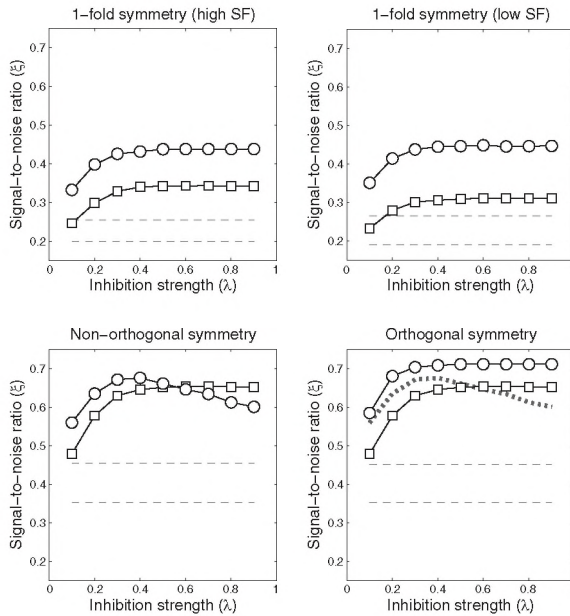


**Figure 2.10.** Signal-to-noise ratios  $\xi$  obtained for symmetrical and random stimuli, indicated by circles and squares, respectively. The dotted lines represent performance in the absence of interaction (inhibition strength  $\lambda = 0$ ), for symmetry (upper dashed line) and random noise (lower dashed line). In the graph on orthogonal symmetry, the signal-to-noise ratio on nonorthogonal symmetry is replotted as a dotted line, showing that the model is consistently more sensitive to orthogonal than to nonorthogonal symmetry, especially for relatively high values of  $\lambda$ .

empirical results can be accounted for by surround inhibition which, for high values of  $\lambda$ , yields both a facilitation in case of orthogonal symmetry and, relative to that, an impediment in case of nonorthogonal symmetry. In other words, it suggests that the special status of orthogonal symmetry is in fact a side-effect of a mechanism which is primarily responsible for mutual inhibition of nonorthogonal orientations.

Notice that ANNs have been used before to detect symmetry in images. For instance, Latimer et al. (1994) showed that ANNs can mimic human anisotropy in the detection of symmetries of various absolute orientations, but their model was restricted in that it pertained to  $6 \times 6$  pixels binary input images. A more versatile model was proposed by Labonté et al. (1993),

wherein symmetry detection was not performed on raw input pixels but rather on features derived from a preliminary grouping stage. Recently, Fukushima & Kikuchi (2006) introduced a complex multi-layer ANN mimicking V1 functionality wherein, similar to our compound model, the first stage involved frequency and orientation-specific spatial filtering of the input image. However, none of these models implemented surround inhibition which, as our empirical results suggest, is crucial to human perception of multiple symmetry. In other words, they cannot account for our finding that orthogonal symmetry is better detectable than nonorthogonal symmetry.

### **2.4.3 Conclusion**

Our study shows that the number of symmetry axes is not the only relevant factor in multiple symmetry perception. Contrary to ideas in the literature, we found no evidence that correlation rectangles facilitate multiple symmetry detection, but we did find evidence that, even in the absence of correlation rectangles, the salience of multiple symmetry is affected by the relative orientation of the symmetry axes. These findings argue against a special status of correlation rectangles in multiple symmetry detection. Rather, they suggest an orientation-dependent interaction between the constituent 1-fold symmetries. By means of a simulation, we demonstrated that surround inhibition might be the neural mechanism underlying our finding that orthogonal symmetry axes are more salient than nonorthogonal symmetry axes.

## 2.5 Appendix A: One-fold symmetry detection model

Our 1-fold symmetry detection model is a slightly modified version of Dakin & Watt's (1994) blob-alignment model. In both models, a stimulus is processed in three stages: a spatial filtering stage, a thresholding stage, and a blob-alignment measurement stage.

First, the image is convolved with an elongated difference-of-Gaussian (DoG) filter oriented orthogonally to the putative symmetry axis. Dakin & Watt used an elongated DoG filter defined by

$$f_s(x, y) = (e^{-y^2/(2s^2)} - \frac{1}{2.23} \cdot e^{-y^2/(2(2.23s)^2)}) \cdot e^{-x^2/2(3s)^2} \quad (2.1)$$

where the space constant  $s$  determines the spatial frequency (SF) sensitivity of the filter. As our stimuli were confined to two SF bands, we used filters at two different spatial scales. Appropriate values for  $s$  were obtained by adjusting the filters' peak SF to roughly match the geometric mean frequencies of the two SF bands.

Second, the convolved image is thresholded to a binary image by setting all luminances in the range  $(\mu - \sigma, \mu + \sigma)$  to 0, and all others to 1, where  $\mu$  is the mean luminance and  $\sigma$  is the standard deviation of the luminance distribution. This yields a number of blobs.

Third, the co-alignment of these blobs along a putative symmetry axis is taken as a measure for the degree of symmetry. This measure is normalized for blob-size and numerosity and it ranges from 0 (totally random) to 1 (perfectly symmetric). Assuming the symmetry axis is located at  $x = 0$ , the alignment measure boils down to

$$A = \frac{1}{M} \cdot \sum_i \exp\left(-\frac{c_i^2}{l_i}\right) \cdot \mu_i \quad (2.2)$$

where  $i$  ranges over the indices of blobs intersecting the symmetry axis,  $M$  is their total mass,  $c_i$  is the abscissa of the centroid of blob  $i$ ,  $l_i$  is its length, and  $\mu_i$  its mass.

This measure differs slightly from Dakin & Watt's measure. As denominator of the argument of the exponential, we chose  $l_i$  instead of  $2l_i^2$ . This gives less weight to the length of the blob, which proved to extract symmetry more reliably in our narrow-band stimuli (Dakin and Watt considered broadband stimuli). A second modification was that we did not take into account blobs in the upper and lower end strips of 30 pixels. The reason is that the filter responds strongly to those parts of the stimulus contour that are approximately tangential to the orientation of the filter (i.e., the parts near both ends of the symmetry axis). Including those parts in our circular stimuli would yield comparatively large blob areas which overemphasize the amount of symmetry in every image, independently of the actually present symmetry (Dakin & Watt considered square-shaped stimuli, for which this artifact does not arise).

In every other respect, we adhered to the model outlined in Dakin & Watt (1994). For each of four different orientations and each of the two scales, the implementation of this model produced a symmetry measure which then served as the external input  $\psi$  to the artificial neural network (see Appendix B).

## 2.6 Appendix B: Artificial neural network dynamics

We derived our artificial neural network from the standard interactive activation and competition (IAC) network (e.g., McClelland & Rumelhart, 1981). We denote the net input and the activation of unit  $i$  at time-cycle  $t$  by  $net_i(t)$  and  $\Omega_i(t)$ , respectively. More specifically, the net input to each unit  $i$  at cycle  $t$  is defined by

$$net_i(t) = \psi_i - \sum_j \lambda \cdot \Omega_j(t)$$

where  $\psi_i$  signifies the external input,  $\lambda \in [0, 1]$  is the inhibitory weight,  $\Omega_j \in [0, 1]$  is the activation of unit  $j$ , while index  $j$  ranges over the units connected to unit  $i$ . The change in activation in unit  $i$ ,  $\Delta\Omega_i$ , is defined by

$$\Delta\Omega_i(t) = (1 - \Omega_i(t)) \cdot net_i(t) - \gamma \cdot \Omega_i(t)$$

for positive net input, and by

$$\Delta\Omega_i(t) = \Omega_i(t) \cdot net_i(t) - \gamma \cdot \Omega_i(t)$$

for negative net input. In both cases,  $\gamma$  is the decay parameter which was empirically set to 0.5. The transfer function of unit  $i$  is defined by

$$\Omega_i(t + 1) = \Omega_i(t) + \tau \cdot \Delta\Omega_i(t)$$

where  $\tau$  is inversely proportional to the temporal resolution of the implementation. The choice of  $\tau$  is not trivial. The theoretical IAC network is a time-continuous system but its implementation is discrete, and artifacts may arise from the fact that the activation of a unit changes in discrete steps. In particular, it can fall out of the defined range ( $\Omega \in [0, 1]$ ). Setting  $\tau = 0.01$  proved to give sufficient temporal resolution to prevent this artifact.

Because the transfer function is recursive, each unit was given an initial activation value of zero (i.e.,  $\forall i : \Omega_i(0) = 0$ ). With respect to the number of cycles, we posed no absolute limit. Rather, a simulation terminated upon

reaching equilibrium. We operationalized equilibrium as being reached when  $\sum |\Delta\Omega_i(t)| < 10^{-5}$ .

## CHAPTER 3

---

### Detection of (anti)symmetry and (anti)repetition: Perceptual mechanisms versus cognitive strategies

---

---

This chapter has been adapted from:  
van der Helm, P. A., & Treder, M. S. (2009). Detection of (anti)symmetry and (anti)repetition:  
Perceptual mechanisms versus cognitive strategies. *Vision Research*, 49, 2754–2763.





Symmetry and repetition are recognized as cues in perceptual organization, but there is disagreement on whether they are detected automatically. This disagreement is resolved by noting that some studies mixed up shape regularities and shape antiregularities (i.e., symmetries and repetitions with mismatches in contour curvature polarity). The results of two experiments indicate that a task-irrelevant regularity is automatically picked up by the visual system, whereas a task-irrelevant antiregularity is not. This suggests that detection of regularities is part of the visual system's intrinsic encoding, whereas detection of antiregularities requires higher cognitive strategies involving selective attention.

### 3.1 Introduction

Detection of regularities such as symmetry and repetition is believed to be an integral part of the perceptual organization process that is applied to any visual input (cf. Tyler, 1994; van der Helm & Leeuwenberg, 1996; Wagemans, 1995). These regularities are therefore said to be visual regularities, that is, regularities the visual system is sensitive to. Pascal (1658/1950) and Mach (1886) already pointed this out, and later, the Gestaltists (Koffka, 1935; Köhler, 1920; Wertheimer, 1912, 1923) put symmetry and repetition forward as relevant cues in the perceptual grouping of stimulus elements into perceived objects. That is, as sustained by Corbalis & Roldan (1974) and Treder & van der Helm (2007), symmetry seems to be a cue for the presence of one object, and repetition seems to be a cue for the presence of multiple objects. Relatively few empirical studies have been devoted to repetition, but symmetry has indeed been shown to play a relevant role in issues such as object recognition (e.g., Pashler, 1990; Vetter et al., 1994), figure-ground segregation (e.g., Driver et al., 1992; Leeuwenberg & Buffart, 1984), and amodal completion (e.g., Kanizsa, 1985; van Lier et al., 1995).

The foregoing suggests that detection of symmetry and repetition is part of the visual system's intrinsic encoding of stimuli. That is, it suggests



**Figure 3.1.** Regularity and antiregularity in two 2-D shapes. (a) Symmetry: the facing sides of the shapes are symmetrical. (b) Repetition: the right-facing sides of the shapes are identical. (c) Antisymmetry: the right-facing sides of the shapes have opposite curvature polarities (i.e., convexities in one side correspond to concavities in the other side) and opposite contrast polarities. (d) Antirepetition: the facing sides of the shapes have opposite curvature polarities and opposite contrast polarities.

that detection of symmetry and repetition occurs automatically, without requiring selective attention to match stimulus parts. This point, however, became the main issue in a debate in which Baylis & Driver (1995) argued that detection of repetition does require selective attention, while Koning & Wagemans (2009) argued that it does not. The latter study was also a reaction to Bertamini et al. (1997) who, although they did not use the terms repetition and selective attention, drew basically the same conclusion as Baylis & Driver did. Resolving this issue is relevant because, as indicated above, it touches upon the very essence of what the perceptual organization process is believed to involve. Also in neuroscience, for instance, there is no consensus about whether or not perceptual organization requires attention (see, e.g., Lamme & Roelfsema, 2000, versus Gray, 1999).

In this article, we argue that Baylis & Driver and Bertamini et al. drew the wrong conclusion for the right reasons, while Koning & Wagemans drew the right conclusion for the wrong reasons. These studies investigated detection of regularity in designated sides of 2-D shapes, closed contours, and projections of slanted 3-D objects, respectively, and we argue that they mixed up perfect regularities and regularities with mismatches in contour curvature polarity. This may be explicated as follows.

Koning & Wagemans looked at symmetry and at what they called repetition but what we call antirepetition (see also Csathó et al., 2003). These features are, in terms of 2-D shapes, shown in Figure 3.1a and Figure 3.1d. Bertamini et al. also looked at only these two features, but they were careful enough to use the fairly neutral terms *reflected contours* and

translated contours. At first sight, it may indeed seem just a matter of terminology, but as we argue in this article, it is much more than that. For instance, one might think that, in Figure 3.1d, the facing sides of the two shapes are identical and therefore exhibit repetition, but this is not the case. These facing sides have opposite contrast polarities at the image level, and currently more relevant, they have opposite curvature polarities (i.e., convexities in one side correspond to concavities in the other side) at the object level, that is, at the level of the perceived shapes. This is why we call it a case of antirepetition or, more generally, a case of antiregularity. Hence, we would say that Koning & Wagemans' and Bertamini et al.'s conclusions, though different, both applied to antirepetition and not, as they suggested, to repetition.

Notice that, in general, stimulus elements can be said to have values in various dimensions (e.g., position and colour), and that we define antiregularity as a form of perturbed regularity in which corresponding elements have opposite values in some dimension (which may imply that the stimulus remains symmetrical in other dimensions). For instance, as we return to in the General discussion, if corresponding dots in an otherwise perfectly symmetrical dot pattern have opposite contrast polarities with respect to the background, then the stimulus is said to exhibit antisymmetry. Likewise, as indicated above, we also speak of antiregularity if corresponding contour elements have opposite curvature polarities.

Be that as it may, to get more clarity on the issue above, we performed experiments using a stimulus manipulation similar to the one introduced by Bertamini et al. and elaborated by Koning & Wagemans (the details of this manipulation are given below). Crucially, however, we added a condition involving what everybody would call repetition (see Figure 3.1b), and to complete the design, we also added a condition involving what we call antisymmetry (defined analogously to antirepetition; see Figure 3.1c). Using another stimulus manipulation (see also below), Baylis & Driver also considered these four stimulus conditions, but they pooled symmetry and antisymmetry under the term symmetry, and they pooled repetition and antirepetition under the term repetition. As we report in this article, however, we found clear qualitative differences between regularity and antiregularity, leading to fundamentally different conclusions than those three studies

drew.

Baylis & Driver concluded that selective attention is involved in the detection of what they called repetition; as said, Bertamini et al. concluded the same, albeit in different words. This conclusion, however, applied to what we call antirepetition, and we found that it does not apply to what everybody would call repetition. Furthermore, Koning & Wagemans concluded that detection of what they called repetition is part of the visual system's intrinsic encoding. Also this conclusion, however, applied to what we call antirepetition, and we found that it only applies to what everybody would call repetition.

To be clear, the authors of those three studies were well aware of the occurrence of opposite curvature polarities in their stimuli. They seemed to argue, however, that these curvature polarities are opposite only at the object level and that, at the image level, one can yet speak of symmetry and repetition (the mismatched contrast polarities in case of 2-D shapes and 3-D objects seem to have been ignored altogether). They further seemed to argue that one should frame perceptual questions in terms of the effect of image properties on the perceptual organization process which, after all, transforms images into perceived objects. This argument is only partly true, however. The perceptual organization process is not a uni-directional bottom-up process from images to objects but is a highly complex and combinatorial process which, for a given image, seems to search for the best-fitting object. This idea stems from the early 20th century Gestaltists (Koffka, 1935; Köhler, 1920; Wertheimer, 1912, 1923) and is nowadays commonly accepted in both cognitive science and neuroscience (see, e.g., Ehrenstein et al., 2003; Gray, 1999).

The foregoing implies that not only image properties but also properties of candidate objects are relevant to the perceptual organization process and that, therefore, such properties should also be taken into account in empirical designs and analyses (i.e., not just afterwards when discussing the data; see also Koning & van Lier, 2003, 2004; Koning & Wagemans, 2009, for convincing evidence that object-level properties may overrule image-level properties). This holds particularly for the kind of experiments considered here. As said, those three studies investigated detection of regularity in designated sides of 2-D shapes, closed contours, and 3-D objects,

respectively. Here, designated means that, for each regularity separately, the participants knew not only which regularity they had to look for but also in which two sides they had to look for this regularity. Notice, however, that participants respond on the basis of what they perceive, that is, on the basis of the perceived objects with all their object-level properties. It is therefore plausible that object-level properties influence their responses. For instance, notice that, in Figure 3.1, the antiregularities yield qualitatively different percepts than those yielded by the regularities.

The foregoing also reveals another methodological problem. That is, in order to perform the task, participants invoke selective attention to focus on the task-relevant sides of the objects they perceive (cf. Ahissar & Hochstein, 2004). This means that it is hard to claim that detection of a feature in the task-relevant sides does or does not require selective attention (which was the question to begin with). Therefore, we proceeded as follows.

## 3.2 Experiment 1

Considering the consistency of the data across those three studies, the stimulus type does not seem decisive, and just as Baylis & Driver, we chose to use stimuli consisting of 2-D shapes. Furthermore, as said, we considered a complete design with the four (anti)regularity conditions depicted schematically in Figure 3.1. These conditions were also considered by Baylis & Driver, but they did not manipulate the task-irrelevant sides, whereas we did – in a way similar to what Bertamini et al. and Koning & Wagemans did, but they did not consider a complete design. To be more specific, Baylis & Driver used only straight task-irrelevant sides (as in Figure 3.1), whereas we used random and congruent task-irrelevant sides (see Figure 3.2). Here, congruent means that the task-irrelevant sides exhibited the same kind of (anti)regularity as the task-relevant sides did. The rationale for this manipulation is as follows (see the General discussion for a theoretical underpinning).

In general, if the visual system is sensitive to a task-relevant feature, then the detection of this feature is bound to be facilitated by the pres-

ence of a congruent task-irrelevant feature (just as, in multiple symmetry, detection of a task-relevant axis is facilitated by the presence of the other axes; Nucci & Wagemans, 2007; Palmer & Hemenway, 1978; Royer, 1981; van der Vloed, 2005; Wenderoth & Welsh, 1998b). Hence, in our stimuli, if a congruent task-irrelevant (anti)regularity yields a facilitating effect (compared to random task-irrelevant sides), then this can be taken as evidence that this task-irrelevant (anti)regularity is detected unconsciously, that is, as part of the visual system's intrinsic encoding and without requiring selective attention.

Notice that, unlike in those other three studies, this approach circumvents the methodological problem mentioned at the end of the Introduction – even though, to participants, there were no differences in procedure and task (in both their and our experiments, the regularity conditions were blocked and participants had to detect "same" or "reflected" relationships between designated task-relevant stimulus sides). That is, those three studies were interested in quantitative differences in detection speed and detection accuracy between the (anti)regularities in the task-relevant sides, and participants were aware that this was at stake. Participants in our experiments also thought that this was at stake, but our interest actually was the qualitative question of whether or not they unconsciously benefited from the congruent (anti)regularities in the task-irrelevant sides.

The latter is therefore also the question our statistical analyses focus on. That is, unlike in those three studies, our analyses do not elaborate on quantitative differences between the four (anti)regularities – partly because our stimuli are not suited to address this quantitative question (which requires, for instance, another control of the distances between task-relevant sides and between task-irrelevant sides), and partly because Baylis & Driver already did a good job in this respect (they found, in our terminology, that symmetry is better detectable than repetition, and that both are better detectable than the two antiregularities; see also our General discussion). Two further differences are worth mentioning. Those three studies looked at (anti)regularity in one and two objects (we return to this in the General discussion), whereas we looked at (anti)regularity in two objects only. Furthermore, for symmetry and antirepetition in two objects, Koning & Wagemans found quantitative but not qualitative differ-

ences between facing and nonfacing task-relevant sides, and we chose to use facing task-relevant sides only.

### 3.2.1 Method

#### 3.2.1.1 Participants

Twenty-five undergraduate students participated in the experiment. They had normal or corrected-to-normal vision and received course credits for their participation.

#### 3.2.1.2 Stimuli

Every stimulus consisted of two black hard-edge shapes on a white background (see Figure 3.2). The luminance of the black and the white areas amounted to  $0.33 \text{ cd/m}^2$  and  $69.50 \text{ cd/m}^2$ , respectively. Each shape was created by filling in a closed contour consisting of two horizontal straight lines connected by two vertical curves. Each curve consisted of five segments that were specified each by the cubic Bézier function

$$B(t) = (1 - t)^3 \cdot P_0 + 3 \cdot t \cdot (1 - t)^2 \cdot P_1 + 3 \cdot t^2 \cdot (1 - t) \cdot P_2 + t^3 \cdot P_3$$

with  $t \in [0, 1]$ , and with control points  $P_1$ ,  $P_2$ ,  $P_3$ , and  $P_4$ . The curves had  $G^0$  continuity, that is, adjacent Bézier segments were connected but did not share a common tangent at the connection point. To avoid very sharp curvatures in the curves, we maintained a minimum vertical distance of  $0.44^\circ$  visual angle (30 px) between both ends of a segment. Each curve was confined to a strip of  $2^\circ$  (80 px) width and  $9.86^\circ$  (400 px) height. The central block between the strips for the left-hand and right-hand curves had a width of  $1.29^\circ$  (50 px). The two shapes were separated by a gap of  $2.57^\circ$  (100 px) width.

We considered four kinds of (anti)regularity, namely, symmetry, repetition, antisymmetry, and antirepetition. In case of symmetry and antisymmetry, corresponding curves were reflected, and in case of repetition and antirepetition, they were translated. For each kind of (anti)regularity, there were two task-relevant sides and two task-irrelevant sides. For symmetry



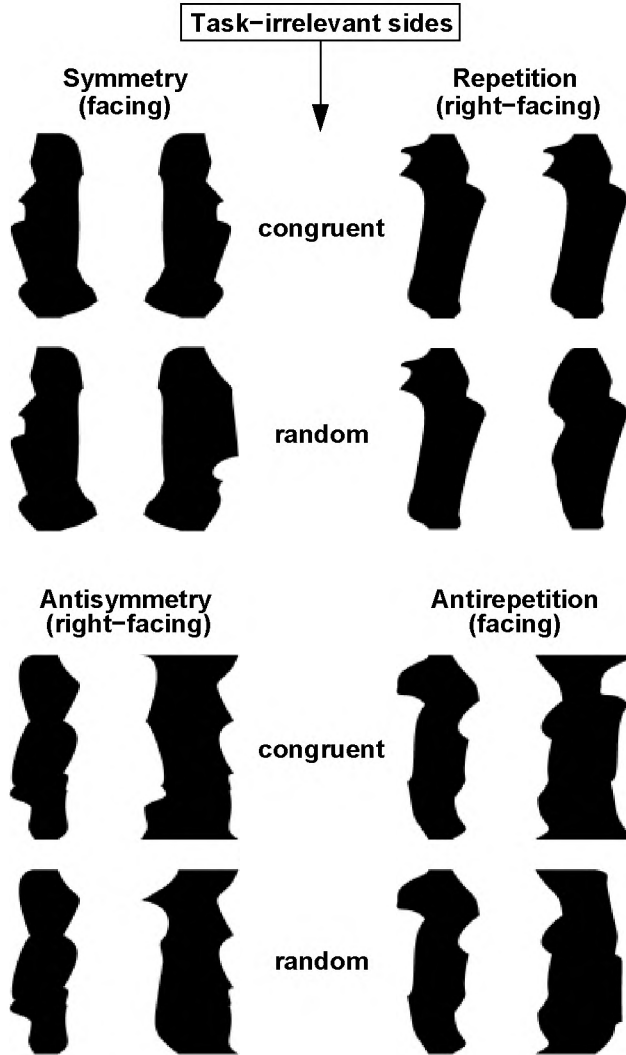


**Figure 3.2.** Experimental conditions in Experiment 1. Participants had to discriminate random from "same" or "reflected" stimulus sides which were indicated as being relevant to the task (the facing sides for symmetry and antirepetition, and the right-facing or left-facing sides for repetition and antisymmetry). To get an optimal assessment of whether the visual system is sensitive to an (anti)regularity, task-irrelevant sides either were random or congruent, where congruent means that they exhibited the same kind of (anti)regularity as the task-relevant sides. This way, we in fact probed whether participants unconsciously picked up the task-irrelevant (anti)regularity (see our rationale in the text).

and antirepetition, the facing sides were task-relevant and the nonfacing sides were task-irrelevant. For repetition and antisymmetry, either the right-facing or the left-facing sides were task-relevant and the other sides were task-irrelevant.

For each kind of (anti)regularity, we considered four subconditions. First, the two crucial subconditions in which the task-relevant sides exhibited the (anti)regularity while the task-irrelevant sides were either random or congruent, that is, exhibited the same kind of (anti)regularity as the task-relevant sides (see Figure 3.2). Second, two sorts of catch trials in which the task-relevant sides were random while the task-irrelevant sides either exhibited the (anti)regularity or were random. For each participant, a set of stimuli was randomly generated using custom MATLAB routines.

### 3.2.1.3 Procedure

A chinrest was used to ensure participants had a constant viewing distance of 60 cm, seated in front of a 19" monitor with a 100 Hz refresh rate and a resolution of 1280 x 1024 px. To prevent tearing artifacts, stimulus presentation was time-locked with the screen's vertical sync. Responses were recorded via a button box which allowed reaction times to be measured with a precision of 1 ms. Participants had to detect whether two designated task-relevant sides, which depended on the kind of (anti)regularity, were the same or reflected (they were not informed about our distinction between regularity and antiregularity). They were instructed to respond as quickly as possible, by pressing a "same" or "reflected" key with their dominant hand when they had detected such a relationship; otherwise, they had to press a "different" key with their nondominant hand.

The experiment was split into four blocks dedicated each to one of the four kinds of (anti)regularity. The order of the blocks was randomized across participants. At the beginning of each block, participants were informed about the relationship to be detected (same or reflected) and they were informed about which sides were task-relevant (by means of a written instruction on the screen, along with sample stimuli in which the two relevant sides in the current block were given by thick red lines). As said, for symmetry and antirepetition, the task-relevant sides were the facing

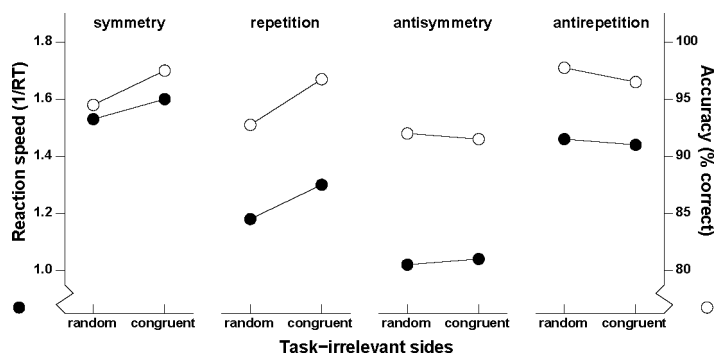


**Figure 3.3.** Results of Experiment 1. The objective was not to investigate quantitative differences between the (anti)regularities but to investigate, for each of them separately, the qualitative question of whether its detection in the task-relevant sides is facilitated by a congruent (anti)regularity in the task-irrelevant sides. In terms of both speed (one divided by reaction time [RT] in seconds) and accuracy (percentage correct), congruent task-irrelevant sides yielded significant facilitating effects for symmetry and repetition, and no significant effects for antisymmetry and antirepetition (see also Table 3.1).

sides. For repetition and antisymmetry, the task-relevant sides (left-facing or right-facing) were counterbalanced across participants.

Each block started with a practice phase of 32 trials, followed by an experimental phase of 120 trials. Each trial commenced with a central fixation dot presented for 600 ms. Following a blank screen lasting for 100 ms, the stimulus appeared and remained until a button was pressed. Auditory feedback was given if the response was wrong. The experiment was self-paced. In total, the experiment comprised 4 [(anti)regularities] x 4 [subconditions] x 30 [stimuli] = 480 experimental trials.

### 3.2.2 Results

Just as in the three studies we criticize, the catch trials merely served to keep participants focused on the task and were not analyzed further. Furthermore, all trials yielding a reaction time (RT) of less than 200 ms were removed. Before analysis, reaction time was turned into reaction speed by the reciprocal transformation  $1/RT$ . The motivation was that reaction time distributions are skewed and that the reciprocal transformation yields more symmetrical distributions (as required for the application of most sta-

tistical models). For the speed analysis, outliers in each subcondition (i.e., values more than  $2.5\sigma$  off mean) were removed. In addition to speed, we also investigated the effects of the experimental manipulations on accuracy in terms of percentage correct. As mentioned, for repetition and antisymmetry, left-facing and right-facing versions were balanced across participants. For the statistical tests, we pooled the data from these two groups because they did not differ significantly in terms of overall speed ( $p = .274$ ) and accuracy ( $p = .63$ ).

First, the data were analysed in  $4 \times 2$  repeated measures ANOVAs. The first factor was the regularity in the task-relevant sides, comprising four levels (symmetry, repetition, antisymmetry, and antirepetition). The second factor was the congruency of the task-irrelevant sides, comprising two levels (congruent and random). For speed, we found main effects of both regularity and congruency,  $F(3, 22) = 31.116$ ,  $p < .001$ , and  $F(1, 24) = 39.857$ ,  $p < .001$ , respectively. The interaction was also significant,  $F(3, 22) = 10.551$ ,  $p < .001$ . For accuracy, we also found main effects of both regularity and congruency,  $F(3, 22) = 7.345$ ,  $p < .001$ , and  $F(1, 24) = 5.18$ ,  $p < .05$ , respectively. The interaction was also significant,  $F(3, 22) = 8.51$ ,  $p < .001$ .

Second, we used a-priori t-tests to investigate, for each (anti)regularity separately, the effect of congruency. For symmetry and repetition, speed was significantly higher in the congruent condition compared to the random condition,  $t(24) = 4.617$ ,  $p < .001$ , and  $t(24) = 7.005$ ,  $p < .001$ , respectively. For antisymmetry and antirepetition, we did not find significant differences ( $p = .279$  and  $p = .399$ , respectively). Furthermore, for symmetry and repetition, also accuracy was significantly higher in the congruent condition compared to the random condition,  $t(24) = 2.115$ ,  $p < .05$ , and  $t(24) = 3.372$ ,  $p < .01$ , respectively. For antisymmetry and antirepetition, we did not find significant differences ( $p = .638$  and  $p = .076$ , respectively). Hence, for symmetry and repetition but not for antisymmetry and antirepetition, participants responded both faster and more accurately when the task-irrelevant sides were congruent (see Table 3.1 and Figure 3.3).

Regularity	Irrelevant sides	RT (ms)	Speed(1/RT)			Accuracy (%correct)		
		Mean	Mean	SEM	$p <$	Mean	SEM	$p <$
Symmetry	random	653.6	1.530	.057		94.5	1.3	
	congruent	624.5	1.601	.055	.001	97.5	.6	.05
Repetition	random	846.4	1.182	.040		92.8	1.1	
	congruent	771.0	1.297	.046	.001	96.8	.6	.01
Antisymmetry	random	884.9	1.015	.054		92.1	1.7	
	congruent	961.6	1.040	.064	.279	91.5	2.5	.638
Antirepetition	random	685.6	1.459	.064		97.7	.6	
	congruent	694.0	1.441	.053	.399	96.4	.7	.076

**Table 3.1.** Results of Experiment 1.

### 3.2.3 Discussion

The significant main effects and interactions we found for regularity and congruency indicate that these factors are perceptually relevant. As said, however, for each (anti)regularity separately, we were interested mainly in whether or not congruent task-irrelevant sides have a facilitating effect on its detectability in the task-relevant sides. We found that a task-irrelevant regularity indeed facilitates the detection of a congruent feature in the task-relevant sides, but that a task-irrelevant antiregularity does not.

This indicates that regularity, even though it is task-irrelevant, is yet picked up by the visual system, whereas antiregularity is not. Hence, it suggests that detection of regularity is part of the visual system's intrinsic encoding, whereas detection of antiregularity is not. It suggests further that detection of antiregularity requires higher cognitive strategies involving selective attention (we return to this in the General discussion).

Considering that the task-irrelevant parts in symmetry gave rise to a facilitating effect even though they were the most eccentric parts, the absence of such an effect for antisymmetry and antirepetition cannot be attributed to the distances between the task-irrelevant parts. Yet, the reflection axes for task-irrelevant sides and task-relevant sides coincide in symmetry but not in antisymmetry. Similarly, the translation distances between task-irrelevant sides and task-relevant sides are equal in repetition but not in antirepetition. One might argue that this in itself could

explain the absence of an effect for antisymmetry and antirepetition. To control for this, we conducted the following experiment.

## 3.3 Experiment 2

### 3.3.1 Method

Unless stated otherwise, the method was identical to the method in Experiment 1.

#### 3.3.1.1 Participants

Thirty-one undergraduate students participated in the experiment. They had normal or corrected-to-normal vision and received course credits for their participation. None of them had participated in Experiment 1.

#### 3.3.1.2 Stimuli

The stimuli were identical to the stimuli used in Experiment 1, except that the widths of stimulus parts were modified to ensure that the distance between the reflection axes for the task-relevant and task-irrelevant sides was equal in symmetry and antisymmetry (see Figure 3.4). Likewise, the modification ensured that the difference in translation distance for task-relevant and task-irrelevant sides was equal for repetition and antirepetition. To this end, the width of the left-hand and right-hand strips was decreased to  $1.54^\circ$  (60 px). Furthermore, for symmetry and repetition, the width of the central block was decreased to zero in the left-hand shape (so that the end points of the contour curves join) and was increased to  $3.09^\circ$  (120 px) in the right-hand shape. For antisymmetry and antirepetition, the width of the central block in both shapes was decreased to zero.

### 3.3.2 Results

First, under the same conditions as in Experiment 1, the data were analysed in  $4 \times 2$  repeated measures ANOVAs. For speed, we found a main effect of regularity,  $F(3, 28) = 21.498$ ,  $p < .001$ . There was no main effect of

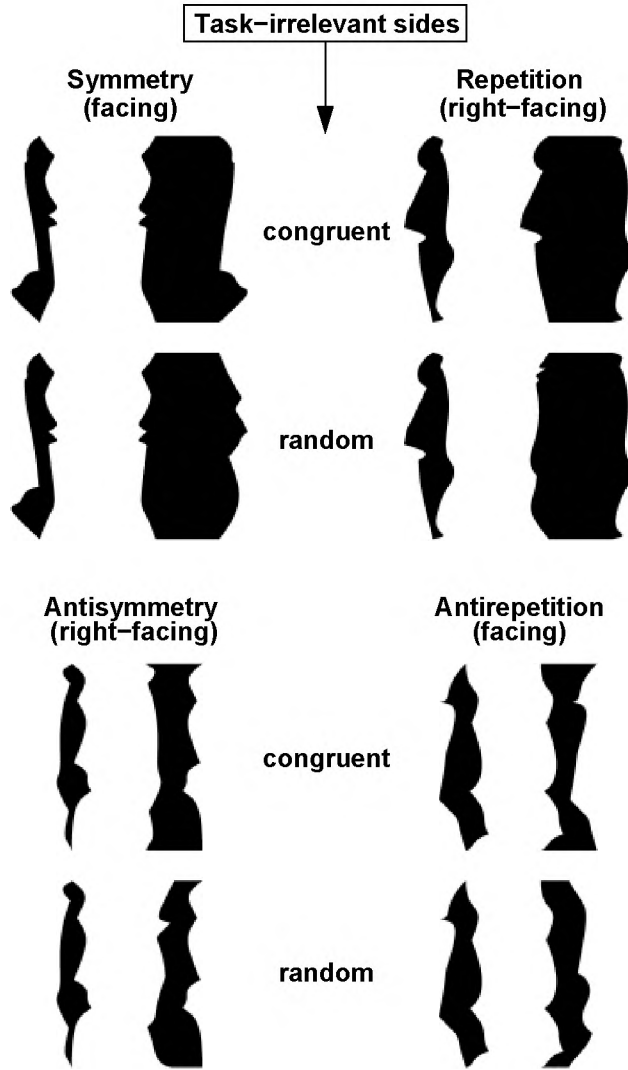


**Figure 3.4.** Experimental conditions in Experiment 2. The design was the same as in Experiment 1, but this time, the widths of stimulus parts were modified to ensure that, for symmetry and antisymmetry, the distance between the reflection axes for the task-relevant and task-irrelevant sides was equal, and that, for repetition and antirepetition, the difference in translation distance for the task-relevant and task-irrelevant sides was equal.

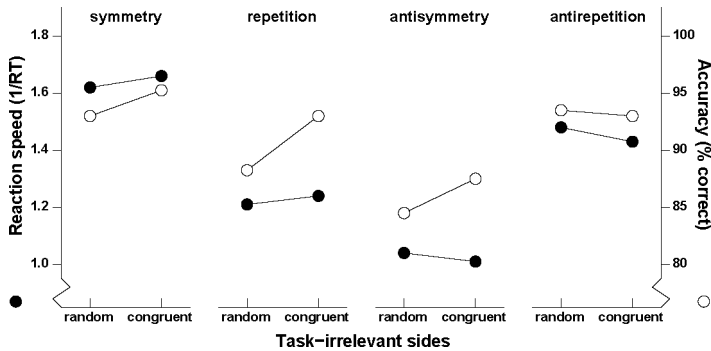


**Figure 3.5.** Results of Experiment 2. In terms of both speed (one divided by reaction time [RT] in seconds) and accuracy (percentage correct), congruent task-irrelevant sides yielded significant facilitating effects for symmetry and repetition. There were no significant effects for antisymmetry and, only in terms of speed, a significant but negative effect for antirepetition (see also Table 3.2).

congruency ( $p = .842$ ), but interaction was significant,  $F(3, 28) = 6.616$ ,  $p < .01$ . For accuracy, we found main effects of both regularity and congruency,  $F(3, 28) = 6.262$ ,  $p < .01$ , and  $F(1, 30) = 9.261$ ,  $p < .01$ , respectively. The interaction was also significant,  $F(3, 28) = 3.393$ ,  $p < .05$ .

Second, we again used a-priori t-tests to investigate the effect of congruency for each (anti)regularity separately. For symmetry and repetition, speed was significantly higher in the congruent condition compared to the random condition,  $t(30) = 2.521$ ,  $p < .05$ , and  $t(30) = 2.221$ ,  $p < .05$ , respectively. For antisymmetry, there was no significant effect of congruency ( $p = .317$ ). For antirepetition, there was a significant effect of congruency,  $t(30) = 3.2$ ,  $p < .01$ , but compared to symmetry and repetition, it was in the opposite direction (i.e., participants responded faster for random task-irrelevant contours). Furthermore, for symmetry and repetition, also accuracy was significantly higher in the congruent condition compared to the random condition,  $t(30) = 2.227$ ,  $p < .05$ , and  $t(30) = 3.529$ ,  $p < .001$ , respectively. For antisymmetry and antirepetition, there were no significant differences ( $p = .130$  and  $p = .580$ , respectively). Hence, again, for symmetry and repetition but not for antisymmetry and antirepetition, participants responded both faster and more accurately when the task-irrelevant sides were congruent (see Table 3.2 and Figure 3.5).



Regularity	Irrelevant sides	RT (ms)	Speed(1/RT)			Accuracy (%correct)		
		Mean	Mean	SEM	$p <$	Mean	SEM	$p <$
Symmetry	random	617.6	1.620	.062		93.0	.9	
	congruent	600.8	1.665	.062	.05	95.3	.9	.05
Repetition	random	826.4	1.210	.053		88.2	2.5	
	congruent	803.4	1.245	.051	.05	93.1	2.1	.001
Antisymmetry	random	958.8	1.043	.097		84.6	2.4	
	congruent	993.6	1.006	.075	.317	87.6	2.6	.130
Antirepetition	random	674.4	1.483	.062		93.6	1.3	
	congruent	699.3	1.430	.059	.01	93.1	1.3	.580

**Table 3.2.** Results of Experiment 2.

### 3.3.3 Discussion

As said, our stimuli were designed specifically to investigate, for each (anti)regularity separately, the qualitative question of whether or not congruent task-irrelevant sides have a facilitating effect on its detectability in the task-relevant sides. This time, we perturbed the global regularity in the regularity conditions, to make it harder to include the task-irrelevant sides. Yet, basically, we found the same pattern of results as in Experiment 1. We again found a facilitating effect in case of symmetry and repetition and not in case of antisymmetry and antirepetition. This strengthens the idea that detection of regularity is part of the visual system's intrinsic encoding, whereas detection of antiregularity is not.

Notice that, by the rationale given earlier, only a positive effect of congruency can be taken as evidence that the visual system is sensitive to the (anti)regularity at hand. Hence, the negative effect of congruency on speed we now found for antirepetition cannot be taken as such evidence (also notice that negative congruency effects were found neither in Experiment 1 nor by Koning & Wagemans, 2009). We think that this negative congruency effect, just as the lack of further effects of congruency for antiregularities, is due to a higher cognitive strategy using selective attention to match stimulus parts. In the next section, we go into more detail on such higher cognitive strategies, but we think that this negative congru-

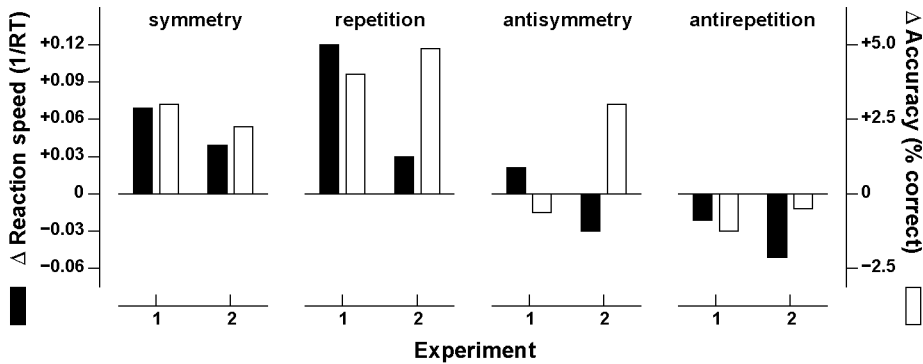


**Figure 3.6.** Summary of the results of Experiments 1 and 2, in terms of congruency effects (participants’ performance in case of congruent task-irrelevant sides minus their performance in case of random task-irrelevant sides). For symmetry and repetition, all congruency effects are significant positive effects, whereas for antisymmetry and antirepetition, all congruency effects are non-significant except for one negative effect (see also Tables 3.1 and 3.2).

ency effect is to be attributed to the small width of the stimuli involved (see Figure 3.4). Due to this small width, participants are faced with two nearby exemplars of what they are looking for, which may slow down such a higher cognitive strategy.

### 3.4 General discussion

The results of our experiments confirm the relevance of the distinction between regularity and antiregularity: a task-irrelevant regularity facilitates the detection of a congruent feature, whereas a task-irrelevant antiregularity does not. In Figure 3.6, we summarized our results in terms of congruency effects as given by participants’ performance in case of congruent task-irrelevant sides minus their performance in case of random task-irrelevant sides. This figure shows a clear qualitative difference between regularities and antiregularities: for symmetry and repetition, all congruency effects are significant positive effects, whereas for antisymmetry and antirepetition, all congruency effects are non-significant except for one negative effect. This suggests that detection of symmetry and repetition is

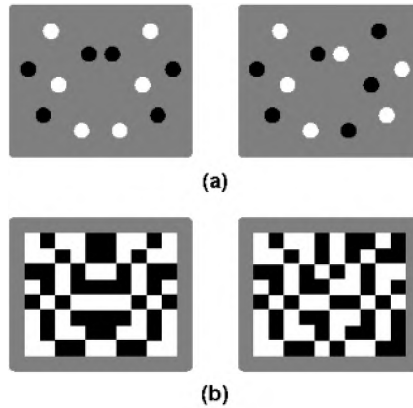


**Figure 3.7.** Symmetry and antisymmetry in (a) dot patterns and (b) checkerboard patterns. In both cases, the antisymmetries arise because symmetrically positioned elements have opposite contrast polarities. In checkerboard patterns, the antisymmetry is detected less easily than in dot patterns (see text for an explanation).

part of the visual system's automatic encoding of stimuli, whereas detection of antisymmetry and antirepetition is not. In other words, our results suggest that symmetry and repetition are visual regularities, whereas antisymmetry and antirepetition are not.

Our finding agrees with Mancini et al.'s (2005) finding for an entirely different stimulus type, as follows. Saarinen & Levi (2000), Tyler & Hardage (1996), Wenderoth (1996), and Zhang & Gerbino (1992) investigated antisymmetry in stimuli consisting of separate elements (dots or blobs), that is, symmetry in which corresponding elements had opposite contrast polarities (see Figure 3.7a). They found merely a minor detectability disadvantage for antisymmetry relative to symmetry, if at all. Mancini et al. argued that there are indeed spatial filters (and maybe neural analogs) which filter out positional information only and which thereby, in this stimulus type, cancel the difference between symmetry and antisymmetry (notice that this would imply that the antisymmetrical nature of these stimuli is not picked up by the visual system). To test this, they turned to checkerboard stimuli in which symmetry and antisymmetry are defined on the contrast dimension alone (see Figure 3.7b). For these stimuli, they did find significant differences in detectability between symmetry and antisymme-

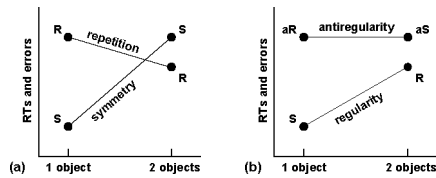


**Figure 3.8.** (a) Sketch of Baylis & Driver’s (1995) summary of their results, which (wrongly) suggests that they replicated Corbalis & Roldan’s (1974) finding that symmetry (S) is better detectable in one object, whereas repetition (R) is better detectable in two objects. (b) Baylis and Driver’s repetition in one object was antirepetition (aR) and their symmetry in two objects was antisymmetry (aS), so that their results actually tell another story, namely, that symmetry is better detectable than repetition and that regularity is better detectable than antiregularity.

try. They concluded therefore that symmetry and antisymmetry do not generally involve similar detection mechanisms and that, unlike symmetry, antisymmetry seems to require the involvement of selective attention – just as we conclude for the form of antisymmetry in the stimulus type we considered.

Notice that, in both stimuli in Figure 3.7, there is a perceptual grouping by colour (which, in symmetrical displays, seems to affect detectability; Morales & Pashler, 1999). However, compared to the dot stimulus in Figure 3.7a, the checkerboard stimulus in Figure 3.7b gives rise to an additional grouping of checkerboard squares into spatially contiguous areas of homogeneous colour (which, in symmetrical displays, also seems to affect detectability; Huang & Pashler, 2002). Hence, here too, object-level properties seem to be the cause of the differences in detectability (see our discussion on this point in the Introduction).

Before we go into more detail on the visual system’s intrinsic encoding in case of regularity and the higher cognitive strategies in case of antiregularity, it is expedient to re-evaluate the three studies we criticise. Therefore, next, we revisit these three studies, but now using our distinction between regularity and antiregularity.

### 3.4.1 Re-evaluating the literature

The study by Baylis & Driver (1995) involved four experiments in which, in designated task-relevant sides of one or two 2-D shapes, participants

had to discriminate random structures from what they called symmetry and repetition. In all conditions, the task-irrelevant sides were straight. Stated in our terminology, they focused in their first three experiments on symmetry in one object, and on antisymmetry and (facing and nonfacing) symmetry in two objects. In their fourth experiment, they focused on antirepetition in one object, and on repetition and (facing) antirepetition in two objects.

In their final analysis, they summarized their results as depicted schematically in Figure 3.8a. This picture suggests that they replicated the results Corbalis & Roldan (1974) found for symmetry and repetition in dot patterns (namely, that symmetry is better detectable in one object, whereas repetition is better detectable in two objects). However, if one honours the distinction between regularity and antiregularity, Baylis & Driver's results yield a fundamentally different picture (see Figure 3.8b). This other picture reveals that they (a) replicated the well-known finding that symmetry is better detectable than repetition is (Bruce & Morgan, 1975; Corbalis & Roldan, 1974; Julesz, 1971; Mach, 1886; Zimmer, 1984), and (b) found that regularity is better detectable than antiregularity is.

The difference between Figure 3.8a and Figure 3.8b shows that our distinction between regularity and antiregularity has fundamental implications for a proper understanding of the data. For instance, Baylis & Driver concluded that repetition is detected by a process of mental imagery involving what they called a jig-saw-matching strategy. Using closed-contour stimuli, Bertamini et al. (1997) investigated this process of mental imagery more deeply and concluded that it involves what they called a lock-and-key-matching strategy. Both ideas, however, make more sense if one realizes that they do not apply to repetition but to antirepetition. That is, in fact, both ideas (a) do not affect the status of repetition, and (b) support the hypothesis that antirepetition is not a feature the visual system is sensitive to, so that its detection requires a higher cognitive strategy.

In a follow-up study using projections of slanted 3-D objects, Koning & Wagemans (2009) looked, in our terminology, at symmetry and antirepetition in facing and nonfacing task-relevant sides of two objects and, crucially, they varied the task-irrelevant sides (in all conditions, these sides could be random, symmetrical, or antirepeated). Their main finding was

that detection of facing and nonfacing symmetry is affected by the task-irrelevant structures, whereas detection of facing and nonfacing antirepetition is not. Notice that we not only replicated this finding but also included antisymmetry and repetition, leading to the broader finding that detection of regularity is facilitated by a congruent task-irrelevant structure, whereas detection of antiregularity is not.

Hence, we would say that also Koning & Wagemans' results (a) do not affect the status of repetition, and (b) support the hypothesis that antirepetition is not a feature the visual system is sensitive to, so that its detection requires a higher cognitive strategy. They, however, argued differently. First, and we agree on this point, they argued that it is preferable to have one account for symmetry and repetition, namely, a structural account which capitalizes on the visual system's intrinsic encoding. Then, however, they argued that this structural account predicts an effect of task-irrelevant structures for symmetry but not for repetition (this should explain they found no effect for what they called repetition). We do not agree with this point. They found no effect for what was actually antirepetition, so, there is neither reason nor need to try to explain this the way they did. Furthermore, our results clearly show that things are different than Koning & Wagemans seemed to believe: They predicted no effect for what they called repetition, but we found an effect for what everybody would call repetition. Indeed, we think it is logically more consistent to interpret this structural account as predicting that both symmetry and repetition are affected by task-irrelevant structures. This is sustained in the next subsection.

### **3.4.2 The visual system's intrinsic encoding**

The foregoing re-evaluation shows that all three studies mixed up repetition and antirepetition, which led to their usage of incomplete designs and analyses. As we mentioned in the Introduction, they seemed to argue that one should frame the problem in image-level terms, that is, not in the object-level terms in which we defined antiregularity. As we also mentioned, however, it is nowadays commonly accepted in both cognitive science and neuroscience that the perceptual organization process is not a

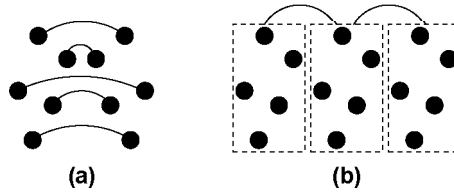


**Figure 3.9.** Holographic structure of symmetry and repetition (the arcs depict the identity relationships a regularity is composed of). (a) Symmetry has a so-called point structure constituted by many identity relationships between elements; this suggests a high weight of evidence for symmetry (and, thereby, a high detectability) and a strong binding of the stimulus into one object. (b) Repetition has a so-called block structure constituted by few identity relationships between repeats; this suggests a low weight of evidence for repetition (and, thereby, a low detectability) and a segmentation of the stimulus into the repeats.

uni-directional process from images to objects but a highly combinatorial process which, for a given image, seems to search for the best-fitting object. As said, this implies that also object-level properties are relevant to the perceptual organization process.

One account of what the best-fitting object is for a given image, is that it is the simplest object among all fitting objects (Hochberg & McAlister, 1953; Leeuwenberg, 1969, 1971; Leeuwenberg et al., 1994; van der Helm, 2000; van der Helm & Leeuwenberg, 2004). In this account, an object is simpler the more regularity it exhibits – that is, of course, regularity the visual system is sensitive to. This simplicity account implies that, in our experiments, the difference in participants' performance between the random and congruent subconditions can be explained by the difference in complexity between the stimuli in these subconditions. This is in fact precisely our underlying idea in arguing that, compared to a random task-irrelevant structure, a congruent task-irrelevant feature facilitates the detection of a task-relevant feature – at least, if both features are features the visual system is sensitive to.

Hence, by giving an underpinning of our rationale rather than an alternative account, this simplicity account indeed explains the positive congruency effects we found for symmetry and repetition. By the same token, it suggests that the lack of positive congruency effects for antisymmetry and antirepetition implies that these antiregularities indeed are not fea-

tures the visual system is sensitive to.

Related to this simplicity account, by the way, is the so-called holographic approach which, based on a mathematical formalization of regularity, provides a fairly comprehensive explanation of visual regularity detection (van der Helm & Leeuwenberg, 1991, 1996, 1999, 2004; see also Csathó et al., 2003, 2004; Nucci & Wagemans, 2007; Treder & van der Helm, 2007; Wenderoth & Welsh, 1998b). Among other things, it explains the earlier-mentioned phenomenon that symmetry is better detectable than repetition is. Here, we do not elaborate on the latter explanation, but it is relevant to note that it is based on the different perceptual structures which symmetry and repetition have according to this mathematical formalization (see Figure 3.9; for details, see van der Helm & Leeuwenberg, 1996). This difference in perceptual structure also corroborates the earlier-mentioned idea that symmetry is a cue for the presence of one object and that repetition is a cue for the presence of multiple objects (Treder & van der Helm, 2007; see also Corbalis & Roldan, 1974). The three studies just re-evaluated related their findings to this idea and they indeed corroborated it insofar as symmetry is concerned, but because they mixed up repetition and antirepetition, they clouded it insofar as repetition is concerned.

One might argue that this idea about object cues could back-fire. After all, in our symmetry condition, the symmetry of the white area between the two black areas might trigger an unintended figure-ground reversal so that this white area becomes, perceptually, the object that is judged by participants (see Figure 3.2 and Figure 3.4). Indeed, we think that, in general, figure-ground coding should be taken into account. However, as we argue next, we do not think it plays an interfering role in the issues addressed here.

This figure-ground argument can hardly be raised against the other conditions and would apply just as well to the three studies just re-evaluated – so, it would not invalidate our arguments against these three studies. Furthermore, in the stimuli considered here, such a figure-ground reversal neither turns regularities into antiregularities nor vice versa – so, it would not invalidate our distinction between regularities and antiregularities. Moreover, if a figure-ground reversal would play a role in the sym-



metry condition so that the central white area becomes the object that is judged, then there is hardly any reason to expect an effect of the task-irrelevant sides, as we nevertheless did find. Finally, neither Baylis & Driver (1995) nor Koning & Wagemans (2009) found qualitative differences between facing and non-facing symmetry in two objects – such differences would be expected if facing symmetry triggers a figure-ground reversal.

### **3.4.3 Cognitive strategies in case of antiregularity**

Although this article focuses mainly on the perceptual question of whether (anti)regularities play a role in the automatic perceptual organization process, it is expedient to also discuss the higher cognitive matching strategy which seems to be applied to detect antisymmetry and antirepetition. We think this matching strategy involves a form of mental translation. Just as Baylis & Driver's (1995) jig-saw matching and Bertamini et al.'s (1997) lock-and-key matching in case of antirepetition, mental translation is a variation on the umbrella theme coined mental rotation (Shepard & Metzler, 1971). There is not much direct evidence for the idea of mental transformations (Bertamini et al., 2002) but, here, we use the term mental rotation merely to refer to "what happens during the execution of a matching task". It indeed applies to a set of still poorly understood phenomena but, for instance, matching entire stimuli is known to be influenced by the perceptual structure of these stimuli (e.g., Koning & van Lier, 2004; Pylyshyn, 1973; Shepard & Metzler, 1971; van Lier & Wagemans, 1998). That is, mental rotation operates on structured object-level representations of stimuli rather than on stimulus-analogous image-level representations. In the experiments considered here, however, participants were asked to match stimulus parts rather than entire stimuli, and this suggests the following.

We think that, in the antiregularity conditions, participants perform mental translation on the stimulus parts to be matched (some of our participants in fact reported spontaneously that they applied a cognitive strategy in these conditions). Also then, however, it is expedient to realize that participants perform their task starting from the objects they perceive. This implies that they have to ignore willfully the objects they perceive and that

they have to focus attention on the parts to be matched (cf. Ahissar & Hochstein, 2004). Such a strategy will therefore hardly be affected by task-irrelevant parts – as corroborated by the lack of positive congruency effects in our antiregularity conditions.

Notice that the foregoing does not explain that performance in the antirepetition condition is good compared to performance in the other three (anti)regularity conditions (see Figure 3.3 and Figure 3.5). We are reluctant, however, to draw conclusions from our results regarding quantitative differences between the four (anti)regularities. After all, as said, our stimuli are not suited to address these quantitative differences, and the difference we found in participants' treatment between the regularity and antiregularity conditions makes us even more reluctant. Yet, on repeated request, we allow ourselves to say the following.

The quantitative difference between symmetry and repetition, on the one hand, probably simply reflects the genuinely perceptual phenomenon discussed earlier, namely, that symmetry is detected more easily than repetition is. The quantitative difference between antisymmetry and antirepetition, on the other hand, is probably due to two factors related to the strategy above, which give facing antirepetition in two objects an advantage over antisymmetry. First, compared to antirepetition, the matching by mental translation in antisymmetry seems to require a more piecemeal treatment of the task-relevant sides. Second, and probably more relevant, the task-relevant sides have to be compared across an object in case of antisymmetry and only across a gap in case of facing antirepetition.

For instance, for nonfacing antirepetition in one object, the task-relevant sides also have to be compared across the object, and for this case, Baylis & Driver (1995) found no quantitative difference with respect to antisymmetry (see Figure 3.8b). Furthermore, facing antirepetition in two objects has an advantage over nonfacing antirepetition not only in one object (as found in all three studies we re-evaluated) but also in two objects (Konig & Wagemans, 2009). This too suggests that, in case of antiregularity, comparisons across gaps are easier than comparisons across objects. Our study does not provide an explanation for this, but it does suggest that an explanation is to be searched for in terms of cognitive strategies rather than in terms of perceptual mechanisms.



## CHAPTER 4

---

### Symmetry and repetition in cyclopean vision: a microgenetic analysis

---

---

This chapter has been adapted from:  
Treder, M. S., & van der Helm, P. A. (2007). Symmetry versus repetition in cyclopean vision:  
A microgenetic analysis. *Vision Research*, 47, 2956–2967.



In four experiments, participants had to detect symmetries or repetitions distributed over two depth planes, under presentation times of 200-1000 ms. Structurally corresponding elements were placed in different planes (Experiments 1a and 1b) or in the same plane (Experiments 2a and 2b). Results suggest (a) an ongoing interaction between regularity cues and depth cues, and (b) that efficient detection of symmetry but not of repetition depends on structural correspondences within depth planes. The latter confirms the idea that, to perceptual organization, symmetry is a cue for the presence of one object whereas repetition is a cue for the presence of multiple objects.

## 4.1 Introduction

To human observers, there are substantial perceptual differences between kinds of visual regularity. Most comparative studies are dedicated to contrasting the two most prominent cases, namely mirror symmetry (henceforth symmetry) and two-fold repetition (henceforth repetition). These studies show consistently that symmetry has a higher goodness than repetition. For instance, symmetry is more salient and more noise-resistant than repetition; furthermore, in terms of the number of stimulus elements covered, symmetry detection seems to propagate exponentially by way of parallel processing whereas repetition detection seems to propagate linearly by way of serial processing (Baylis & Driver, 1994; Bruce & Morgan, 1975; Corbalis & Roldan, 1974; Csathó et al., 2003; Fitts et al., 1956; Julesz, 1971; Mach, 1886; van der Helm & Leeuwenberg, 1996, 1999, 2004; Zimmer, 1984).

In fact, symmetry and repetition seem to have opposite effects on the perceptual formation of objects. Symmetry seems to integrate pattern halves into perceived wholes, while repetition rather seems to signal the presence of two distinct objects (for a tentative explanation, see van der Helm & Leeuwenberg, 1996; for accounts of the general problem of perceptual object formation, see e.g. Feldman, 1999, and van der Helm et al., 2003). There are some empirical indications for this dichotomy. For in-

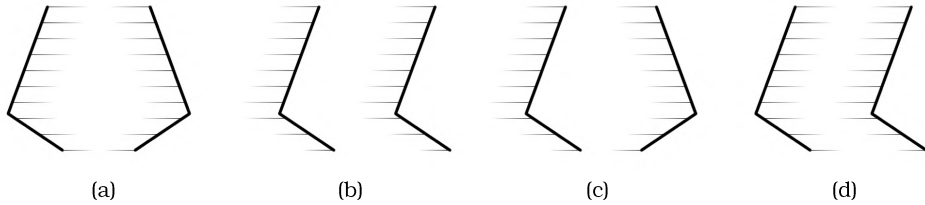


**Figure 4.1.** Schematic overview of stimuli used by Baylis and Driver (1995, 2001). The vertical contours belong to surfaces with interiors indicated by horizontal stripes. In the top row, contour polarity (i.e., concavity/convexity) goes along with the regularity between the contours. We therefore call (a) a true symmetry and (b) a true repetition. In the bottom row, contour polarity goes against the regularity between the contours. We therefore call (c) an antisymmetry and (d) an antirepetition.

stance, Baylis & Driver (1995, 2001) had participants discriminate symmetric from asymmetric and repetitive from non-repetitive vertical curves which were part of the contour of either the same object or different objects. They found that symmetric curves are detected more easily than repeated curves when they belong to the same object, whereas repeated curves are detected more easily than symmetric curves when they belong to different objects. However, it is questionable to speak of symmetry in the two-object stimuli and of repetition in the one-object stimuli because, in these cases, the contour polarity of the curves goes against the regularity (see Figure 4.1). Hence, in these cases, we would rather speak of antisymmetry and antirepetition. A similar argument applies to Bertamini et al. (1997), who compared symmetry to what we would call antirepetition.

Stronger evidence stems from an experiment conducted by Corbalis & Roldan (1974). They had participants discriminate between symmetric and repetitive patterns in which the pattern halves were either adjacent or separated by a fixed distance. They found that symmetry is more salient than repetition when there is no spatial separation between the pattern halves but not when there is a spatial separation between the pattern halves. Apparently, manipulation of the distance between pattern halves within the projection plane has different, if not opposite, effects on symmetry as compared to repetition.

In this study, we put visual regularity in direct competition with another significant determinant of perceptual organization, namely, stereoscopic

depth. When relative disparity exceeds a certain threshold (Yakushijin & Ishiguchi, 1999), it provides metrical information about distances and locations in depth (cf. Burge et al., 2005). As a consequence, depth influences the grouping of parts into objects, because spatially contiguous parts tend to be perceived as belonging to the same object. However, the processing of relative disparity takes time to become effective (Ritter, 1980), and we wondered whether and, if so, how this affects regularity perception. That is, we think that both regularity perception and stereopsis are ongoing processes, and in this study, we investigate the interaction between these two ongoing processes. This issue may be introduced as follows.

Hitherto, comparative studies on symmetry and repetition in depth are rare. It is true that van der Vloed et al. (2005) investigated the effect of linear perspective on the discriminability of symmetry and repetition, and that Farell (2005) probed the detectability of visual regularities defined by disparity values, but to our knowledge, there are no comparative studies on stereoscopic manipulations of symmetry and repetition. Only for symmetry alone, several studies did examine detectability in stereoscopic space; this is discussed next.

The first explorations into symmetry and binocular viewing were conducted by Julesz (1960, 1966). He demonstrated that a binocular symmetry percept can arise even in the absence of monocular symmetry and that monocular symmetry can be destroyed by appropriate binocular cues. These findings led him to conclude that symmetry detection is preceded or dominated by stereo vision. This is in line with Ishiguchi & Yakushijin (1999) who had participants discriminate between patterns consisting of two or three depth planes with varying interplanar distances. They found that the disparity threshold to distinguish between depth planes is not affected by the structure (symmetry or random) of the patterns in each plane. Furthermore, Yakushijin & Ishiguchi (1999) found that, when symmetry and noise are placed in different depth planes, the detectability of symmetry in the symmetry plane is unaffected by the noise plane, provided that the relative disparity between the planes is sufficiently large. Finally, Bertone & Faubert (2002) found that the detectability of symmetry deteriorates with increasing disparity when pattern halves are put into different depth planes. However, even for large disparities, symmetry detection re-



mained feasible. Apparently, to a certain extent, depth separation induced by binocular disparity can be overcome.

At first glance, these results seem to be contradicted by Locher & Smets (1992), who proposed that symmetry is detected before the integration of figural and disparity cues. However, these two points of view do not have to exclude each other. In contrast to classical views which state that grouping is preattentive and operates on the retinal image, recent research suggests that perceptual grouping can be influenced significantly by factors such as lightness constancy, amodal completion and binocular disparity (Palmer, 2002; Palmer et al., 2003). Furthermore, whether or not grouping is preceded by these factors seems to depend strongly on exposure time: For short exposure times, subjects seem to base their response on retinal properties while the aforementioned factors come into play for long exposure times (Schulz & Sanocki, 2003).

These effects may partly be due to the fact that different features of the visual input are processed in functionally more or less specialized streams (Ungerleider & Mishkin, 1982; for recent evidence, see Borowsky et al., 2005). While shape processing seems largely confined to the ventral stream, stereoprocessing seems to occur in both dorsal and ventral areas (Chandrasekaran et al., 2007; Neri, 2004). This suggests that there is a certain degree of neural dissociation but also interaction between shape processing and stereoprocessing. Consequently, the detection of visual regularities in a stereoscopic context (with visual regularity co-defining a Gestalt and disparities encoding its location) is probably a dynamic process in which different forces of perceptual organization dominate at different points in time.

A comprehensive approach to the detection of visual regularities in depth thus requires a microgenetic analysis of the interaction between the ongoing processes of regularity perception and stereopsis (to be clear, the concept of microgenesis refers to the development on a brief present-time scale of, in this case, a percept; see, e.g., Sekuler & Palmer, 1992). To this end, in our experiments, both temporal and spatial aspects of the stimulus material were manipulated. With respect to the temporal domain, we varied presentation time from 200 ms to 1000 ms to probe the detection mechanism at different stages of visual processing. With respect to the

spatial domain, we subjected regularities to various kinds of stereoscopic manipulations to test the resistance of the detection mechanism to spatial displacements of pattern elements. First, for symmetry in Experiment 1a and for repetition in Experiment 1b, we investigated the effects of assigning non-corresponding disparity values to structurally corresponding elements (yielding one regularity spread out across two depth planes). Second, in Experiments 2a and 2b, we compared this to the effects of assigning corresponding disparity values to structurally corresponding elements (yielding two depth planes featuring one regularity each).

## **4.2 Experiments 1a and 1b**

### **4.2.1 Method**

#### **4.2.1.1 Participants**

In each of the experiments, 22 subjects participated (no overlap between the two groups). The participants were either undergraduate students or volunteers with normal or corrected-to-normal vision and good stereopsis. To assess whether participants were able to perceive stereoscopic depth, we had them look at stereoscopic dot displays while wearing shutter glasses and asked them to describe their percept. In return for their participation, they received either course credits or money.

#### **4.2.1.2 Apparatus**

The experiments were run on a standard PC with a 19" monitor with a 140 Hz refresh rate and a resolution of 1024 × 768 pixels. The screen was viewed through a 16 cm × 16 cm hole in a black piece of cardboard; this was done because pilot experiments suggested that viewing the stimuli through such a hole eases stereopsis when the cardboard has a few centimeters offset from the screen. During the experiment, participants wore wireless CrystalEyes 3 shutter glasses. An infrared emitter synchronized the shutter glasses with the refresh rate of the screen. Responses were recorded via a button box.

### 4.2.1.3 Stimuli

Stimuli consisted of 60 dark grey discs with a diameter of  $0.42^\circ$  of visual angle on a light grey background. The luminance of the discs amounted to  $0.63 \text{ cd/m}^2$  and the luminance of the background was  $28.49 \text{ cd/m}^2$ . The whole pattern had a size of  $12^\circ \times 12^\circ$  of visual angle. Stereoscopically, stimuli comprised three depth planes, two frontoparallel target planes constituting the regularity or its random counterpart (20 discs in total, 10 discs per target plane), and a frontoparallel noise plane in the background (40 discs). The position of the first target plane in stereoscopic space coincided with the computer screen. The relative disparity to the second target plane and the noise plane amounted to  $+26.4'$  and  $+49'$  (i.e., target plane 2 was located behind target plane 1 and the noise plane was the hindmost plane; see Figure 4.2a). The noise plane was included not only to control task difficulty but also to stimulate an effective usage of binocular cues. That is, participants can perform the task more efficiently when using binocular cues to separate the noise plane from the target planes (see also Yakushijin & Ishiguchi, 1999).

The target planes were constructed by starting from planar regular or random patterns. In Experiment 1a, the symmetry patterns were generated by randomly placing 10 discs in one half of a pattern and then reflecting this pattern half about a vertical axis. For the repetition patterns in Experiment 1b, this pattern half was copied without reflection. To generate random patterns, discs in the left-hand and right-hand halves were distributed randomly. Both Experiment 1a and Experiment 1b contained three stimulus conditions, namely, *LR* (left-right), *Opp* (opposite), and *Base* (baseline). These conditions differed in the way the discs were assigned disparity values to place them in one of the two target planes, as follows.

In the *LR* condition, the discs were assigned disparity values such that the pattern halves were placed in different planes. In the *Opp* condition, the symmetry or repetition pairs were divided randomly into two subsets of equal size. In one subset, the left-hand disc of each pair was placed in the first target plane and the right-hand disc in the second target plane; in the second subset, the disparities were reversed. Figure 4.2b schematically

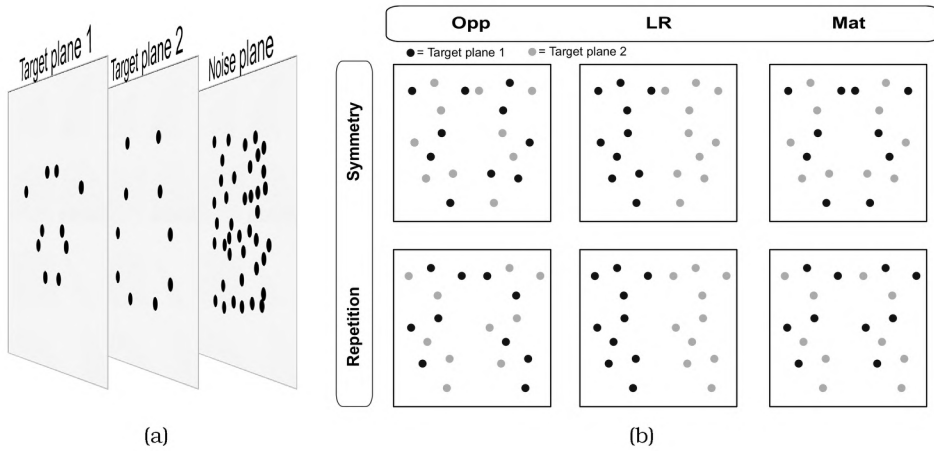


**Figure 4.2.** Overview of the stimuli used in our experiments. (a) Schematic side view of the depth planes. From left to right: target plane 1, target plane 2, and noise plane. From the subject's perspective, target plane 1 was the foremost frontoparallel plane. In this example, the arrangement of discs corresponds to the *Mat* condition for symmetry. (b) Sketch of the pattern types *Opp* (opposite), *LR* (left-right), and *Mat* (matched) for symmetry (first row) and repetition (second row). Just for illustration purposes, the noise plane is omitted, and the discs are coloured light and dark to indicate on which target plane they are located. The additional *Base* condition simply featured a regularity confined to a single plane and is not displayed here.

depicts the *LR* and *Opp* stimuli used in the experiments. The frontoparallel projection of the two target planes always yielded a perfect planar regularity, irrespective of the manipulation performed. In both experiments, we also included a baseline condition *Base* with only one target plane, that is, all discs were assigned the same disparity, thus confining the regularity to either the first or the second target plane. To the random counterparts of these three conditions, the same manipulations were performed. The assignment of disparity values was counterbalanced within each condition.

#### 4.2.1.4 Procedure

Participants were seated at 65 cm from the computer screen. Participants in Experiment 1a performed a symmetry present/absent task. In each trial, either a symmetric or a random stimulus was presented and participants had to press a button with their dominant hand when they saw symmetry and another button with their non-dominant hand when they did

not. Participants in Experiment 1b performed a repetition present/absent task and had to indicate their choice analogously.

A series of 60 practice trials preceded the experimental phase. During practice, stimulus presentation ended only when participants responded. This was necessary, because many participants initially needed a few seconds to get used to the unusual sensation of stereoscopic depth on a computer screen. During the practice phase, visual feedback was given immediately after the response. Immediately after the practice phase, the experimental phase commenced. It was split into five blocks featuring the presentation times 200, 400, 600, 800, and 1000 ms, respectively. The order of presentation times was randomized across participants.

At the beginning of each trial, a fixation cross was presented for 500 ms. To minimize a fixation bias towards one of the target planes, the fixation cross was presented stereoscopically in between the two target planes. Subsequently, the stimulus appeared on the screen. Following the offset of the stimulus, participants were given three seconds to respond. After the response and an inter-trial interval of 100 ms, the next trial commenced automatically. Each time after 120 trials, a break was given and the percentage of correct responses during the last block was displayed. In total, each experiment comprised 5 (presentation times)  $\times$  3 (pattern types: *LR*, *Opp*, and *Base*)  $\times$  2 (regular and random)  $\times$  20 (measurements) = 600 trials.

### 4.2.2 Results

For each experiment separately, and based on hits and correct rejections,  $d'$  was calculated for every combination of presentation time (200, 400, 600, 800, and 1000 ms) and pattern type (*Base*, *LR*, and *Opp*). Compared to the baseline, performance on the other pattern types was significantly lower. For symmetry, repeated measures ANOVAs yielded  $F(1, 21) = 58.596$ ,  $p < .001$ , and  $F(1, 21) = 98.838$ ,  $p < .001$ , for *LR* and *Opp*, respectively. For repetition, the corresponding values were  $F(1, 21) = 9.237$ ,  $p < .01$ , and  $F(1, 21) = 86.448$ ,  $p < .001$ . However,  $d'$  was merely an intermediate step in the specification of a more interesting dependent variable which may be introduced as follows.

By definition, prolonged viewing eases the task and thus enhances  $d'$ , irrespective of the presence of binocular depth cues. Furthermore, perceptual dissociation of the target and noise planes, which is increasingly feasible with increasing presentation time, gives an additional boost to performance. Indeed, we found that  $d'$  increases with presentation time in all conditions, but because of these factors, this does not allow for a straightforward comparison of the pattern types across presentation times. To eliminate these factors from our measurements, we calculated relative performance, that is, the performance on *LR* and *Opp* relative to the baseline *Base*. We defined relative detectability  $\Delta d'$  by

$$\Delta d'_x = d'_x - d'_{Base}$$

where  $d'_x$  corresponds to  $d'$  obtained for a pattern type  $x \in \{LR, Opp\}$ , while  $d'_{Base}$  corresponds to  $d'$  obtained for the baseline condition. In other words,  $\Delta d'$  for the *LR* condition was derived by subtracting  $d'$  in the *Base* condition from  $d'$  in the *LR* condition. Correspondingly,  $\Delta d'$  for the *Opp* condition was derived by subtracting  $d'$  in the *Base* condition from  $d'$  obtained in the *Opp* condition. This subtraction eliminates the facilitating effects of longer presentation times and of the perceptual dissociation of the target and noise planes, so that any effect found for  $\Delta d'$  can be attributed to the kind of manipulation applied to the regularities. A set of repeated measures ANOVAs was performed on the obtained  $\Delta d'$  (note that a main effect on  $\Delta d'$  for *LR* or *Opp* is statistically equivalent to an interaction in terms of  $d'$  between the baseline and *LR* or *Opp*).

*Effects of pattern type.* For symmetry, participants performed significantly better in the *LR* condition as compared to the *Opp* condition, with  $F(1, 21) = 25.088$ ,  $p < .01$  (see Figure 4.3a). This difference was not significant at a presentation time of 200 ms ( $p = .342$ ), but was significant at 400 ms,  $t(21) = 2.104$ ,  $p < .05$ , and later. For repetition, the same pattern was found, that is,  $LR > Opp$  with  $F(1, 21) = 55.512$ ,  $p < .01$  (see Figure 4.3b); this time, the difference between *LR* and *Opp* is already evident at a presentation time of 200 ms,  $t(21) = 2.883$ ,  $p < .01$ .

*Time effects.* We also investigated whether there were effects of presentation time in each of the conditions. For *Opp*, there was a negative time

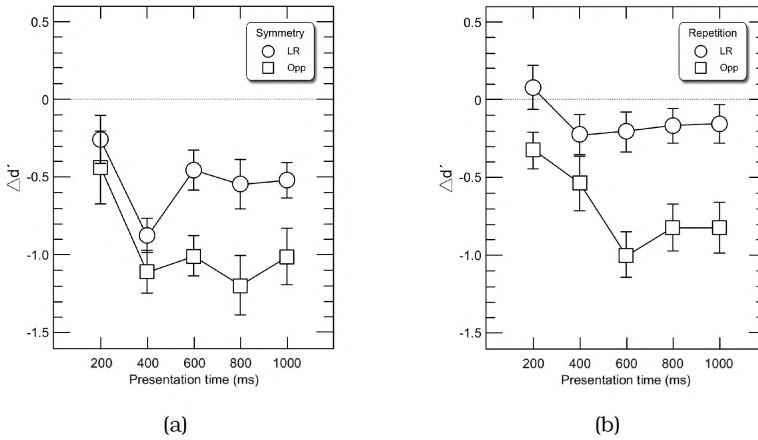


**Figure 4.3.** (a) Results of experiment 1a:  $\Delta d'$  on symmetry as a function of presentation time. The *LR* curve (circles) shows a performance dip at 400 ms. The *Opp* curve (squares) also drops at 400 ms and then levels off. The dips suggest the *LR* and *Opp* depth segregations do not agree with the perceptual structure of symmetry. (b) Results of experiment 1b:  $\Delta d'$  on repetition as a function of presentation time. Just as for symmetry, the *Opp* curve (squares) drops with increasing presentation time and then levels off, but the *LR* curve (circles) is hardly affected by presentation time. This suggests that the *Opp* segregation does not agree with the perceptual structure of repetition but that the *LR* segregation does.

effect on both symmetry and repetition, with  $F(4, 18) = 4.150$ ,  $p < .05$ , and  $F(4, 18) = 3.025$ ,  $p < .05$ , respectively. For *LR*, we found a negative effect of time on symmetry, with  $F(4, 18) = 3.234$ ,  $p < .05$ , but not on repetition ( $p = .588$ ). The time effect on symmetry in the *LR* condition was solely due to a performance drop at 400 ms. That is, two-sided t-tests revealed that relative performance at 400 ms was significantly worse than at the immediately preceding (200 ms) and following (600 ms) levels of presentation time, with  $t(21) = 3.393$ ,  $p < .01$ , and  $t(21) = -2.313$ ,  $p < .05$ , respectively; if the 400 ms condition was removed from the analysis, the main effect disappeared ( $p = .57$ ).

### 4.2.3 Discussion

To allow a comparison between symmetry and repetition across different presentation times, we introduced  $\Delta d'$  as a measure of relative detectability, specifying  $d'$  in the *LR* and *Opp* conditions relative to the baseline.

Because the effects of both prolonged viewing and target-noise separation are eliminated by this measure, any remaining effect can be attributed to the kind of manipulation applied to the stimuli. For both symmetry and repetition, we found that detection is impaired more in the *Opp* condition than in the *LR* condition. These differences are also reflected in the patterns of interaction between regularity and depth over time.

For symmetry, we found significant time effects for both kinds of manipulations (see Figure 4.3a). From 200 ms to 400 ms, relative performance drops in both conditions. After that, however, the curves for *LR* and *Opp* diverge. For *Opp*, the low relative performance at 400 ms persists, but for *LR*, relative performance recovers nearly to the level it had at 200 ms. For repetition, we only found a time effect in the *Opp* condition, where relative performance declines from 200 ms to 600 ms and then levels off. Although the performance drop is less severe than it is for the *Opp* condition in symmetry, the course of relative performance across presentation time is comparable for both regularities. This suggests that the stimulus segmentation triggered by the depth segregation in the *Opp* condition is compatible neither with the perceptual structure of symmetry nor with the perceptual structure of repetition. Conversely, in the *LR* condition, repetition shows no time effect whereas symmetry does; this suggests that the stimulus segmentation triggered by the depth segregation in the *LR* condition agrees with the perceptual structure of repetition but conflicts with the perceptual structure of symmetry.

Our finding in the *LR* condition seems a stereoscopic analogue of Corbalis & Roldan's (1974) finding that separating pattern halves within the projection plane enhances the detectability of repetition but impairs the detectability of symmetry. However, in our experiment, repetition in the *LR* condition was detected not better but actually slightly worse than in the baseline condition. This raises the question of whether, compared to the baseline condition, the *LR* condition might be more complex just because it contains an additional depth plane. Another question is whether, for symmetry, the performance dip in the *LR* condition is due to the depth segregation *per se* or due to a conflict with the perceptual structure of symmetry. These two questions were investigated further in Experiments 2a and 2b, in which the *LR* condition was contrasted to a condition in which



structurally corresponding elements were assigned corresponding disparity values, yielding two depth planes featuring one regularity each.

## 4.3 Experiments 2a and 2b

### 4.3.1 Method

#### 4.3.1.1 Participants, apparatus, and procedure

Twenty-one subjects participated in Experiment 2a (on symmetry) and 20 subjects participated in Experiment 2b (on repetition). None of them had participated in Experiments 1a or 1b; 11 of the subjects in Experiment 2a had participated first in Experiment 2b, but a post-hoc analysis showed no significant difference ( $p = .908$ ) in performance between this group and the naive subjects. The parameters of the apparatus and the procedure were the same as in Experiments 1a and 1b.

#### 4.3.1.2 Stimuli

Just as in Experiments 1a and 1b, we created the *Base* condition (with one regularity in one target plane) and the *LR* condition (with one half of a regularity in one target plane and the other half in the other target plane). The *Opp* condition, however, was now replaced by the *Mat* (matched) condition in which structurally corresponding elements had the same disparity, yielding two planar regularities, one in each target plane (see Figure 4.2b). To the task, one of the planes was redundant because regularity could be judged on the basis of only one plane, so that the presence of an additional depth plane was the main difference with respect the baseline condition.

### 4.3.2 Results

For each experiment separately, we again calculated  $d'$  for every combination of presentation time and pattern type. Also this time, all manipulations caused a significant deterioration in performance compared to the baseline. For symmetry, repeated measures ANOVAs yielded  $F(1, 20) =$

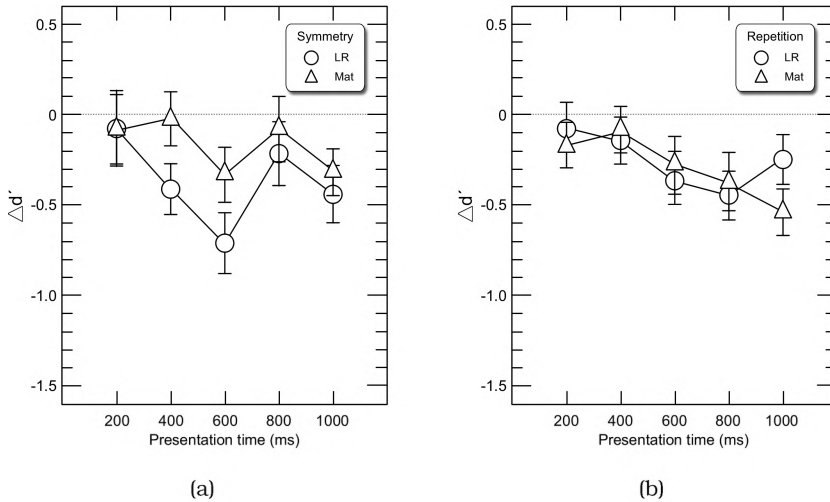


**Figure 4.4.** (a) Results of experiment 2a:  $\Delta d'$  on symmetry as a function of presentation time. The *LR* curve (circles) shows a performance dip at 600 ms. The *Mat* curve (triangles) has as similar slope, but there is no dip. The fact that *Mat* > *LR* suggests that symmetry is more salient when there are structural correspondences within depth planes. (b) Results of experiment 2b:  $\Delta d'$  on repetition as a function of presentation time. Both curves are hardly affected by presentation time. The fact that *Mat*  $\approx$  *LR* suggests that repetition, unlike symmetry, does not depend on structural correspondences within depth planes.

11.969,  $p < .01$ , and  $F(1, 20) = 5.396$ ,  $p < .05$ , for *LR* and *Mat*, respectively. For repetition, the corresponding values were  $F(1, 19) = 17.302$ ,  $p < .001$ , and  $F(1, 19) = 20.561$ ,  $p < .001$ . As before, a more interesting analysis involved repeated measures ANOVAs performed on  $\Delta d'$  to compare the effects of the manipulations with each other.

*Effects of pattern type.* For symmetry, participants performed significantly better in the *Mat* condition than in the *LR* condition,  $F(1, 20) = 4.627$ ,  $p < .05$  (see Figure 4.4a). The difference between *LR* and *Mat* was not significant at 200 ms ( $p = .965$ ), 800 ms ( $p = .523$ ), and 1000 ms ( $p = .457$ ), but was significant at 400 ms,  $t(20) = 2.926$ ,  $p < .01$ , and at 600 ms,  $t(20) = 2.189$ ,  $p < .05$ . For repetition, no significant difference between *LR* and *Mat* was found ( $p = .741$ ; see Figure 4.4b).

*Time effects.* There were no significant time effects for both manipulations of both regularities. However, in the *LR* condition, two-sided t-tests

for symmetry revealed a dip in performance just as observed in Experiment 1a. From 200 ms to 600 ms, performance dropped significantly,  $t(20) = 2.674$ ,  $p < .05$ ; subsequently, performance increased nearly significantly from 600 ms to 800 ms,  $t(20) = -2.23$ ,  $p = .051$ . Such a dip was absent in the *Mat* condition.

### 4.3.3 Discussion

The stimuli in the *Mat* condition are similar to those in the *Base* condition in the sense that regularities are confined to single planes, but the stimuli in the *Mat* condition have two target planes while those in the *Base* condition have only one. The worse performance in the *Mat* condition relative to the *Base* condition suggests therefore that the addition of an extra depth plane *per se* increased task difficulty (the *Mat* stimuli also have fewer elements per plane than the *Base* stimuli but, if anything, we think this would give *Mat* an advantage rather than a disadvantage over *Base*). This implies that the *Mat* vs *LR* comparison is most appropriate to pinpoint differences between symmetry and repetition, because both *Mat* stimuli and *LR* stimuli contain two target planes (with the same number of elements per plane).

For symmetry, we found that  $Mat > LR$  in terms of relative performance. This suggests that symmetry detection is at its best whenever structurally corresponding elements are in the same depth plane. Furthermore, relative performance in the *Mat* condition showed no time effect, while for *LR*, we again found a performance dip as also observed in Experiment 1a (this time, it occurs at 600 ms instead of 400 ms). The absence of a time effect for *Mat* suggests that the presence of two target planes *per se* is not enough to trigger such a performance dip. Rather, the re-occurring performance dip for *LR* supports our earlier suggestion that such a dip occurs only when the stimulus segmentation triggered by depth cues disagrees with the perceptual structure of symmetry. The dip, and the varying presentation time it occurs at, also indicate that depth perception and symmetry perception interact in a dynamic way.

For repetition, we found that  $Mat \approx LR$ , even though inspection of one plane sufficed in the *Mat* condition whereas participants were forced to

compare pattern halves across two planes in the *LR* condition. This supports our earlier suggestion that the stimulus segmentation triggered by the depth segregation in the *LR* condition agrees with the perceptual structure of repetition. Thus, overall, repetition detection is more robust to depth segregation than symmetry detection is.

## 4.4 General discussion

Marr (1982) argued that a full understanding of a perceptual phenomenon requires an combination of complementary approaches at three different levels of description, namely the computational level, the algorithmic level, and the implementational level. More generally, these levels can also be called the goal level, the method level, and the means level, respectively, so that the combination can be said to give an understanding of how the goal is reached by a method that is allowed by the means (cf. van der Helm & Leeuwenberg, 2004). In accordance with this scheme, we next discuss the mental representation of visual regularities (computational level), the microgenesis of visual regularity in depth, both empirically and theoretically (algorithmic level), and evidence from neuroimaging studies on the possible interaction of visual regularity and stereoscopic depth (implementational level).

### 4.4.1 Computational: The mental representation of regularity

In the traditional transformational approach, visual regularities are conceived as configurations that are invariant under motion, that is, under rigid translations or rotations (Garner, 1974; Palmer, 1983). For instance, a mirror symmetry is invariant under a 3-D rotation about the symmetry axis, and an infinite repetition is invariant under a translation the size of one repeat. Because symmetry halves and repeats, respectively, are identified with each other by these transformations, both symmetry and repetition are thus predicted to have a representation involving a block structure (see Figure 4.5ab). As a consequence, the transformational ap-

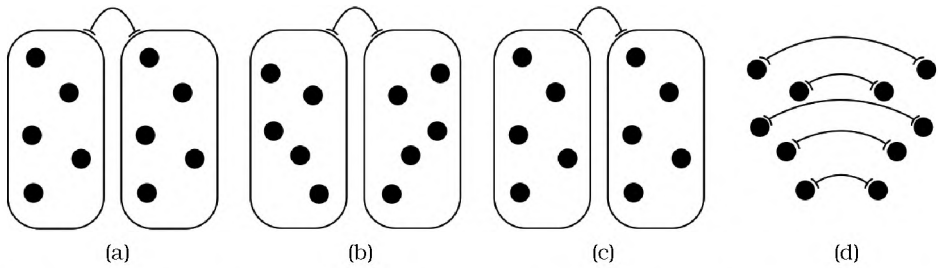


**Figure 4.5.** Structural relationships in symmetry and repetition. According to the transformational approach, both repetition (a) and symmetry (b) have a block structure. According to the holographic approach, repetition has a block structure (c) but symmetry has a point structure (d).

proach predicts equivalent goodness effects for symmetry and repetition. However, this is contradicted by virtually all comparative studies.

More recently, based on a mathematical formalization of regularity (van der Helm & Leeuwenberg, 1991), the holographic approach proposed to conceive visual regularities as configurations that are invariant under growth (van der Helm & Leeuwenberg, 1996, 1999, 2004). To put it simple, a repetition remains a repetition when expanded by one repeat, and a symmetry remains a symmetry when expanded by one symmetry pair. Because repeats and symmetry pairs, respectively, mark the size of the expansion steps, repetition is again predicted to have a representation involving a block structure but, this time, symmetry is predicted to have a point structure (see Figure 4.5cd). As corroborated by a quantitative goodness model (van der Helm & Leeuwenberg, 1996), this difference in representational structure agrees with many goodness effects reported in the literature, such as the higher saliency of symmetry and its greater resistance to perturbation in comparison to repetition.

Although stereoscopic factors lie outside the scope of both approaches, we can nevertheless examine whether the effects of the manipulations in our experiments agree with their basic tenets. For the transformational approach, this is not the case, because it predicts equivalent representational structures for symmetry and repetition. After all, our results suggest that the *LR* segregation agrees with the perceptual structure of repetition but not with the perceptual structure of symmetry. This finding is compatible

with the holographic approach. The holographic point structure of symmetry, on the one hand, implies that a planar symmetry is built from many relationships between symmetrically positioned elements, which suggests a strong binding between the pattern halves; the holographic block structure of repetition, on the other hand, implies that a planar two-fold repetition is built from only one relationship between two repeats, which suggests a segmentation rather than a binding between the pattern halves (for more details on this, see van der Helm & Leeuwenberg, 1996). This implies that the depth segregation between the pattern halves in the *LR* condition goes against the holographic structure of symmetry but not of repetition.

The difference between the holographic structures of symmetry and repetition agrees with the idea that, to perceptual organization, symmetry is a cue for the presence of one object whereas repetition is a cue for the presence of multiple objects. This idea already has been around for a while but, so far, the empirical evidence was weak. As we mentioned in the Introduction, Baylis & Driver's (1995, 2001) and Bertamini et al.'s (1997) seemingly supporting evidence is confounded by the usage of antisymmetry and antirepetition as controls (see Figure 4.1). Only Corbalis & Roldan's separation of the pattern halves in the projection plane can be said to yield supporting evidence, although their manipulation of the physical distance between corresponding elements in a stimulus somewhat at odds with the idea of perceived objectness. We now found that efficient detection of symmetry but not of repetition depends on structural correspondences within depth planes. We think this provides stronger evidence for the idea of perceived objectness, because in our stimuli, we manipulated not the physical distance but the perceived distance between corresponding elements in a stimulus (i.e., the depth planes were perceived depth planes). This implies that any grouping or segmentation is solely due to internal perceptual organization processes (for a similar argument, see Khuu & Hayes, 2005). Next, we go into more detail on these processes.

#### 4.4.2 Algorithmic, part 1: The microgenesis of regularity

Symmetry detection is feasible under presentation times as short as 10 ms (Locher & Wagemans, 1993), and virtually all studies on symmetry perception use short presentation times, say, 50-150 ms (e.g., Barlow & Reeves, 1979; Carmody et al., 1977; Csathó et al., 2003; Julesz, 1971; Locher & Wagemans, 1993). In comparison to symmetry detection, the processing of relative disparity (disparity between objects) lags behind, becoming effective for exposures of 120 ms or longer (Ritter, 1980). Hence, for short presentation times, one would expect the symmetry percept to be based on the retinal image alone. Our data support this hypothesis. Although the *LR* and *Opp* manipulations yield substantially different depth percepts, there is no difference in performance at 200 ms presentation time. This is plausible considering that, at the retinal level, the *LR* and *Opp* manipulations yield parafoveal symmetries with equal eccentricity. This is shown next.

Assume that, in a symmetry,  $P(x, y)$  and  $P'(-x, y)$  specify the mirror-symmetric points in a coordinate frame in which the symmetry axis coincides with the  $y$ -axis. Suppose that, for every symmetry pair, one of the points is horizontally shifted by adding a constant  $c$  to its  $x$ -coordinate. The pattern then still has one symmetry axis but, now, located eccentrically at  $x = c/2$  irrespective of whether the shifted points all lie on one side of the pattern (as occurs in the *LR* condition) or are distributed across both sides (as occurs in the *Opp* condition). In the *Mat* condition, conversely, one half of the symmetry pairs are shifted and the other half of the symmetry pairs are left at their original position. This yields two symmetries, one fovea-centered symmetry and one symmetry located eccentrically at  $x = c/2$ . The percept thus boils down to a jittered foveal symmetry, but compared to *LR* and *Opp*, the saliency-increasing (foveal symmetry) effect probably cancels out the saliency-decreasing effect (jitter). In total, this suggests that  $LR \approx Opp \approx Mat$ , which is what we found. In other words, the effects on symmetry at 200 ms can be accounted for in terms of the retinal image. This also implies, however, that the subsequent divergence of the *LR* and *Opp* curves is not explicable in terms of the retinal image.

The re-occurring performance dip in the *LR* condition must be an effect of stereo processing, because the *LR* and *Opp* stimuli do not differ before disparities have been processed.

In repetition, a basic characteristic is that the intra-pair distance between corresponding elements is the same, say  $D$ , for all pairs. At the retinal level, the *LR* segregation corresponds to a shift of the left-hand or right-hand half of the pattern, which either increases or decreases the intra-pair distance for all pairs by the same amount, that is, the new intra-pair distance is again the same for all pairs. By the *Mat* segregation, repetition pairs are shifted, so that, again, the intra-pair distance remains the same for all pairs. The *Opp* segregation, however, does not preserve this characteristic. In one half of the pairs, the left-hand element is shifted, say by a horizontal distance  $c$ , yielding a new intra-pair distance of  $D - c$ ; in the other half of the pairs, the right-hand element is shifted, yielding a new intra-pair distance of  $D + c$ . In total, this suggests that  $Mat \approx LR > Opp$ , which is what we found not only for short presentation times but also for longer ones.

Hence, our data suggest that regularity detection shifts from a retinal frame of reference to a stereoscopic frame of reference. This indicates a genuine interaction between regularity cues and depth cues, that is, not merely an interference of regularity detection by stereo processing. This is clear for repetition: spreading structurally corresponding elements across depth planes does not necessarily hinder the repetition percept. Rather, the detectability of repetition depends on whether the depth segregation agrees with the perceptual structure of repetition. Next, we discuss this issue more theoretically.

#### **4.4.3 Algorithmic, part 2: Regularity-detection anchors in depth**

Jenkins (1983) proposed that the regularity-detection mechanism uses virtual lines between corresponding elements as the first-order anchors to propagate from. In both symmetry and repetition, these virtual lines exhibit orientational uniformity; in addition, the virtual lines are midpoint collinear in symmetry and have a constant length in repetition. Wage-



mans (Wagemans, 1995; Wagemans et al., 1991, 1993) noticed that orientational uniformity and midpoint collinearity also hold for the virtual lines in skewed symmetry which, nevertheless, is less salient than nonskewed symmetry. He therefore proposed additional second-order anchors in the form of trapezoids (in symmetry) and parallelograms (in repetition), composed of two virtual lines each. These second-order anchors are distorted by skewing, which explains the lesser saliency of skewed symmetry. Because the first-order and second-order anchors as such do not yet explain that symmetry is more salient than repetition, van der Helm & Leeuwenberg (1999) proposed in addition that symmetry detection propagates exponentially but that repetition detection propagates linearly (they inferred this directly from the holographic approach in van der Helm & Leeuwenberg, 1996).

So far, the foregoing ideas about first-order and second-order anchors have been applied only to retinal projections of visual regularities. The question now is whether these ideas are consistent with our findings for regularities in stereoscopic space. Because both midpoint co-planarity (the 3-D analogue of 2-D midpoint collinearity) in symmetry and constant length in repetition are preserved under all three stereoscopic manipulations, these segregations should manifest themselves in violations of the first-order orientational uniformity or in perturbations of the second-order anchors.

*Symmetry.* In both *LR* and *Opp* stimuli, structurally corresponding elements are spread across two depth planes. The angle of a virtual line relative to the frontal plane is larger the closer the elements are to the symmetry axis. Therefore, both *LR* and *Opp* stimuli violate orientational uniformity. In *LR* stimuli, the angles of all virtual lines are either positive or negative while, for *Opp* stimuli, both positive and negative angles occur. Hence, the degree of violation is higher for *Opp* than for *LR*. In *Mat* stimuli, all angles are zero, thus preserving orientational uniformity, and only in *Mat* stimuli, the second-order trapezoids remain intact. In total, this suggests that  $Mat > LR > Opp$ , which is what we found for presentation times of 400 ms and 600 ms.

*Repetition.* In *LR* stimuli, all virtual lines have the same angle relative to the frontal plane, thus preserving orientational uniformity. In *Opp* stim-

uli, orientational uniformity is violated, because both positive and negative angles occur. In *Mat* stimuli, all angles are zero, thus again preserving orientational uniformity. Furthermore, in *LR* and *Mat* stimuli but not in *Opp* stimuli, the second-order parallelograms remain intact. In total, this suggests that  $Mat \approx LR > Opp$ , which is what we found for presentation times of 200–800 ms.

The preceding analysis shows that our findings for regularities in stereoscopic space can be understood by considering the proposed first-order and second-order anchors of the regularity-detection mechanism in a stereoscopic frame of reference. This gives further support to the idea of a genuine interaction between regularity cues and depth cues. In the next subsection, we review neuroimaging studies on stereopsis and regularity processing to examine the neural plausibility of such an interaction between regularity and depth cues.

#### **4.4.4 Implementational: Neural interaction of regularity and depth**

Stereopsis cannot be pinpointed to be implemented in a specialized neural location. Rather, stereopsis-related activation has been found in many areas, such as V3, V3A, MT+, and parietal regions (e.g., Fortin et al., 2002; Gulyás & Roland, 1994; Merboldt et al., 2002). However, peak activation is usually found in extrastriate areas V3 and V3A (Backus et al., 2001; Gillaie-Dotan et al., 2002; Kourtzi & Kanwisher, 2001; Kwee et al., 1999; Mendola et al., 1999; Negawa et al., 2002; Ptito et al., 1993). Furthermore, there seems to be a neural differentiation between absolute disparity processing and relative disparity processing. While dorsal areas V3A, MT+ and V7 code absolute disparity but not relative disparity, ventral areas hV4 and V8 are sensitive to both (Neri et al., 2004). Single-cell studies in monkeys support the involvement of higher ventral stream areas in disparity-defined shape processing (e.g., Janssen et al., 2000a,b, 2003). Finally, Brouwer et al. (2005) found transient activation in areas V4d-topo, V3A, and V7, correlated with the onset of stereoscopic perception. They also found sustained activation in areas V4v, VP, and LOC, correlated with the

stereoscopic percept. They proposed that the latter areas code for shapes defined by disparity.

In contrast to stereopsis, regularity detection has only recently become a topic in neuroimaging. While an initial study reported DLO (dorsolateral occipital cortex) to be involved in symmetry perception (Tyler et al., 2005), a follow-up study reported a more distributed pattern of activation (Sasaki et al., 2005). That is, this follow-up study reported high levels of activation in V3A, V4, V7, and LOC, marginal activation in V3, and virtually no symmetry-specific activity elsewhere. More recently, Chen et al. (2007) showed that frontally viewed faces also increase activation in these areas relative to their phase-scrambled versions, and they argued that these areas may also feed the adjacent OFA (occipital face area), which seems to be involved in processing specific to facial symmetry.

Evidently, there are common sites of activation for processing related to stereopsis and symmetry detection, namely, extrastriate area V3A and ventral stream area LOC. Symmetry detection could be mediated by stereoprocessing directly via interactions in these regions, or indirectly via feedback loops to V1.

To elaborate on the latter, Lee et al. (1998) proposed that V1 might serve as a high resolution buffer used for computations by extrastriate visual areas. This suggests that recurrent feedback from stereoprocessing in V3A might be relayed to symmetry processing areas via V1. This does not seem very plausible, however. First, so far, neuroimaging studies did not report V1 activation related specifically to symmetry detection. Second, although V3A showed the strongest response in stereoprocessing, it codes only absolute disparity, but relative-disparity processing is needed in our stimuli.

In contrast, LOC is associated with object perception (Grill-Spector, 2003; Malach et al., 1995) and, as mentioned, it has been proposed to be involved in coding disparity-defined shapes. This makes LOC a good candidate for the locus of symmetry-depth interaction. The foregoing suggests that this interaction might take the form of a direct competition between the stimulus interpretation defined by disparity versus the stimulus interpretation defined by regularity.

## **4.5 Conclusion**

Regularity and depth are not processed one after the other. We presented psychophysical, theoretical, and neurofunctional evidence that both regularity detection and stereo processing are ongoing processes that interact dynamically over time. During this interaction, the detection of symmetry and repetition shifts from a retinal frame of reference to a stereoscopic frame of reference, yielding effects that depend on the regularity at hand. That is, efficient detection of symmetry depends on structural correspondences within depth planes, but efficient detection of repetition does not. This confirms the idea that, to perceptual organization, symmetry is a cue for the presence of one object whereas repetition is a cue for the presence of multiple objects.



## CHAPTER 5

---

### Integration of structure-from-motion and symmetry during surface perception

---

---

This chapter has been adapted from:  
Treder, M. S., & Meulenbroek, R. G. J. (in press). Integration of structure-from-motion and  
symmetry during surface perception. *Journal of Vision*.



Sinusoidal motion of elements in a random-dot pattern can elicit a striking percept of a rotating volume, a phenomenon known as structure-from-motion (SFM). We demonstrate that if the dots defining the volume are 2D mirror-symmetric, novel 3D interpretations arise. In addition to the classical rotating cylinder, one can perceive mirror-symmetric, flexible surfaces bending along the path of movement. In three experiments, we measured the perceptual durations of the different interpretations in a voluntary control task. The results suggest that motion signals and symmetry signals are integrated during surface interpolation. Furthermore, the competition between the rotating cylinder percept and the symmetric surfaces percept is resolved at the level of surface perception rather than at the level of individual stimulus elements. Concluding, structure-from-motion is an interactive process that incorporates not only motion cues but also form cues. The neurofunctional implication of this is that surface interpolation is not fully completed in its designated neural 'engine', MT/V5, but rather in a higher-tier area such as LOC which receives input from MT/V5 and which is also involved in symmetry detection.

## 5.1 Introduction

The principal task of the human visual system is to establish a 3D representation of the visual environment. To this end, it uses a plenitude of depth cues, for instance, ocular cues such as accommodation and binocular disparity, and pictorial cues such as linear perspective, shading, and texture gradients (e.g., Palmer, 1999; Todd, 2004).

Another important source for the extraction of structural 3D information is visual motion. Even in the absence of other depth cues, motion can convey rich information about object structure. In a particularly compelling illustration of this phenomenon, coined kinetic depth effect or structure-from-motion (SFM), sinusoidally moving dots evoke a strong percept of volumetric form (Braunstein, 1962; Green, 1961; Todd & Norman, 1991;



Treue et al., 1991, 1995; Wallach, 1953; for a review, see Andersen & Bradley, 1998; see Movie 1a<sup>1</sup>). The present consensus on the functional implementation of SFM seems to be that, first, the local velocities of individual dots are integrated to derive a global velocity field. Second, mental representations of surfaces are constructed based on this velocity field and they are updated and refined across time (Andersen & Bradley, 1998; Hildreth et al., 1990; Hol et al., 2003; Treue et al., 1991, 1995; Ullman, 1984).

Neurofunctional research attempted to pinpoint the neural correlates of SFM. Bradley et al. (1998) presented evidence from monkey research suggesting MT/V5 as the neural analog of surface interpolation. They showed that, in a bistable rotating cylinder stimulus, the activity of MT/V5 triggered by moving elements is higher when these elements are perceived as being part of the front surface rather than part of the back surface. MT/V5 was also shown to be sensitive to speed gradients, to encode the orientation of surfaces tilted in depth, and to be affected by attention to motion-defined surfaces, with similar results for humans and monkeys (Martinez-Trujillo et al., 2005; Orban et al., 1999; Treue & Andersen, 1996; Vanduffel et al., 2002a; Wannig et al., 2007; Xiao et al., 1997). Nonetheless, there is no stringent evidence requiring that the computation of surfaces is also fully completed in this area. In fact, the involvement in SFM of a number of other cortical areas such as V3A and the lateral occipital complex (LOC) suggests that SFM is supported by a widespread cortical network (Brouwer & van Ee, 2007; Orban et al., 1999; Paradis et al., 2000; Vanduffel et al., 2002a).

Many of these areas are involved not only in motion processing but also in the processing of static form. For instance, (Murray et al., 2003) showed that part of the LOC is activated both by SFM stimuli and by 3D line drawings. Using simultaneous EEG and MEG recordings, Jiang et al. (2008) revealed subsequent activations of MT, LOC and ventral temporal regions to motion-defined 3D shapes. Most importantly, activity in LOC was associated with induced gamma synchronization, a hallmark of perceptual binding.

---

Quicktime movies are included in the online version obtainable at [www.journalofvision.org](http://www.journalofvision.org). Captions belonging to the movies are attached at the end of this chapter.

Despite the remarkable overlap between brain regions involved in SFM and form processing (for a review, see Kourtzi et al., 2008), there have been no complementary reports in the psychophysical literature demonstrating that the computation of motion-defined surfaces is affected by form cues. On the contrary, it has been argued that the spatial structure of dots defining, for instance, a rotating cylinder, does not affect surface interpolation (Li & Kingdom, 2001; Treue et al., 1991).

In this article, we show that structure-from-motion and symmetry are integrated during surface perception, and that this interaction entails novel 3D interpretations. The starting point for this study was an informal observation by the first author which was further substantiated during a pilot experiment with sixteen naive participants. If the parallel projection of dots attached to a rotating cylinder yields a random dot pattern in 2D, the classical interpretations are perceived, that is, a clockwise or counterclockwise rotating cylinder, or two convex or concave surfaces (Movie 1a; Chen & He, 2004; Hol et al., 2003), are perceived. If, however, the parallel projection yields a pattern that is mirror-symmetric about the vertical midline in 2D, a number of additional 3D interpretations arise which have not been covered in the literature yet (Figure 5.1 and Movie 1b). All novel interpretations have in common that one usually perceives two moving surfaces that are mirror-symmetric about a symmetry plane whose 2D projection coincides with the vertical midline. In contrast to the rigid rotating cylinder percept, these surfaces are flexible and they bend along the perceived path of movement. Participants did not report these percepts when exposed to random dot stimuli, suggesting that the perception of symmetric surfaces is linked to the symmetry of the stimulus.

The novel interpretations can be roughly classified according to two characteristics. First, the symmetric surfaces can be perceived as either colliding at the vertical midline and then bouncing off in the opposite direction (colliding surfaces), or as crossing by each other at the vertical midline without any physical contact (crossing surfaces). Second, motion can be cyclic, in which case each surface returns to its perceived 3D position within one cycle of sinusoidal motion, or winding, in which case the surfaces are perceived to wind forward or backward, resembling the movement of a snake (Figure 5.2).

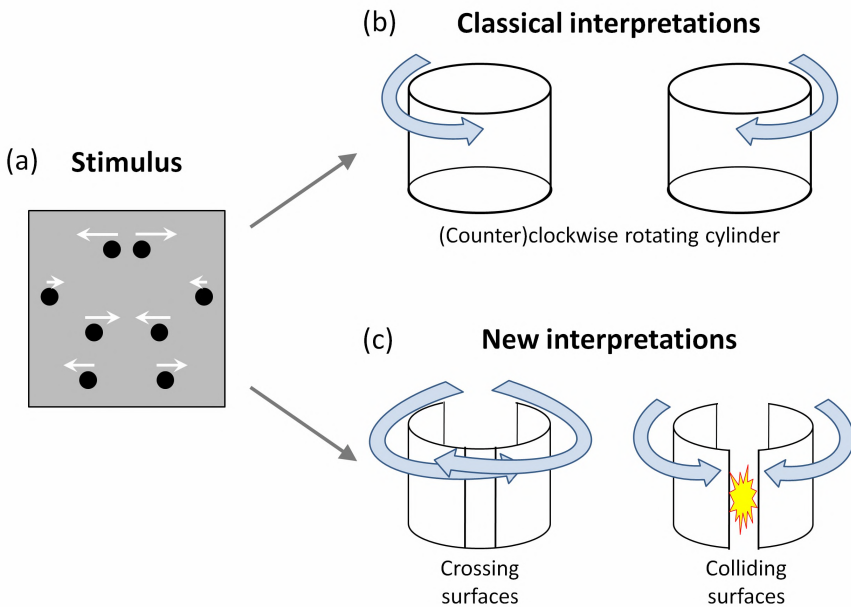


**Figure 5.1.** Perceptual interpretations of the symmetric motion pattern. (a) Schematic display of the physical stimulus, consisting of a dot pattern which is symmetric about the vertical midline. For simplicity, only 8 dots are depicted. As indicated by the white arrows, symmetric dots move in opposite directions with the same velocity so that symmetry is preserved through time. (b) Classical 3D interpretations, a clockwise or counterclockwise rotating cylinder. (c) Novel 3D interpretations, two (or more) symmetric surfaces. At the vertical midline, symmetric elements meet and they can be perceived as crossing by each other without physical contact (crossing surfaces) or as colliding and then bouncing off each other in the opposite direction (colliding surfaces).

The preponderance of perceptual interpretations that are given by a conjunction of motion and symmetry (for convenience, we will use the term symmetry to refer to mirror-symmetry) leads for an integration of motion signals and symmetry signals during surface interpolation. To establish the role of symmetry in the new interpretations, we conducted Experiment 1 wherein we presented only symmetric SFM stimuli. Participants were asked to attempt to perceive either a rotating cylinder or symmetric surfaces, and we measured the perceptual durations of these two interpretations as a function of a number of viewing conditions.

To our knowledge, this is the first empirical study linking symmetry processing and SFM. It is only in computer vision that this link has received

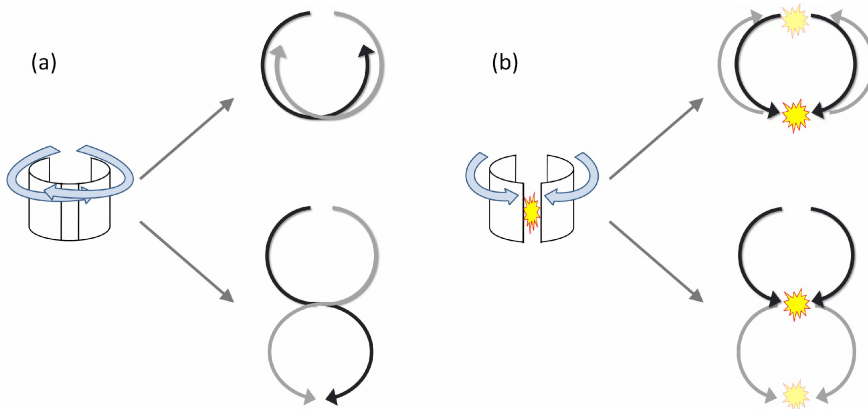


**Figure 5.2.** For each type of symmetric percept, there is a number of possible interpretations of the motion direction. In the schematic examples given here, motion is either cyclic (top row) or winding (bottom row). Movement is sketched from a top-down perspective, with the observer looking from below. Only one cycle is shown for each type of motion; the type of motion keeps repeating upon subsequent cycles. (a) Two possible interpretations of motion direction for the crossing surfaces percept. One surface is depicted as black, the other as grey. In the top view represents, both surfaces rotate continuously about the midpoint in opposite directions. In the bottom view, the surfaces wind forward towards the observer, crossing by each other without perceived physical contact. (b) Two possible interpretations of motion direction for the colliding surfaces percept. In the top view, cyclic motion is shown, with symmetric surfaces moving towards the observer (black arrows), then colliding, reversing direction, and moving back in the other direction (grey arrows). In the bottom view, symmetric surfaces move towards the observer (black arrows), collide, and then move on in the same direction (grey arrows) and keep moving forward. It is also possible to perceive motion in the opposite direction (i.e., surfaces receding from the observer).

some attention. There, symmetry was shown to boost the efficiency of SFM algorithms (Mitsumoto et al., 1992; Poggio & Vetter, 1992; Rothwell et al., 1993; Zabrodsky & Weinshall, 1997).

## 5.2 Experiment 1

Experiment 1 was conducted to substantiate the claim that symmetry processing is involved in the perception of symmetric surfaces. The starting point was the fact that motion processing and symmetry processing have different signatures in terms of eye movements. To be more clear, the efficacy of symmetry detection peaks when the symmetry axis is foveated and it has been shown to drop with increasing eccentricity of the symme-

try axis, at least for static stimuli (e.g., Gurnsey et al., 1998; Herbert & Humphrey, 1996; Saarinen, 1988). In contrast, for the rotating cylinder percept, Hol et al. (2003) showed that perceptual duration is not affected by viewing condition.

Consequently, if symmetry processing is involved in the perception of symmetric surfaces, foveation of the symmetry axis should enhance the perceptual duration of the symmetric surfaces percept. To test this, we introduced four viewing conditions, namely central fixation, bottom fixation (below the stimulus but still on the symmetry axis), left fixation and a free viewing condition. Considering the free viewing condition, we expected that participants focus on the symmetry axis if they were cued to perceive the symmetric surfaces but not if they were cued to perceive the rotating cylinder.

## **5.2.1 Method**

### **5.2.1.1 Apparatus**

We used a Tobii 1750 integrated eye tracker to display stimuli and to register eye movements concurrently. The refresh rate of the 17" screen amounted to 75 Hz and the resolution was  $1280 \times 1024$  px<sup>2</sup>. The sampling rate of the eye tracker was 50 Hz. Viewing distance was about 67 cm. Although Tobii is quite robust to head movements within a certain range, participants were asked to move their head as little as possible throughout the experiment. Participants' button responses were recorded using a button box with a 1 ms temporal accuracy. Stimulus presentation and data acquisition were performed using Neurobehavioural Systems Presentation. This software was complemented by Tobii's eye tracking software and a Presentation interface.

### **5.2.1.2 Participants**

Sixteen right-handed undergraduate students participated in this experiment. All participants were naive with respect to the purpose of the experiment and they had normal or corrected-to-normal vision. None of them had participated in the pilot experiment.

### 5.2.1.3 Stimuli

Parallel projections of dots on a rotating cylinder were used as stimuli. Each stimulus consisted of 48 elements that were uniformly distributed on the cylinder surface and that moved according to a sinusoidal velocity function. During the pilot phase, this number of elements proved most promising in evoking both the rotating cylinder percept and the novel percepts reliably.

All elements were symmetric about the vertical midline of the stimulus. To produce 2D symmetry starting from the cylinder, half of the elements was randomly placed on one half of the cylinder. Subsequently, this half was copied and shifted onto the other half, resulting in the 2D projection being symmetric. In 2D, the two elements in each symmetry pair had equal-magnitude, opposite-sign movement vectors, so that perfect bilateral symmetry was preserved through time.

We also took care of an uncontrolled variable that we became aware of during the pilot experiment. Participants reported that, on some occasions, they perceived four or even six symmetric surfaces. Apparently, clusters of elements were grouped on basis of the relative proximity of the elements on the cylinder surface. We will address a possible implication of this finding in the General Discussion. For the experiments at hand, it was more important to keep this factor under control. Therefore, we imposed a spatial contiguity constraint on the stimulus. This means that, during stimulus generation, the first element was placed randomly on the cylinder surface; each subsequent element was placed randomly, too, but it was constrained to be within the vicinity (80 px) of at least one previously placed element. This method assured that, in the symmetric interpretations, the number of perceived surfaces was always two.

Dot diameter was 10 px or about  $0.22^\circ$  of visual angle. The placement of the elements was limited to a window of  $400 \times 400$  px<sup>2</sup> or  $8.9^\circ \times 8.8^\circ$  of visual angle. The actual height of a stimulus could be lower than 400 px since elements were randomly placed. Angular velocity was  $90^\circ/\text{s}$  and element positions were updated in every frame. All elements were white and the color of the background was set to mean grey value. All stimuli were randomly generated during the experiment and each stimulus was

centered on the screen. Movie 2 gives a sample stimulus.

#### **5.2.1.4 Procedure**

Our aim was to measure perceptual durations of the rotating cylinder percept and the symmetric surfaces percept as a function of exogenous (stimulus characteristics) and endogenous (voluntary control, eye movements) parameters. For classical SFM percepts, it was shown earlier that perceptual switches are subject to voluntary control, but only within certain limits imposed by stimulus and task parameters (Brouwer & van Ee, 2006; Hol et al., 2003; Klink et al., 2008; Raemaekers et al., 2009). To measure perceptual durations, we adopted the procedure used in Hol et al.'s (2003) study on the effects of attention on SFM. The procedure was as follows.

Each trial was initiated via a button press. Subsequently, a cue was presented, indicating which kind of interpretation, the rotating cylinder or the symmetric surfaces, participants should attempt to perceive. The physical stimulus was always symmetric, irrespective of which percept was cued. Upon another button press, a fixation dot appeared and remained on the screen until the end of the trial. Participants had to fixate this dot. After 1 s, the stimulus appeared and remained on the screen for 20 s. The task of the participants was to press the left button as soon as they clearly perceived the cued percept, and to press the right button when the percept switched to the other stimulus class, when it became ambiguous, or when depth was not perceived any more. Participants were told that the exact type of movement (clockwise or counterclockwise rotation in case of the rotating cylinder percept, and cyclic or winding motion in case of the symmetric surfaces percept) was irrelevant and that they should also ignore perceived switches of movement direction.

To test the effects of eye movements, we introduced four viewing conditions. First, central fixation, wherein a fixation dot was presented in the center of the stimulus, on the symmetry axis. Second, bottom fixation, wherein the fixation dot was presented 10 px below the stimulus, however still aligned with the symmetry axis; since stimulus height varied due to the random placement of dots, the absolute distance between the fixation dot and the center of the stimulus necessarily also varied in the bottom fix-

ation condition. Third, left fixation, wherein the fixation dot was presented 100 px to the left of the center, which is halfway between the symmetry axis and the left border of the stimulus. Finally, free viewing, wherein there was no fixation dot.

In the first three viewing conditions, participants were told to strictly fixate the fixation dot. In the free viewing condition, eye movements were unrestricted; participants were instructed, however, to try to move their eyes in such a way that the cued percept could be best perceived. The same kind of symmetric dot pattern was presented in each trial, irrespective of which percept was cued.

Each experiment was preceded by a demonstration, wherein a number of sample stimuli were shown and the possible percepts were explained. All participants were able to perceive the different interpretations. Usually, the rotating cylinder interpretation was perceived first. When instructed to focus on the symmetry axis, participants could readily perceive the symmetric surfaces interpretation. After the demonstration, they completed a practice phase, with one practice trial given for each of the eight subconditions in a random order. This was followed by the experimental phase.

We used two different kinds of cues, one for the rotating cylinder and one for the symmetric surfaces. Also, in order to record eye movements, the eye tracker was calibrated before the start of the experiment. The total number of trials amounted to 2 [percept conditions]  $\times$  4 [viewing conditions]  $\times$  8 [measurements] = 64. The order of trials was randomized.

### **5.2.1.5 Dependent variable**

To measure the perceptual salience of the different percepts, we used perceptual duration as a dependent variable, as specified in Hol et al. (2003). Perceptual duration refers to the total amount of time the cued interpretation is perceived within a trial. Since each stimulus was presented for 20 s, duration was bracketed between 0 s (when the cued interpretation was not perceived at all) and 20 s (when the cued interpretation was perceived all the time). Note that Hol et al. also introduced reaction time, defined as the first point in time wherein the cued interpretation is perceived, as a second dependent measure, which is not considered here. In our opinion,



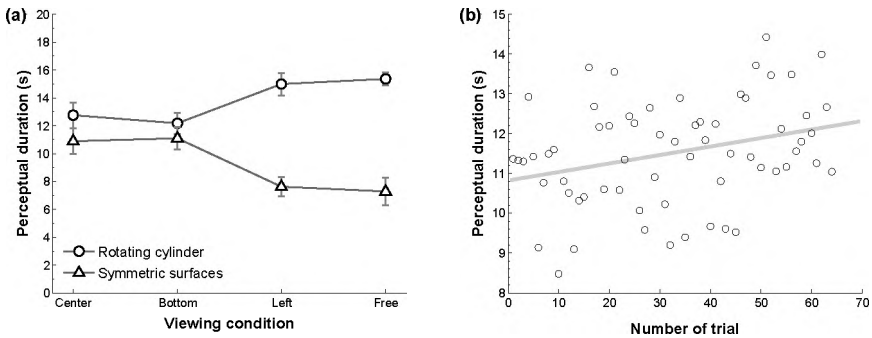


**Figure 5.3.** Perceptual durations in Experiment 1 as a function of percept and viewing condition. Connecting lines have been added for illustrative purposes. Error bars represent 1 S.E.M. Overall, perceptual duration was higher for the rotating cylinder percept than for the symmetric surfaces percept. The perception of symmetric surfaces was more sustained under central or bottom fixation (i.e., when the symmetry axis was fixated) than under left fixation or free viewing. The opposite pattern is found for the rotating cylinder percept, suggesting that the symmetric surfaces percept and the rotating cylinder percept engage in perceptual competition.

it does not add substantial information because it is negatively correlated with perceptual duration, at least for long perceptual durations. We verified this negative correlation by re-running our analyses for reaction time and, as expected, we found opposite patterns of results for perceptual duration and for reaction time (i.e., long perceptual durations corresponded to short reaction times, and vice versa).

## 5.2.2 Results

*Perceptual durations.* We investigated the perceptual durations using a  $2 \times 4$  (Percept  $\times$  Viewing Condition) repeated measures ANOVA. The results are depicted in Figure 5.3a. Overall, the rotating cylinder was perceived more often than the symmetric surfaces (Percept;  $F(1,16) = 44.289$ ,  $p < .001$ ). There was no main effect of Viewing Condition ( $p = .619$ ), but there was a significant interaction between Percept and Viewing Condition,  $F(3,14) = 13.89$ ,  $p < .001$ . Using post-hoc tests, perceptual durations for the rotating cylinder percept and the symmetric surfaces percept were analyzed separately. A Bonferroni-corrected  $\alpha$ -value of  $0.05/6 = 0.0083$  was used.

For the rotating cylinder percept, there was no significant difference in perceptual duration between central fixation and bottom fixation ( $p = .487$ ), and also no difference between left fixation and free viewing ( $p = .535$ ) in terms of perceptual duration. However, there was a significant difference between these two pairs of conditions ( $p < .001$ ). In other words, the rotating cylinder percept was more persistent when fixation was off the symmetry axis (left fixation) or when participants viewed freely than when participants had to fixate the symmetry axis (central fixation and bottom fixation).

The opposite pattern of results was found for the symmetric surfaces condition. Again, there was no significant difference between central fixation and bottom fixation ( $p = .762$ ), and no difference between the left fixation and free viewing ( $p = .756$ ). Also again, there was a significant difference between these two pairs of conditions ( $p < .001$ ), but this time, the difference was in the opposite direction.

To investigate whether voluntary control of the perceptual interpretation gets more effective with time, we fitted a regression line through the perceptual durations as a function of trial number. As depicted in Figure 5.4b, the analysis reveals a positive trend, albeit small. The slope for the rotating cylinder percept was positive (15.88 ms / trial) but not significantly different from zero ( $p = .232$ ), and likewise for the symmetric surfaces percept (24.85 ms / trial;  $p = .084$ ).

*Eye movements.* We examined the fixation conditions and the free viewing condition separately. In all fixation conditions, mean eye position was within one standard deviation of the corresponding fixation dot position. In paired-samples t-tests conducted for x and y dimensions separately, we did not find any significant differences between the conditions in terms of means (all  $p$  values  $> .101$ ) and standard deviations (all  $p$  values  $> .104$ ) of the fixation data.

We also investigated whether there was a difference in terms of the number of saccades between the three fixation conditions. To estimate the number of saccades from the raw data, we applied a spatiotemporal fixation filter consisting of two sliding averaging windows. As Figure 5.4a illustrates, participants made slightly less than one saccade per trial on average. A repeated measures ANOVA did not show any systematic re-

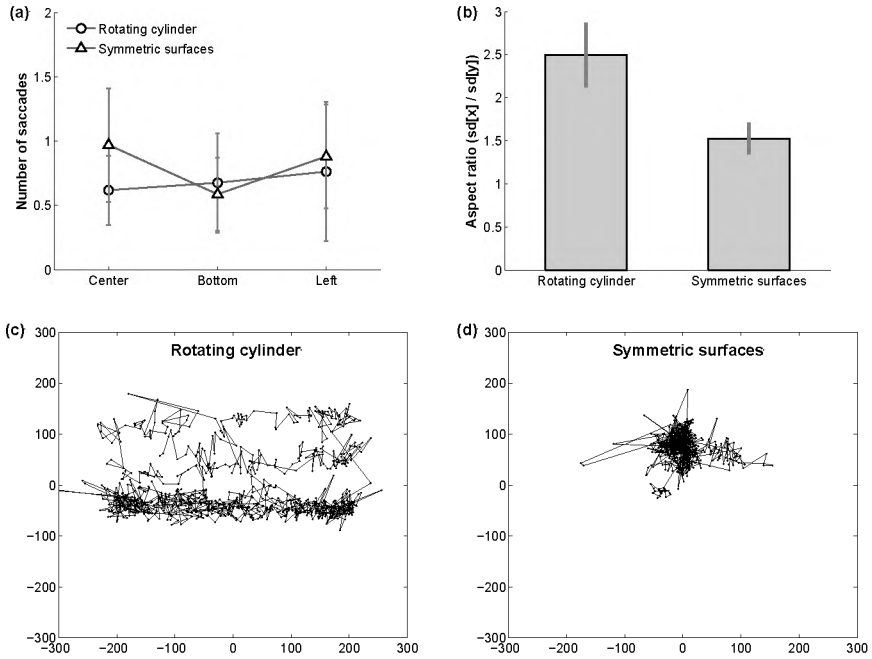


**Figure 5.4.** Results of the analysis of the eye movements data in Experiment 1. (a) Number of saccades as a function of fixation condition (center, bottom, left). Connecting lines have been added for illustrative purposes. (b) Aspect ratio of the extent of horizontal eye movements relative to vertical eye movements in the free viewing condition. The ratio is higher for the rotating cylinder percept, indicating more horizontal (potentially smooth pursuit) eye movements when the rotating cylinder is perceived than when symmetric surfaces are perceived. Error bars in (a) and (b) represent 1 S.E.M. (c) Eye movement trace for the rotating cylinder percept in the free viewing condition. The plot depicts raw data points from one single trial. The coordinate system is centered on the midpoint of the stimulus and fixation coordinates are plotted in pixels. The data on the rotating cylinder percept shows predominantly horizontal eye movements. (d) Eye movement trace for the symmetric surfaces in the free viewing condition, taken from the same participant as the previous plot. The data points culminate at the center of the stimulus.

relationship between number of saccades and experimental condition (all  $p$  values  $> .424$ ), suggesting that participants were fixating equally well in all fixation conditions.

For the free viewing conditions, we were interested in whether there was a qualitative difference in terms of eye movements between the rotating cylinder condition and the symmetric surfaces condition. Figure 5.4cd gives eye movement traces for the rotating cylinder and the symmetric surfaces conditions. The plots suggest that participants performed rather horizontal eye movements and fixations off the symmetry axis in the rotating cylinder condition, but tried to stick to the symmetry axis in the symmetric surfaces condition. To quantify this, we calculated the aspect ratio for the rotating cylinder and symmetric surfaces conditions, that is, the extent of the eye movements along the  $x$  dimension (width) divided by the extent of the eye movements along the  $y$  dimension (height). To this end, we used the standard deviations along each dimension (an alternative would be to take the minimum and maximum values along the  $x$  and  $y$  dimensions, but these values are more susceptible to outliers than the standard deviation). Figure 5.4b depicts the aspect ratio for the rotating cylinder and symmetric surfaces conditions. A paired-samples  $t$ -test revealed that the aspect ratio is indeed different between these two conditions,  $t(16) = 2.404$ ,  $p < .05$ .

### 5.2.3 Discussion

Both the rotating cylinder and the symmetric surfaces could be perceived under all viewing conditions, but we found different effects of viewing condition on the perceptual durations of the two percepts (Figure 5.3a).

For the symmetric surfaces percept, perceptual duration is highest for central fixation and bottom fixation. In other words, efficient perception of the symmetric surfaces requires foveation of the symmetry axis, which suggests that symmetry processing is involved in the perception of symmetric surfaces (see Gurnsey et al., 1998; Herbert & Humphrey, 1996; Saarinen, 1988).

For the rotating cylinder percept, the opposite pattern of results was found. In contrast to Hol et al. (2003), who used similar viewing conditions and who did not find an effect of viewing condition on perceptual dura-

tion, we found that it is higher for free viewing and left fixation than when the symmetry axis is fixated. This pattern of results suggests that there is a direct perceptual competition between the rotating cylinder interpretation and the symmetric surfaces interpretation. Furthermore, the fact that, for each fixation condition, the perceptual duration for the rotating cylinder percept and the symmetric surfaces percept adds up to more than 20 s suggests that voluntary control is involved in the perception of these stimuli, as proposed in other studies on SFM (Brouwer & van Ee, 2006; Hol et al., 2003; Klink et al., 2008). This is in line with the first author's own observations and some informal reports by participants. We analyzed whether voluntary control improves with time and we found a small positive trend for both percepts (Figure 5.3b), but it was not significant in either case.

In terms of eye movements, we found that participants made slightly less than one saccade per trial (Figure 5.4a). This is less than Brouwer & van Ee (2006) reported using a different paradigm (about 10 saccades / min), but it is roughly in the same order of magnitude. Comparing the aspect ratios in the free viewing condition, we found that participants perform relatively more horizontal eye movements when they try to perceive the rotating cylinder than when they try to perceive symmetric surfaces (Figure 5.4b). This suggests that smooth pursuit might have been involved in the perception of the rotating cylinder but not in the perception of symmetric surfaces. The temporal resolution of our eye tracker is too low for a comprehensive analysis of smooth pursuit eye movements, but Brouwer & van Ee (2006) already presented evidence that voluntary control of a bistable rotating sphere is improved with smooth pursuit.

To sum up, first, foveation of the symmetry axis enhances perceptual durations of the symmetric surfaces percept, suggesting that symmetry signals are integrated during SFM processing. Second, we found evidence that the rotating cylinder percept and the symmetric surfaces percept engage in perceptual competition, and showed that voluntary control seems to be involved in resolving this competition. In the SFM literature, it is proposed that the surface level is crucial to perceptual competition (Brouwer & van Ee, 2006; Hol et al., 2003; Klink et al., 2008; Treue et al., 1991, 1995). Furthermore, there is evidence that, in bistable stimuli, surfaces can be

the target of visual attention (Wannig et al., 2007). In light of this, perceptual competition between the different interpretations is most probably resolved at the level of surface perception.

A control experiment, reported next, served to corroborate the idea that the symmetric surfaces percept stems from an interaction between SFM processing and symmetry processing.

### 5.3 Experiment 2

In the stimuli used in Experiment 1, symmetry was defined by perfect point-to-point correspondences between individual dots. Consequently, the dots of each symmetry pair met at the symmetry axis, where net motion (i.e., the sum of motion vectors) amounted to zero. Qian & Andersen (1994) advocated that this kind of motion balance affects motion transparency (i.e., the perception of multiple transparent moving surfaces, a prerequisite for perceiving a rotating cylinder). They presented stimuli consisting of pairs of horizontally moving dots, whereby the dots in each pair had opposite motion vectors. Motion transparency was drastically reduced when the dots in each pair were vertically aligned, that is, when local net motion amounted to zero. To rule out that this motion balance (rather than symmetry processing) underlies the symmetric surfaces percept, we performed a control experiment using also symmetric stimuli whereby motion is not balanced. The rationale was that, if motion balance underlies the symmetric surfaces percept, no symmetric surfaces would be perceived with unbalanced symmetric stimuli.

To create unbalanced symmetric stimuli, we exploited the well-documented fact that symmetry detection is quite robust to various kinds of distortions, such as the addition of noise dots, spatial jittering of symmetry dots, or phase randomization in the frequency domain (Barlow & Reeves, 1979; Dakin & Herbert, 1998; Rainville & Kingdom, 2002; Wagemans et al., 1993). As explicated in the method, a manipulation similar to spatial jitter was applied to remove motion balance but still preserve symmetry on a rough spatial scale. To further corroborate the importance of the interrelated surfaces, rather than explicit point-to-point correspondences, in the

perception of symmetric surfaces, we also added a limited-lifetime condition whereby dot pairs were constantly replaced by new randomly placed dot pairs.

### **5.3.1 Method**

#### **5.3.1.1 Apparatus**

Stimuli were displayed on a 19" monitor at a refresh rate of 100 Hz. Viewing distance was 60 cm and a chinrest was used to restrict head movements. The resolution of the screen was  $1280 \times 1024$  px<sup>2</sup>.

#### **5.3.1.2 Participants**

Twenty-two right-handed undergraduate students participated in this experiment. All participants were naive with respect to the purpose of the experiment and they had normal or corrected-to-normal vision. None of the participants had participated in the previous experiment or in the pilot experiment.

#### **5.3.1.3 Stimuli**

Stimulus parameters were largely identical to the stimulus parameters used in Experiment 1, except for the following. In Experiment 2, our stimuli featured element symmetries and surface symmetries. Element symmetries were identical to the stimuli used in Experiment 1, that is, random dots reflected about the vertical midline, with point-to-point correspondences and, hence, motion balance being preserved. Movie 3a gives a sample stimulus. To create surface symmetries, a spatial jitter manipulation was applied. First, a perfectly symmetric dot pattern was generated. With an unconstrained spatial jitter manipulation, dots could fall out of the boundaries of the original symmetric surfaces. To prevent this, we calculated the convex hull as an approximation of the surface border. The convex hull is the smallest subset of dots of the cluster which, when connected by straight lines, encloses the whole cluster. Then, the dots were randomly shuffled, but only within the borders of the specified surface. By

this, the dots were not symmetric any more but the two surfaces they specified were still symmetric on a rough spatial scale. Movie 3b gives a sample stimulus. In two additional conditions, we applied element symmetry and surface symmetry to stimuli with limited-lifetime dots. In these stimuli, elements disappeared after 120 ms and were instantly replotted at new, randomly chosen locations within the convex hull. To maintain perfect element symmetry, symmetric elements were removed and replotted pair-wise. For surface symmetries, elements were also replotted pair-wise, but the elements of each pair were not symmetric about the vertical midline. Movies 3c and 3d give sample stimuli for element symmetry and surface symmetry with limited-lifetime dots. In all conditions, dot diameter was 10 px, which amounted to about  $0.25^\circ$  of visual angle. The stimulus was constrained to a  $400 \times 400$  px<sup>2</sup> window ( $10.27^\circ \times 9.86^\circ$  of visual angle).

To substantiate the claim that surface symmetry contains 2D symmetry information at a rough spatial scale, we performed a multi-scale symmetry analysis based on Barlow and Reeves' (1979) symmetry detection algorithm. The results, depicted in Figure 5.5, show that surface symmetry contains substantial 2D symmetry information, especially at lower spatial scales. Note that simultaneous processing of symmetry at multiple spatial scales has been demonstrated in humans (e.g., Julesz & Chang, 1979; Rainville & Kingdom, 1999, 2002).

#### 5.3.1.4 Procedure

The procedure was largely identical to the procedure used in Experiment 1. Participants completed 2 [percept conditions]  $\times$  4 [pattern types]  $\times$  9 [measurements] = 72 trials and the order of trials was again randomized.

#### 5.3.2 Results

Again, we subjected perceptual durations to a repeated measures ANOVA. The results are depicted in Figure 5.6. There were significant effects of both Percept and Pattern Type,  $F(1,22) = 5.228$ ,  $p < .05$ , and  $F(3,20) = 3.374$ ,  $p < .05$ , respectively. Interaction was highly significant,  $F(3,20) = 44.997$ ,  $p < .001$ . Using post-hoc tests, perceptual durations for the rotating cylinder percept and the symmetric surfaces percept were analyzed separately. A



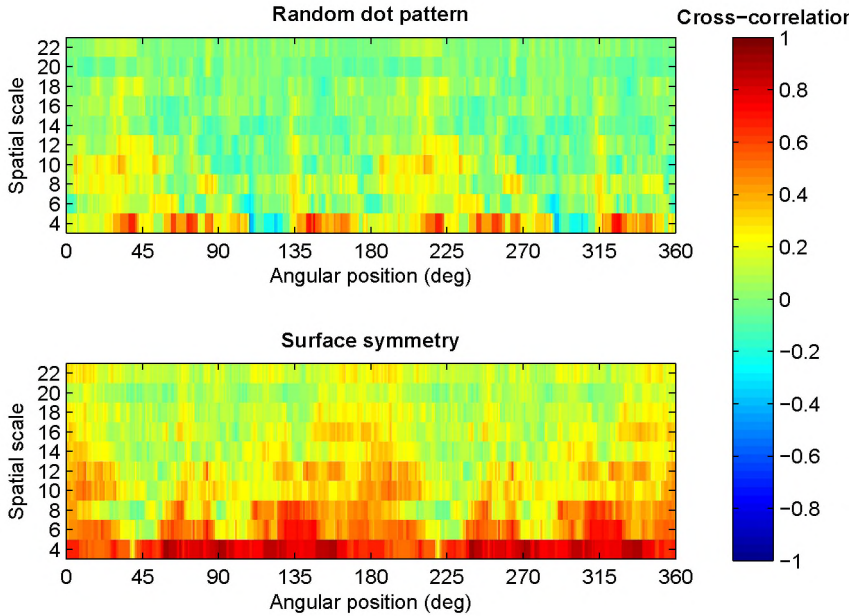


**Figure 5.5.** Multi-scale analysis of symmetry for two sample stimuli, a random dot pattern yielding the classical rotating cylinder percept (top row) and a surface symmetry (bottom row). Symmetry was extracted from static frames for each of the 360 angular positions of the stimulus, depicted along the x-axis, and for ten different spatial scales, depicted along the y-axis. Based on Barlow & Reeves' (1979) symmetry detection algorithm, the image was subdivided into  $S \times S$  square-shaped bins for each value  $S$  of spatial scale, and the numbers of elements contained in each bin were counted. The amount of symmetry was then operationalized as the normalized cross-correlation between the bins on the left and the right stimulus halves for each frame  $\times$  spatial scale combination. The corresponding cross-correlations are depicted in color-coded form, with high correlation signifying high amounts of symmetry. Due to the random placement of dots, spurious symmetry is always present in random dot patterns (red and orange spots), especially at low spatial scales. Although the surface symmetry lacks fine-grained symmetry information, it features high correlations throughout the motion cycle (i.e., at virtually all angular positions) on a rough scale, and symmetry information also extends into higher spatial scales than in the random dot pattern. Mean cross-correlations were determined for 100 random dot stimuli and 100 surface symmetries. An independent samples t-test showed that there is significantly more symmetry information in surface symmetries than in random dot patterns ( $p < .00001$ ).

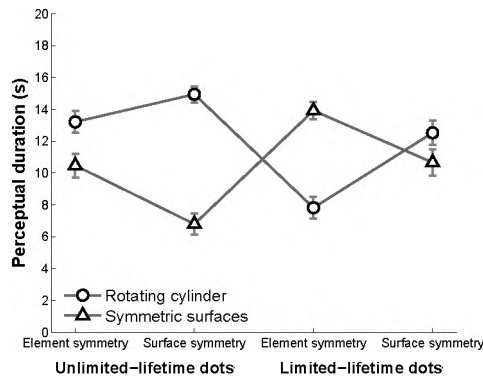


**Figure 5.6.** Perceptual durations in Experiment 2 as a function of stimulus type, with separate lines for the rotating cylinder condition and the symmetric surfaces condition. Connecting lines have been added for illustrative purposes. Error bars represent 1 S.E.M. The results show that the symmetric surfaces can be perceived in the surface condition but that perceptual duration is lower than for element symmetry. This accords with the fact that, in 2D, surface symmetry is 'noisy' due to the spatial jitter manipulation, and it supports the involvement of symmetry processing in the perception of symmetric surfaces. Furthermore, the pattern of results for the rotating cylinder condition is reversed even in the surface conditions, which suggests that the competition between these two percepts is resolved at the surface level rather than at the element level.

Bonferroni-corrected  $\alpha$ -value of  $0.05/6 = 0.0083$  was applied. For the symmetric surfaces percept, we found that perceptual duration is higher for element symmetry than for surface symmetry, for both unlimited-lifetime dots ( $p < .001$ ) and for limited-lifetime dots ( $p < .001$ ). Furthermore, perceptual duration was longer than in the unlimited-lifetime condition, for both element symmetry ( $p < .001$ ) and surface symmetry ( $p < .001$ ). The exactly reverse pattern of results was obtained for the rotating cylinder, with all differences being significant.

### 5.3.3 Discussion

The results show that explicit point-to-point correspondences are not required for perceiving symmetric surfaces. In line with the fact that symmetry is perfect in the element symmetry condition and 'noisy' in the surface symmetry condition, we found that perceptual durations of the symmetric surfaces are longer for the former type of stimulus than for the latter.

Again, this evidence pleads for the genuine involvement symmetry processing in the perceptual construction of surfaces.

Additionally, we found that symmetric surfaces can be perceived with limited-lifetime dots. Moreover, perceptual durations of the symmetric surfaces are higher with limited-lifetime dots than with unlimited-lifetime dots. The latter finding could be due to the fact that the effective (or perceived) dot density is higher when dots are constantly replotted. This results in a more accurate and, therefore, more symmetric representation of the surface than with unlimited-lifetime dots. Alternatively, the increase in perceptual durations might also be due to impoverished motion signals with limited-lifetime dots, decreasing the dominance of the rotating cylinder percept and, thereby, increasing perceptual duration of the symmetric surfaces percept. However, we doubt that this alternative argumentation can fully explain the results at hand. First of all, the presentation duration of the dots (120 ms) was clearly above point-lifetime threshold (50-85 ms; Treue et al., 1991), so that one would not expect depth-from-motion analysis to be seriously obstructed by this manipulation. Second, effective dot density is higher with limited-lifetime stimuli than with unlimited-lifetime stimuli, which should support rather than hamper 3D perception. Third, participants were firmly instructed to respond only to surfaces moving in 3D, not to the percept of a 2D symmetric pattern, so that a decrease in the quality of depth perception should have decreased perceptual durations for both kinds of interpretations.

Another observation made in this experiment is that colliding surfaces are not perceived in the surface symmetry condition, although they can be perceived in the element symmetry conditions. While this might not be surprising, it seems reasonable to assume that it is the ambiguity introduced by the mutual occlusion of symmetric dots at the symmetry axis in the element symmetry condition. Once being occluded, it is ambiguous as to which element is which. If this kind of identity ambiguity is indeed responsible for the colliding surfaces percept, 'labeling' the elements should affect which of interpretations is perceived. This issue was addressed in the next experiment.

## 5.4 Experiment 3

In this experiment, we investigated whether it is the ambiguity caused by the mutual occlusion of dots meeting at the symmetry axes which is responsible for the fact that both crossing surfaces and colliding surfaces can be perceived with the same stimulus. To resolve this ambiguity, we 'labeled' elements by using both circles and triangles as element shapes. For the rotating cylinder, Li & Kingdom (1998, 1999, 2001) already showed that the visual system is sensitive to the 'labeling' of elements by means of unique features such as orientation, luminance polarity, and spatial frequency.

### 5.4.1 Method

#### 5.4.1.1 Apparatus

The same apparatus was used as in Experiment 2.

#### 5.4.1.2 Participants

Seventeen right-handed undergraduate students participated in this experiment. All participants were naive with respect to the purpose of the experiment and they had normal or corrected-to-normal vision. None of the participants had participated in the previous experiments or in the pilot experiment.

#### 5.4.1.3 Stimuli

Stimulus parameters were largely identical to the stimulus parameters used in Experiment 2, except for the following. Now, stimulus elements consisted of circles and triangles. Circle diameter and triangle height and width was 13 px (about  $0.33^\circ$  of visual angle); the elements were slightly larger than in Experiments 1 and 2 to make circles and triangles better distinguishable. The discriminability of the two kinds of elements was informally verified during the demonstration of the stimulus.

In each stimulus, half of the elements consisted of circles and the other half consisted of triangles. To vary the amount of ambiguity, we introduced

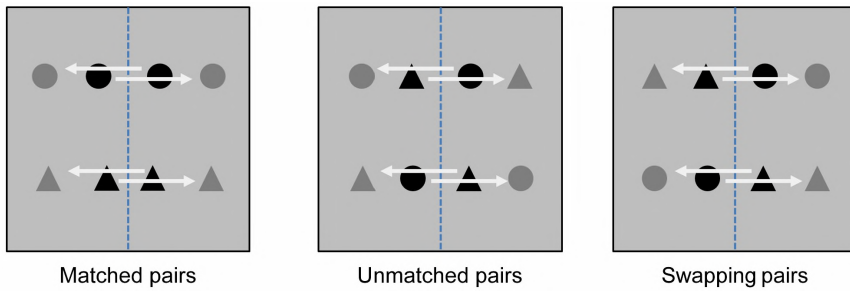


**Figure 5.7.** Schematic sketch of the three stimulus conditions in Experiment 3. Four elements are shown in each display, before (black) and after (grey) crossing the symmetry axis. Arrows indicate the direction of motion. (a) Matched pairs condition. Symmetric elements have equal shapes, and shape does not change after they cross the symmetry axis. This stimulus is analogous to the stimulus used in Experiment 1 and it is compatible with all percepts investigated in Experiment 3 (i.e., rotating cylinder, colliding surfaces, and crossing surfaces). (b) Unmatched pairs condition. Symmetric elements have different shapes, that is, one element is a triangle and the other element is a circle. This stimulus is compatible with the crossing surfaces percept and the rotating cylinder percept but not with the colliding surfaces percept. (c) Swapping pairs condition. As in the unmatched pairs condition, symmetric elements have different shapes. However, when crossing the symmetry axis, the elements swapped shapes, that is, a triangle becomes a circle and vice versa. This stimulus is compatible with the colliding surfaces percept but not with the crossing surfaces percept or the rotating cylinder percept.

three shape pairing conditions. Figure 5.7 gives a schematic overview of these conditions. In the matched pairs condition, the two elements in each symmetry pair had identical shapes. By this, identity ambiguity was preserved so that this condition functioned as a baseline condition. In the unmatched pairs condition, each symmetry pair consisted of one triangle and one circle. In the swapping pairs condition, the elements of each symmetry pair also had different shapes. However, when crossing the midline, the elements swapped shapes. In the unmatched pairs condition and in the swapping pairs condition, identity ambiguity is resolved. More specifically, the unmatched pairs condition yields a stimulus which is compatible with the crossing surfaces interpretation but incompatible with the colliding surfaces interpretation. In contrast, the swapping pairs condition yields a stimulus which is not compatible with the crossing surfaces interpretation but which is compatible with the colliding surfaces interpretation.

#### 5.4.1.4 Procedure

The procedure was largely identical to the procedure used in Experiment 1. In Experiment 3, we investigated the rotating cylinder percept and the symmetric surfaces percept, too, but the symmetric surfaces cue was split into a colliding surfaces cue and a crossing surfaces cue (see Figure 5.1c), so that there were three different cues in total. Participants completed 3 [percept conditions]  $\times$  3 [element shape conditions]  $\times$  8 [measurements] = 72 trials.

#### 5.4.2 Results

We subjected perceptual durations to a 3  $\times$  3 (percept  $\times$  element shape) repeated measures ANOVA. The results are depicted in Figure 5.8. There were significant effects of both Percept and Element Shape,  $F(2,17) = 42.447$ ,  $p < .001$ , and  $F(2,17) = 8.934$ ,  $p < .01$ , respectively. Interaction was also significant,  $F(4,15) = 16.061$ ,  $p < .001$ . Using post-hoc tests, perceptual durations were analyzed separately for the three different percepts. A Bonferroni-corrected  $\alpha$ -value of  $0.05/9 = 0.0056$  was applied.

For the rotating cylinder, perceptual duration was higher for unmatched pairs than for matched pairs ( $p < .05$ ) or swapping pairs ( $p < .05$ ), but this was not significant under the modified  $\alpha$ -value. There was no significant difference between the latter two conditions ( $p = .767$ ). For the crossing surfaces percept, matched pairs tended to produce a higher perceptual duration than both unmatched pairs ( $p = .076$ ) and swapping pairs ( $p = .066$ ), but these effects were also not significant. Similarly, for the colliding surfaces percept, perceptual duration was higher for matched pairs than for unmatched pairs ( $p < .001$ ) and for swapping pairs ( $p < .05$ ), although the latter difference was not significant under the modified  $\alpha$ -value. Moreover, swapping pairs yielded a higher perceptual duration than the unmatched pairs ( $p < .001$ ).

#### 5.4.3 Discussion

The results show that the type of shape pairing affects perceptual durations, especially in the colliding surfaces condition, which indicates that

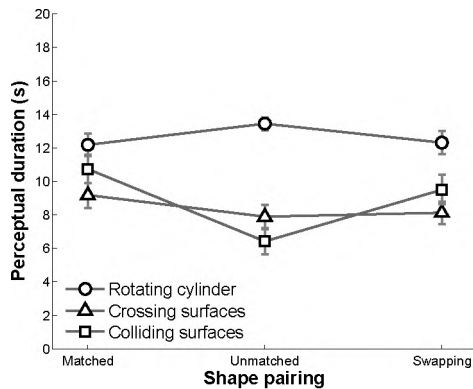


**Figure 5.8.** Perceptual durations in Experiment 3 as a function of shape pairing, for each percept (rotating cylinder, colliding surfaces, and crossing surfaces) separately. Connecting lines have been added for illustrative purposes. Error bars represent 1 S.E.M. The figure shows that disambiguation of the stimulus increases perceptual durations of the corresponding percept, albeit by a small magnitude. In case of the rotating cylinder percept, perceptual duration is highest for the unmatched pairs condition, which most uniquely specifies the rotating cylinder. Interestingly, although disambiguation also increases perceptual duration for the colliding surfaces condition, the matched pairs condition yields even higher durations for both kinds of symmetric surfaces percepts. This is despite the matched condition being ambiguous. Probably, this effect is due to the fact that, in the matched pairs condition, the stimulus is perfectly symmetric even on a fine scale, that is, the elements themselves are not only positioned symmetrically, they are also symmetric with respect to each other.

identity ambiguity plays a role in the perception of symmetric surfaces. The effects are small, however, so that even interpretations which are not compatible with the stimulus manipulation can be readily perceived (in these cases, elements seem to change their shape when crossing the vertical midline). Possibly, these effects might be increased by increasing the difference between the elements, for instance by 'labeling' elements with additional stimulus dimensions, such as size or color.

The pattern of effects is different for each kind of percept. In case of the rotating cylinder, unmatched pairing elicits the highest perceptual duration. This is according to the expectation because unmatched pairings give the most unique specification of a rotating cylinder. Disambiguation also has a positive effect on the colliding surfaces percept but not on the crossing surfaces percept.

For both types of symmetric surfaces percepts, the ambiguous matched pairs condition yielded longer perceptual durations than the non ambigu-

ous conditions. A possible explanation is that, in the matched pairs condition, fine-scale symmetry is preserved but it is violated in the other conditions. In other words, in the matched pairs condition, not only the positioning of elements is symmetric; the elements themselves are also symmetric with respect to each other. Together with the previous experiment, this suggests that the symmetric surfaces percepts are supported by symmetry processing at both fine and rough spatial scales simultaneously.

## 5.5 General discussion

Most research on multi-stable stimuli points at the competition between high-level perceptual interpretations rather than low-level stimulus features (e.g., Grunewald et al., 2002; Kornmeier & Bach, 2005; Parker et al., 2002; Tong et al., 1998). Similarly, in the SFM literature, it has been argued that the competition between different perceptual interpretations, for instance, clockwise versus counterclockwise rotating cylinders, is resolved at the level of surface perception (e.g., Brouwer & van Ee, 2006; Hol et al., 2003; Klink et al., 2008; Treue et al., 1991, 1995). For instance, Brouwer & van Ee (2006) showed that, if the surface of a rotating cylinder features a patch with a high dot density, perceived rotation direction tends towards the motion direction of the surface containing the patch. Crucially, the same effect is found if the patch contains no dots at all, although elements moving in the opposite direction are visible through the gap. This suggests that the dominance of a perceptual interpretation depends on the salience of the motion and not so much on the competition between individual elements.

In all of our experiments, perceptual durations for the different interpretations added up to more than 20 s (22–24 s in Experiments 1 and 2, and up to about 32 s in Experiment 3), which suggests that voluntary control is involved in surface perception. This implicates that perceptual competition takes place at a level of processing that can be targeted by voluntary control. We propose that this level is the level of surface perception, because the different interpretations of the symmetric motion stimulus differ mainly in the perceived spatial arrangement of surfaces. The importance



of surfaces in visual perception was corroborated by Wannig et al. (2007), who showed that visual attention can target motion-defined surfaces and that, moreover, attention to surfaces modulates the activity of MT/V5 neurons. Given this evidence, it seems safe to conclude that the perceptual competition between the rotating cylinder percept and the symmetric surfaces percept is also resolved at the level of surface perception.

The present stimulus is truly multi-stable in the sense that there is not only competition between the rotating cylinder and symmetric surfaces, but there is also competition between different rotating cylinders (clockwise or counterclockwise rotation, and concave or convex surfaces) and different symmetric surfaces (crossing or colliding surfaces, and cyclic or winding motion). In the next two sections, we will expand on the possible determinants of the different symmetric surfaces interpretations and on the implications of the results for the neural implementation of structure-from-motion.

### **5.5.1 Perceptual competition between different symmetric surfaces percepts**

As outlined in the Introduction and as illustrated in Figures 5.1 and 5.2, symmetric surfaces can be perceived in a number of different variations. Two sources of ambiguity seem to govern the competition between these different interpretations.

*Ambiguous depth order.* In patterns of sinusoidally moving dots, depth order is inherently ambiguous. In the rotating cylinder interpretation, the same physical stimulus may be perceived as rotating clockwise or counterclockwise. Surface convexity/concavity can be assigned to the front and back surfaces independently from each other, so that one can also perceive two frontoparallel convex or concave surfaces (Hol et al., 2003).

Symmetry partly resolves this ambiguity by establishing relative depth relationships. Symmetrical elements 'like to be' in the same depth plane and symmetry detection is hampered if symmetric elements are forced on different depth planes via stereo information (Treder & van der Helm, 2007). Therefore, in a symmetric interpretation of the stimulus, symmetric elements are assigned equal depth values. Consequently, what is an

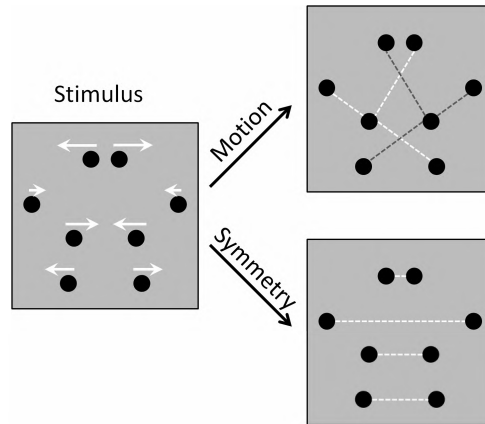


**Figure 5.9.** Grouping by motion (common fate) versus grouping by symmetry. As illustrated here, the two principles of grouping yield conflicting perceptual interpretations. In accordance with the rotating cylinder percept, grouping by motion (common fate) implies that elements moving in the same direction are grouped together, as indicated by the dashed lines. The two resulting surfaces are perceived as being situated in two different depth planes. By this, symmetry is broken because there is no global symmetry plane in 3D. Grouping by symmetry implies that symmetrical elements are grouped together. This implies that symmetrical elements (moving in opposite directions) are located in the same depth plane, which is not reconcilable with the rotating cylinder percept.

ambiguity of rotation direction in the rotating cylinder percept translates to an ambiguity of surface motion direction. Surfaces can be perceived as moving forward (towards the observer), as moving backward (away from the observer), or as moving in cycles. Figure 5.9 illustrates the conflict between grouping by motion and grouping by symmetry.

*Ambiguous element identity.* In perfectly symmetric stimuli, elements of symmetry pairs occlude each other at the vertical midline. When the elements move apart again, there is ambiguity as to which element is which. As shown in Experiment 3, 'labeling' alone does not resolve this ambiguity completely, but, as illustrated in Experiment 2, preventing these occlusions by using surface symmetry rather than element symmetry makes the colliding surfaces interpretation disappear.

While the exact type of the symmetric surfaces percept is specified by these ambiguities, the number of perceived surfaces is not. In the pilot experiment, we noticed that the number of perceived symmetric surfaces can differ from stimulus to stimulus. We conjecture that this is caused

by inhomogeneities in dot density due to the random placement of dots. For the rotating cylinder, patches of high or low dot density have been shown to affect perceptual reversals of rotation direction (Brouwer & van Ee, 2006). For the symmetric surfaces, patches with a relatively high density of elements are perceptually segregated from other patches. That is, surface interpolation takes place between the elements within the patches but, unlike in the rotating cylinder, surface is not extrapolated beyond the patches, resulting in a number of detached moving surfaces. The importance of high intensity patches is illustrated in Movie 4, where a limited-lifetime dot pattern is shown. In contrast to the stimuli used in Experiment 2, the dots are not replotted within pre-specified high-density surfaces but rather randomly on the screen. The rotating cylinder can still be perceived with this stimulus, but the perception of symmetric surfaces collapses. Due to the unconstrained repositioning of symmetry pairs, high density clusters of dots are only transient, counteracting a stable and continuous representation of symmetric surfaces.

The results presented in this study also constrain models about the neural implementation of SFM. Neurally, SFM is supported by a cortical network spanning areas from the ventral and dorsal stream, such as MT/V5, V3A, and LOC (Orban et al., 1999; Paradis et al., 2000; Raemaekers et al., 2009; Vanduffel et al., 2002b). Interestingly, 2D symmetry has been associated with high levels of activation in V3A and LOC (the designated region for feature integration), too, but there was no symmetry-specific activation in MT/V5, the presumed 'engine' of surface interpolation (Sasaki et al., 2005; Tyler et al., 2005). If, however, symmetry signals are not processed in or feedboxed to MT/V5, this implies that the interpolation of the symmetric surfaces is not completed in MT/V5 but rather in a higher-tier area such as LOC.

### **5.5.2 Conclusion**

In this study, we demonstrated the emergence of novel interpretations of the rotating cylinder stimulus when the underlying dot pattern is 2D symmetric. The results of three studies suggest that the new percepts are due to an interaction between SFM processing and symmetry processing and,

furthermore, that the competition between motion-based percepts (i.e., the rotating cylinder) and symmetry-based percepts (i.e., the symmetric surfaces) is resolved at the level of surface perception. This shows that structure-from-motion is a highly interactive process that incorporates not only motion cues but also form cues.

## Movie captions

*Movie 1.* These two movies contrast the classical SFM stimulus and the symmetric motion stimulus. (a) A classical SFM stimulus consisting of 48 randomly positioned dots moving according to a sinusoidal velocity function. The classical interpretation, that is, a cylinder rotating clockwise or counterclockwise can be readily perceived. It is also possible to perceive two convex or concave surfaces (Hol, Koene, and van Ee, 2003). (b) A symmetric motion stimulus. The stimulus was generated in the same way as the random dot stimulus, but this time, dots are located symmetrically about the vertical midline throughout the whole motion cycle (as can be easily verified when one halts the movie). As before, the classical rotating cylinder can be perceived. In addition to this, one can also perceive multiple symmetric surfaces. The surfaces either cross by or collide and bounce off each other at the vertical midline. The percept is most salient under strict fixation of the symmetry axis. If you have difficulties in perceiving the symmetric surfaces, move your mouse pointer to the center of the stimulus and fixate it.

*Movie 2.* The stimulus type used in Experiment 1. To control the number of emerging symmetric surfaces, a spatial contiguity constraint (i.e., each dot has at least one neighbour within 80 px vicinity) was applied in all experiments.

*Movie 3.* Sample stimuli used in Experiment 2. Each movie represents one of the four stimulus conditions. Note that, for the sake of comparability, all stimuli are based on the same surfaces. (a) Element symmetry. This stimulus is identical in its parameters to the stimuli used in Experiment

1. (b) Surface symmetry. Here, the dots are not symmetric with respect to each other, but the two dot clouds yield roughly symmetric surfaces. (c) Element symmetry with limited-lifetime dots. At each moment in time, the display is perfectly symmetric, but elements are constantly being replaced within the boundaries of the pre-specified symmetric regions. One can readily perceive symmetric surfaces. (d) Surface symmetry with limited-lifetime dots. At every moment in time, the display is not symmetric on a dot level, but yet, surface symmetry is easily perceived.

*Movie 4.* A symmetric motion stimulus with limited-lifetime dots. The rotating cylinder can be readily perceived. However, the perception of symmetric surfaces collapses. When symmetric 3D structure is perceived at all, then it is volatile and limited to the lifetime of certain clusters of dots.

## CHAPTER 6

---

Discussion

---



The results of this thesis strongly favor the idea that symmetry detection is an ongoing, non-modular, and highly interactive process that affects, and is affected by, other visual processes. In this last chapter, I evaluate the contribution of the present work and place the findings in the context of prior evidence. This thesis is closed with critical notes on present research and a rundown of possible future investigations.

## 6.1 Status quo

Before discussing the contribution of this thesis to the field of symmetry perception, it is expedient to recap the state of knowledge. For succinctness, this overview will be given in an itemized form:

- symmetry detection operates on 2D projections of 3D objects
- focused attention is not necessary for symmetry processing
- symmetry detection is quick, sensitive to deviations from perfect symmetry, and robust to noise
- the salience of symmetry varies with the orientation of symmetry axis, with the most salient axes being, in order of salience, vertical, horizontal, left/right oblique axes
- generally, the salience of symmetry increases with the number of symmetry axes
- symmetry detection is most efficient when the symmetry axis is foveated, but performance can be equated across stimulus eccentricities by appropriate up-scaling with eccentricity
- the uptake of symmetry information is limited but it is scale invariant
- neurally, symmetry processing is supported by a widespread network of visual areas, including V3A, V7, and LOC



The results of this thesis join this knowledge as follows.

Chapter 2 focused on the interaction between component symmetries in a multiple symmetry. Two characteristics of multiple symmetry were investigated which, in perfect symmetry, are tied to the number of symmetry axes. First, additional structural relationships that multiple symmetry gives rise to and, second, the relative orientation of symmetry axes. Using a number of noise manipulations, these factors were decoupled from the number of symmetry axes. The results suggest that, first, the additional structural relationships contained in multiple symmetry are not picked up during symmetry processing. Second, the relative orientation of symmetry axes affects symmetry detection. In other words, the salience of symmetry is not only affected by the absolute orientation of single symmetry axes, but also by the relative orientation of multiple symmetry axes.

Chapter 3 focused on the interaction between symmetry and repetition and the processing of contours. Based on theoretical grounds, a distinction was made between regularity with matched contour polarity (symmetry and repetition) and a regularity with a mismatch in contour polarity (antisymmetry and antirepetition). The results underpin that this distinction is more than a terminology-issue. The processing of symmetry and repetition is facilitated if task-irrelevant contours exhibit the same regularity, but the processing of antisymmetry and antirepetition is not facilitated if task-irrelevant contours exhibit the same antiregularity. This implies that the definition of symmetry and repetition in visual perception needs to be narrowed, because not all regularities that have been called symmetry and repetition qualify as such.

Chapter 4 focused on the interaction between symmetry and repetition processing and stereoprocessing. Symmetry and repetition information was placed on two stereoscopic depth planes such that relationships between symmetric or repeated elements were preserved within a depth plane or spread out across two depth planes. Additionally, the process of interaction was temporally traced by using presentation times ranging from 200 ms to 1000 ms. The results suggest, first, that the processing of regularity can change from a retinotopic to a stereoscopic frame of reference. Second, the results are in line with the idea that symmetry is a one-object cue and repetition is a multiple-objects cue. Although it was not an explicit subject

of the study, some information about the relative strength of symmetry and repetition processing and stereoprocessing may be inferred from the data. If regularity cues and stereo cues are not reconcilable, the conflict is solved in favor of stereoprocessing. In other words, in these situations, depth segmentation by stereo information cannot be overcome by either symmetry or repetition.

Chapter 5 focused on the interaction between symmetry processing and motion processing. Adding symmetry to random dot structure-from-motion (SFM) stimuli gave rise to a range of novel depth percepts. In these stimuli, grouping by motion and grouping by symmetry enables conflicting perceptual interpretations. However, in contrast to the case of stereo information presented in Chapter 4, there is no clear dominance of symmetry-based percepts or motion-based percepts. Within limits, observers can perceive either interpretation at will.

## 6.2 Notes on empirical research

The rest of this chapter zooms out of the central focus of this thesis – symmetry interactions – to take a peek at more general empirical and theoretical issues in symmetry research. This section leads off with a few remarks on stimulus construction and a small rundown of ready-to-go experiments.

In vision research, an inherent paradox and often criticized point is that it seeks to understand vision in the natural environment by placing par-

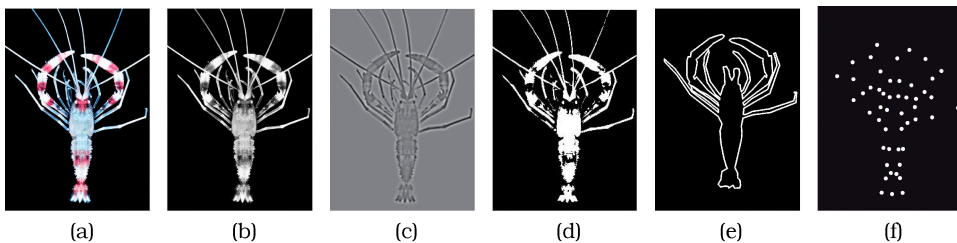


**Figure 6.1.** Levels of abstraction of a visual stimulus, taking the *Stenopus Hispidus* shown in Chapter 1 as an example. (a) Original color image. (b) Image without color information. (c) Image with restricted spatial frequency content. (d) Image without texture information (black-white). (e) Polygon. (f) Dot pattern.

ticipants in highly artificial environments, the very simple reason being that in order to establish a causal relationship between an independent variable (e.g., a stimulus manipulation) and a dependent variable (e.g., psychophysical performance) one has to assure that every aspect of the stimulus except the factor under survey is constant across experimental conditions. This was one of the reasons for the use of abstract stimuli introduced in Chapter 1 and it enabled the acquisition of a large amount of knowledge about symmetry processing.

The good of using abstract stimuli notwithstanding, there are also reasons to also consider complex stimuli in symmetry research. First of all, symmetry detection is an interactive process, which means that it is also affected by other ongoing processes that act upon other features of the stimulus. Hence, it is not for granted that its characteristics established with rather impoverished stimuli also surface under more natural viewing conditions. In other words, complex stimuli can be used as a means to underpin the generalizability of experimental results. Second, complex stimuli may expose aspects of symmetry processing that are not evident in, say, random dot stimuli. To illustrate this, I will give two examples from the literature.

Evans et al. (2000) investigated the perception of symmetry in complex biological images using almost perfectly symmetric images of insects and crustaceans. Perfectly symmetric counterparts were generated by reflecting the left or right halves of the animals about the vertical midline. As baselines, the authors also included abstract versions of the stimuli by turning the images into white silhouettes or into dot patterns by placing dots at locations of conspicuous features of the animal. The results showed that symmetry axis orientation effects known from earlier studies also apply to complex biological images but that, moreover, symmetry detection in these stimuli is easier, suggesting that observers also exploit information on dimensions other than form (e.g., color or texture) to judge symmetry. In the present thesis we did not use stimuli as complex as those used by Evans et al. (2000), but in comparison to many other studies the level of complexity of symmetry processing that we addressed was relatively high.

In another study, Rhodes et al. (2005) investigated the detection of symmetry in frontal views of faces. They showed that the detection of symme-

try is better for upright faces than for inverted faces and contrast-reversed faces, although they all share the same low-level statistics. Furthermore, unlike low-level mechanisms in symmetry detection, symmetry detection in faces was affected by spatial scale. These findings suggest that there might be processes specialized to extracting symmetry from faces.

These two studies testify that the use of complex stimuli can be revealing. Naturally, stimulus complexity is a continuum, so that the contributions of different features can be assessed by varying the complexity of a stimulus. For instance, as Figure 6.1 shows, information on particular feature dimensions (e.g., color, texture, spatial frequency) can be selectively removed to focus on particular features of interest.

In the rest of this sections, a number of further experiments on symmetry perception is outlined based on research reported in this thesis and questions raised by the literature that have not yet been answered.

### 6.2.1 More interactions: symmetry versus texture

This thesis investigated some interactions between symmetry processing and the processing of other visual cues. One out of the numerous features that were not addressed is texture. Texture refers to the visual properties of surfaces. Often, they can be expressed in terms of image statistics, such as orientation content and spatial frequency content. It is unclear whether

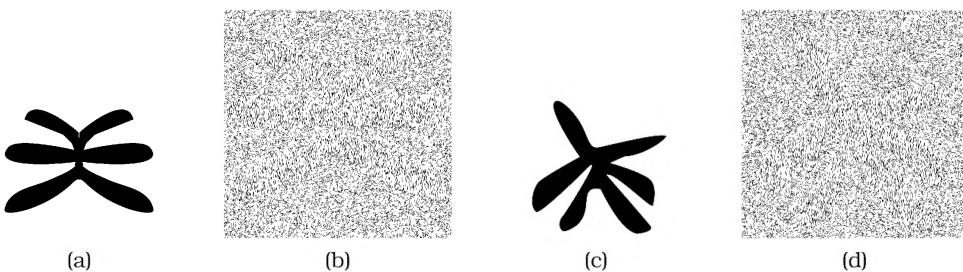


**Figure 6.2.** Possible stimuli for an experiment on the interaction between symmetry processing and shape from texture. (a) Symmetric basis shape. (b) Shape embedded in noise. Noise consists of short, randomly placed and randomly oriented lines. In the area given by the basis shape, all lines are vertical (100% coherence). (c) Random basis shape. (d) Same shape embedded in noise. Again, the shape is given by 100% coherent lines.

symmetry processing can aid in the extraction of shape from texture. To investigate this, one could make use of shapes that are defined by texture alone, such as shapes defined by the coherent orientation of lines. An example is given in Figure 6.2.

Note that, in these stimuli, lines are not positioned symmetrically, so that there is little explicit symmetry information in the image. Yet, the representation extracted from the symmetric basis shape in Figure 6.2 will give a more symmetrical shape than the representation extracted from the random basis shape, and it might be that this additional 'goodness' of the shape facilitates shape from texture processing. The experimental task would have to ensure that participants do not use the marginal image symmetry in the symmetric stimuli as a direct cue. To achieve this, one could, for instance, introduce a two-intervals forced-choice task whereby participants have to compare either two symmetric or two random shapes, rendering symmetry an uninformative cue. The task could then boil down to, for instance, indicating which of the two presented stimuli had more extremities (for instance, the examples in Figure 6.2 all have six extremities).

### 6.2.2 Symmetry integration across spatial scales

As reviewed in Chapter 1, Dakin & Herbert (1998) showed that, in dense noise, the integration of symmetry is limited to a spatial region that inversely scales with spatial frequency. However, they used only bandlimited

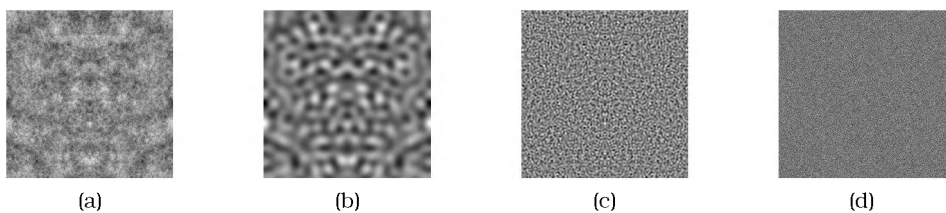


**Figure 6.3.** A broadband symmetry with a  $1/f^2$  spectral slope and its three component bands. (a) Broadband symmetry. (b) Low spatial frequency band. (c) Mid spatial frequency band. (d) High spatial frequency band. By splitting a stimulus into its component bands, the size of the symmetric patch can be varied within each band independently with no effect on other spatial scales.

stimuli. This raises the question about what the size of the symmetry integration region (IR) is in broadband stimuli. After all, broadband stimuli contain information at many spatial scales. To investigate this, one could use a broadband stimulus and tile it into, for instance, three component symmetries occupying different spatial frequency bands, as depicted in Figure 6.3. By varying the size of the symmetrical patch at each spatial scale separately, one could explore how symmetry information is integrated in broadband stimuli.

### 6.2.3 Symmetry integration: the role of redundancy

Rainville & Kingdom (2002) showed that the scale of the symmetry integration region is determined by information density, that is, the number of elements per unit area. The spatial extent of the integration region is such that a constant number of elements is integrated. This suggests that the integration of symmetry is to be understood in information-theoretic terms. If this is so, the spatial extent of the integration region should grow when the symmetry information becomes more redundant. One possibility to increase redundancy is to add more symmetry axes. In a 2-fold sym-

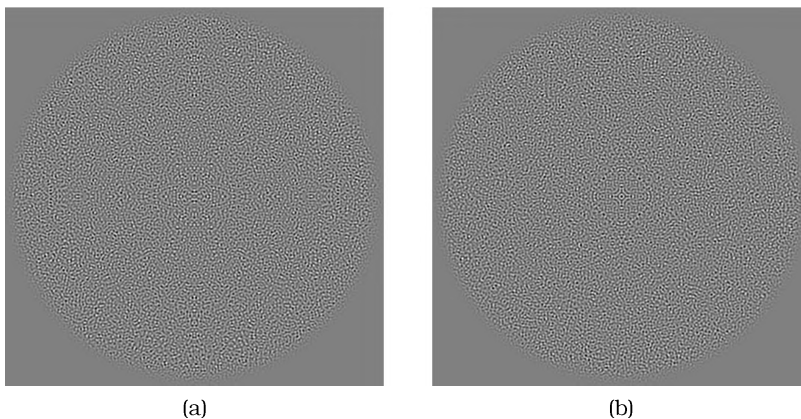


**Figure 6.4.** Bandpass noise patterns containing central symmetric patches. (a) Two-fold symmetry (vertical and horizontal). Except for the border, the whole pattern is symmetric. (b) Four-fold symmetry (vertical, horizontal, and left/right oblique), whereby the symmetry information is restricted to a small central patch.

metry, for instance, unique information is contained in one quadrant; the rest of the stimulus can be obtained by reflecting about the vertical and the horizontal midline. In 4-fold symmetry, only one eighth of the stimulus contains unique information. Apart from stimulus redundancy, one might also investigate temporal redundancy by varying presentation time. More information should be integrated if there is more time to do so, at least within certain limits imposed by, for instance, the drop of spatial acuity in the periphery.

### 6.2.4 Symmetry as a depth cue

As stated in Chapter 1, symmetry might not only signal the presence of objects. Once detected, it is also a rich source of information about the orientation of objects. As Figure 6.5 indicates, the parallelity of the virtual lines becomes a gradient of angles with respect to a horizontal line in the 2D projection of a slanted pattern. This gradient gets steeper the farther the symmetry is slanted away from the frontal plane. The visual system, if it were sensitive to the orientation of dipoles (i.e., symmetry pairs), could exploit this systematicity to deduce depth information. This issue could be

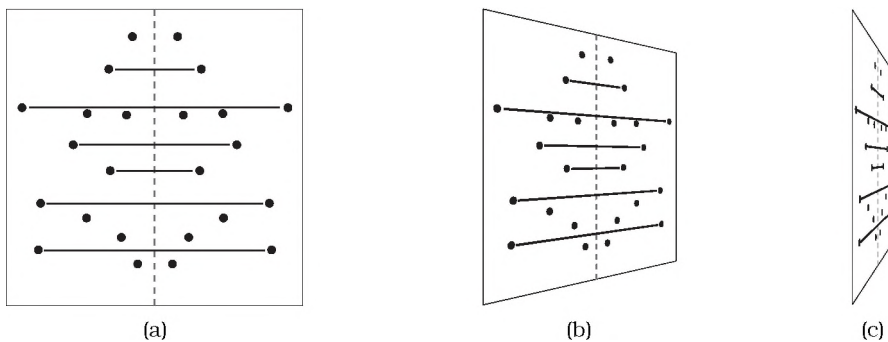


**Figure 6.5.** Different depth views of the same dot pattern. The dashed vertical line indicates the symmetry axis. Solid black lines connect symmetric dots for six of the symmetry pairs. (a) Frontoparallel view of a dot pattern. Virtual lines are parallel with respect to each other. (b) The same dot pattern slanted by  $40^\circ$ . The 2D projection yields lines that are not parallel any more but, rather, converging towards a vanishing point. (c) The same dot pattern slanted by  $80^\circ$ . The difference between the virtual lines in terms of their 2D orientation is larger than for a  $40^\circ$  slant.

investigated using dot stimuli if one would eliminate the depth cues depth cues emanating from the contour of the stimulus by viewing it through an aperture. If the efficacy of depth judgments for symmetric patterns was indeed higher than for random patterns, this would provide direct evidence that the visual system can exploit the orientation of dipoles as a depth cue.

### **6.3 Notes on theoretical research**

There are several models on symmetry perception and all seem to capture some, but not all, known features of symmetry detection. For instance, the transformational approach and the holographic approach specify the structural relationships that play a role in symmetry and other kinds of regularities. The bootstrapping approach points out that the detectability of symmetry can be well predicted by taking into account certain geometric relationships between stimulus elements (although, as we demonstrated in Chapter 2, this does not hold for correlation rectangles). Spatial filtering models, in turn, emphasize the importance of low-level visual processes. They construe symmetry detection as a sequence of mostly primitive filtering operations.

The Achilles heel of many models on symmetry perception, especially representational and process models, is their stimulus specificity. Most models are conceptualized and tested within the framework of a specific kind of stimulus, and sometimes even a specific kind of noise. For instance, the transformational approach (Palmer, 1983), the holographic approach (van der Helm & Leeuwenberg, 1996, 1999, 2004), the Voronoi tessellation model (Dry, 2008), and the bootstrapping approach (Wagemans et al., 1991, 1993) seem to be tailored to dot stimuli. Moreover, the holographic approach makes quantitative predictions for random noise manipulations but not for more realistic manipulations such as jitter. The transformational approach does not really deal with any kind of noise (except for stating that a noisy symmetry does not qualify as a symmetry), and the bootstrapping model, although predicting that jitter hampers symmetry detection, does not make any corresponding quantitative predictions.



The crucial point is that these models rely on discrete information (i.e., sparse stimuli consisting of individual elements), so they collapse when exposed to dense noise stimuli, whether pixel noise or bandpass filtered. Possibly, there are ways to conceive of extensions of the models that would include different kinds of noise and different kinds of stimuli. For instance, one could argue that these models should be understood to act upon discrete features or primitives that are extracted by prior visual processing. However, as long as these extensions and features are not specified and tested using various stimulus manipulations, the models will be of limited application value and probably cannot hold as general models of symmetry perception (although this might not be their pretension).

The appeal of spatial filtering models in this respect is that they are not plagued by the necessity of a discrete representation of stimulus parts. They work simply on raw visual input and, in subsequent stages, on filter output. This is not to say that spatial filtering models are completely stimulus aspecific. One can conceive of manipulations where some spatial filtering models fail but our visual system does not. To give an example, many spatial filtering models cannot be applied when the elements constituting the symmetry have different spatial frequency content, as depicted in Figure 6.6. Obviously, spatial filtering models are limited, too.

As said, all types of models seem to capture relevant aspects of symmetry

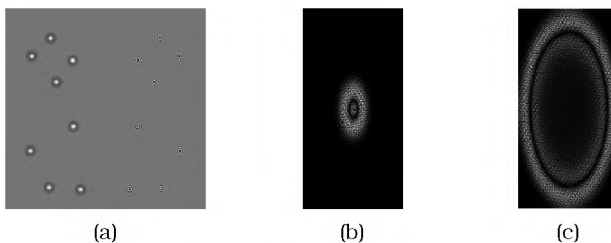


**Figure 6.6.** A dot pattern comprised of elements with different spatial frequency content. (a) The left half of the pattern contains dots with relatively low spatial frequency content, while the right half features high spatial frequency dots. (b) Amplitude spectrum for the left half of the pattern, demonstrating the dominance of low spatial frequencies. (c) Amplitude spectrum for the left half of the pattern, demonstrating the dominance of high spatial frequencies. Despite the different frequency content, the symmetry can be easily perceived.

perception. A comprehensive model would have to bring these aspects together. It should implement known characteristics of symmetry perception such as scale invariance and the effects of different noise manipulations on detectability. At the same time, it should be neurally plausible. In the light of these requirements, spatial filtering models might turn out to be the most promising type of model to depart from. First, they are abstract enough to be able to describe symmetry processing as a multi-stage process. Second, at least for a part, they capitalize on mechanisms which are known to exist in visual cortex. Third, they are applicable to all kinds of stimuli. Fourth, they implicitly implement some of the characteristics of symmetry addressed in more abstract models. To give an example for the last point, the bootstrapping approach points out the importance of orthogonality of symmetry pairs with respect to the symmetry axis; this idea is supported by experimental findings showing that skewed symmetry is more difficult to detect than perfect symmetry (e.g., Wagemans et al., 1992, 1993). A similar reliance on orthogonality is evident in Dakin & Watt's (1994) spatial filtering model; the model employs filters orthogonal to the symmetry axis. Although this was not explicitly tested, it is quite evident that filter output would decrease with increasing skew of the symmetry (whether this decrease is congruent with human performance is to be verified, of course).

## 6.4 Prospect

Symmetry processing, even though just a cogwheel in the large visual clockwork, continues being an intriguing and astonishing subject of research. So far, its versatility resisted all attempts to capture it in a comprehensive model. Although there is now an extensive body of evidence, the research field does not seem yet to be at the verge of comprehension. Therefore, future work will have to focus on a tighter convergence of psychophysical, neurophysiological, and theoretical work, investigating symmetry perception in isolation and in interaction with other visual processes. Eventually, this should lead to the emergence of a comprehensive and plausible model of symmetry perception.



---

## Bibliography

---

- Ahissar, M., & Hochstein, S. (2004). The reverse hierarchy theory of visual perceptual learning. *Trends in Cognitive Sciences*, *8*, 457–464.
- Andersen, R. A., & Bradley, D. C. (1998). Perception of three-dimensional structure from motion. *Trends in Cognitive Sciences*, *2*, 222–228.
- Backus, B. T., Fleet, D. J., Parker, A. J., & Heeger, D. J. (2001). Human cortical activity correlates with stereoscopic depth perception. *Journal of Neurophysiology*, *86*, 2054–2068.
- Barlow, H. B., & Reeves, B. C. (1979). The versatility and absolute efficiency of detecting mirror symmetry in random dot displays. *Vision Research*, *19*, 783–793.
- Baylis, G. C., & Driver, J. (1994). Parallel computation of symmetry but not repetition within single visual shapes. *Visual Cognition*, *1*, 377–400.
- Baylis, G. C., & Driver, J. (1995). Obligatory edge assignment in vision: The role of figure and part segmentation in symmetry detection. *Journal of Experimental Psychology: Human Perception and Performance*, *21*, 1323–1342.
- Baylis, G. C., & Driver, J. (2001). Perception of symmetry and repetition within and across visual shapes: Part-descriptions and object-based attention. *Visual Cognition*, *8*, 163–196.
- Beh, H. C., & Latimer, C. R. (1997). Symmetry detection and orientation perception: Electrocortical responses to stimuli with real and implicit axes of orientation. *Australian Journal of Psychology*, *49*, 128–133.
- Benard, J., Stach, S., & Giurfa, M. (2006). Categorization of visual stimuli in the honeybee *Apis mellifera*. *Animal Cognition*, *9*, 257–270.
- Bertamini, M., Friedenberg, J., & Argyle, L. (2002). No within-object advantage for detection of rotation. *Acta Psychologica*, *111*, 59–81.
- Bertamini, M., Friedenberg, J., & Kubovy, M. (1997). Detection of symmetry and perceptual organization: The way a lock-and-key process works. *Acta Psychologica*, *95*, 119–140.
- Bertone, A., & Faubert, J. (2002). The interactive effects of symmetry and binocular disparity on visual surface representation [Abstract]. *Journal of Vision*, *2*, 94a.
- Blakemore, C., & Campbell, F. W. (1969). On the existence of neurones in the human visual system selectively sensitive to the orientation and size of retinal images. *Journal of Physiology*, *203*, 237–260.

- Borowsky, R., Loehr, J., Kraushaar, G., Kingstone, A., & Sarty, G. (2005). Modularity and intersection of "what", "where" and "how" processing of visual stimuli: A new method of fMRI localization. *Brain Topography*, *18*, 67–75.
- Bradley, D. C., Chang, G. C., & Andersen, R. A. (1998). Encoding of three-dimensional structure-from-motion by primate area MT neurons. *Nature*, *392*, 714–717.
- Braunstein, M. L. (1962). Depth perception in rotating dot patterns: effects of numerosity and perspective. *Journal of Experimental Psychology*, *64*, 415–420.
- Bredfeldt, C. E., & Ringach, D. L. (2002). Dynamics of spatial frequency tuning in macaque V1. *Journal of Neuroscience*, *22*, 1976–1984.
- Brouwer, G. J., & van Ee, R. (2006). Endogenous influences on perceptual bistability depend on exogenous stimulus characteristics. *Vision Research*, *46*, 3393–3402.
- Brouwer, G. J., & van Ee, R. (2007). Visual cortex allows prediction of perceptual states during ambiguous structure-from-motion. *The Journal of Neuroscience*, *27*, 1015–1023.
- Brouwer, G. J., van Ee, R., & Schwarzbach, J. (2005). Activation in visual cortex correlates with the awareness of stereoscopic depth. *The Journal of Neuroscience*, *25*, 10403–10413.
- Bruce, V. G., & Morgan, M. J. (1975). Violations of symmetry and repetition in visual patterns. *Perception*, *4*, 239–249.
- Burge, J., Peterson, M. A., & Palmer, S. E. (2005). Ordinal configural cues combine with metric disparity in depth perception. *Journal of Vision*, *5*, 534–542.
- Carmody, D. P., Nodine, C. F., & Locher, P. J. (1977). Global detection of symmetry. *Perceptual & Motor Skills*, *45*, 1267–1273.
- Cham, T.-J., & Cipolla, R. (1994). Skewed symmetry detection through local skewed symmetries. In *Proceedings of the conference on British machine vision (vol. 2)*.
- Chandrasekaran, C., Canon, V., Dahmen, J. C., Kourtzi, Z., & Welchman, A. E. (2007). Neural correlates of disparity-defined shape discrimination in the human brain. *Journal of Neurophysiology*, *97*, 1553–1565.
- Chen, C.-C., Kao, K.-L. C., & Tyler, C. W. (2007). Face configuration processing in the human brain: The role of symmetry. *Cerebral Cortex*, *17*, 1423–1432.
- Chen, X., & He, S. (2004). Local factors determine the stabilization of monocular ambiguous and binocular rivalry stimuli. *Current Biology*, *14*, 1013–1017.
- Corbalis, M. C., & Roldan, C. E. (1974). On the perception of symmetrical and repeated patterns. *Perception & Psychophysics*, *16*, 136–142.
- Csathó, Á., van der Vloed, G., & van der Helm, P. A. (2003). Blobs strengthen repetition but weaken symmetry. *Vision Research*, *43*, 993–1007.

- Csathó, Á., van der Vloed, G., & van der Helm, P. A. (2004). The force of symmetry revisited: symmetry-to-noise ratios regulate (a)symmetry effects. *Acta Psychologica*, *117*, 233–250.
- Dakin, S. C., & Herbert, A. M. (1998). The spatial region of integration for visual symmetry detection. *Proceedings of the Royal Society of London B*, *265*, 659–664.
- Dakin, S. C., & Watt, R. J. (1994). Detection of bilateral symmetry using spatial filters. *Spatial Vision*, *8*, 393–413.
- Delius, J. D., & Nowak, B. (1982). Visual symmetry recognition by pigeons. *Psychological Research*, *44*, 199–212.
- Driver, J., Baylis, G. C., & Rafal, R. D. (1992). Preserved figure-ground segregation and symmetry perception in visual neglect. *Nature*, *360*, 73–75.
- Dry, M. J. (2008). Using relational structure to detect symmetry: a Voronoi tessellation based model of symmetry perception. *Acta Psychologica*, *128*, 75–90.
- Ehrenstein, W. H., Spillmann, L., & Sarris, V. (2003). Gestalt issues in modern neuroscience. *Axiomathes*, *13*, 433–458.
- Erkelens, C. J., & van Ee, R. (2007). Monocular symmetry in binocular vision. *Journal of Vision*, *7*, 5.
- Evans, C. S., Wenderoth, P., & Cheng, K. (2000). Detection of bilateral symmetry in complex biological images. *Perception*, *29*, 31–42.
- Farrell, B. (2005). The perception of symmetry in depth [Abstract]. *Journal of Vision*, *5*, 519a.
- Feldman, J. (1999). The role of objects in perceptual grouping. *Acta Psychologica*, *102*, 137–163.
- Fitts, P., Weinstein, M., Rappaport, M., Anderson, N., & Leonard, J. (1956). Stimulus correlates of visual pattern recognition: A probability approach. *Journal of Experimental Psychology*, *51*, 1–11.
- Fortin, A., Ptito, A., Faubert, J., & Ptito, M. (2002). Cortical areas mediating stereopsis in the human brain: a PET study. *Neuroreport*, *13*, 895–898.
- Friedenberg, J., & Bertamini, M. (2000). Contour symmetry detection: the influence of axis orientation and number of objects. *Acta Psychologica*, *105*, 107–118.
- Fukushima, K., & Kikuchi, M. (2006). Symmetry axis extraction by a neural network. *Neurocomputing*, *69*, 1827–1836.
- Garner, W. R. (1974). *The processing of information and structure*. Potomac, MD: Erlbaum.
- Gillaie-Dotan, S., Ullman, S., Kushnir, T., & Malach, R. (2002). Shape-selective stereo processing in human object-related visual areas. *Human Brain Mapping*, *15*, 67–79.

- Giurfa, M., Eichmann, B., & Menzel, R. (1996). Symmetry perception in an insect. *Nature*, 382, 458–461.
- Glachet, R., Lapreset, J. T., & M-Dhome (1993). Locating and modelling a flat symmetric object from a single perspective image. *CVGIP: Image Understanding*, 57, 219–226.
- Glass, L. (1969). Moiré effect from random dots. *Nature*, 223, 578–580.
- Graham, N. V. S. (1989). *Visual pattern analyzers*. Oxford University Press.
- Grammer, K., Fink, B., Møller, A. P., & Manning, J. T. (2005). Physical attractiveness and health: comment on Weeden and Sabini (2005). *Psychological Bulletin*, 131, 658–661.
- Grammer, K., Fink, B., Møller, A. P., & Thornhill, R. (2003). Darwinian aesthetics: sexual selection and the biology of beauty. *Biological reviews of the Cambridge Philosophical Society*, 78, 385–407.
- Grammer, K., & Thornhill, R. (1994). Human (*homo sapiens*) facial attractiveness and sexual selection: the role of symmetry and averageness. *Journal of Comparative Psychology*, 108, 233–242.
- Gray, C. M. (1999). The temporal correlation hypothesis of visual feature integration: still alive and well. *Neuron*, 24, 31–47.
- Green, B. F. (1961). Figure coherence in the kinetic depth effect. *Journal of Experimental Psychology*, 62, 272–282.
- Grill-Spector, K. (2003). The neural basis of object perception. *Current Opinion in Neurobiology*, 13, 159–166.
- Grunewald, A., Bradley, D. C., & Andersen, R. A. (2002). Neural correlates of structure-from-motion perception in macaque V1 and MT. *The Journal of Neuroscience*, 22, 6195–6207.
- Gulyás, B., & Roland, P. E. (1994). Binocular disparity discrimination in human cerebral cortex: Functional anatomy by positron emission tomography. *Proceedings of the National Academy of Sciences of the United States of America*, 91, 1239–1243.
- Gur, M., Kagan, I., & Snodderly, D. M. (2005). Orientation and direction selectivity of neurons in V1 of alert monkeys: functional relationships and laminar distributions. *Cerebral Cortex*, 15, 1207–1221.
- Gurnsey, R., Herbert, A. M., & Kenemy, J. (1998). Bilateral symmetry embedded in noise is detected accurately only at fixation. *Vision Research*, 38, 3795–3803.
- Hamada, J., & Ishihara, T. (1988). Complexity and goodness of dot patterns varying in symmetry. *Psychological Research*, 50, 155–161.
- Herbert, A. M., & Humphrey, G. K. (1996). Bilateral symmetry detection: testing a 'callosal' hypothesis. *Perception*, 25, 463–480.

- Hildreth, E. C., Grzywacz, N. M., Adelson, E. H., & Inada, V. K. (1990). The perceptual buildup of three-dimensional structure from motion. *Perception & Psychophysics*, *48*, 19–36.
- Hochberg, J. E., & McAlister, E. (1953). A quantitative approach to figural "goodness". *Journal of Experimental Psychology*, *46*, 361.
- Hol, K., Koene, A., & van Ee, R. (2003). Attention-biased multi-stable surface perception in three-dimensional structure-from-motion. *Journal of Vision*, *3*, 486–498.
- Howard, I. P. (1982). *Human visual orientation*. New York: Wiley.
- Huang, L., & Pashler, H. (2002). Symmetry detection and visual attention: a "binary-map" hypothesis. *Vision Research*, *42*, 1421–1430.
- Hubel, D. H., & Wiesel, T. N. (1968). Receptive fields and functional architecture of monkey striate cortex. *Journal of Physiology*, *195*, 215–243.
- Höfel, L., & Jacobsen, T. (2007). Electrophysiological indices of processing aesthetics: Spontaneous or intentional processes? *International Journal of Psychophysiology*, *65*, 20–31.
- Ishiguchi, A., & Yakushijin, R. (1999). Does symmetry structure facilitate the depth separation between stereoscopically overlapped dot planes? *Perception & Psychophysics*, *61*, 151–160.
- Jacobsen, T., & Höfel, L. (2003). Descriptive and evaluative judgment processes: behavioral and electrophysiological indices of processing symmetry and aesthetics. *Cognitive, Affective and Behavioral Neuroscience*, *3*, 289–299.
- Janssen, P., Vogels, R., Liu, Y., & Orban, G. A. (2003). At least at the level of inferior temporal cortex, the stereo correspondence problem is solved. *Neuron*, *37*, 693–701.
- Janssen, P., Vogels, R., & Orban, G. A. (2000a). Selectivity for 3D shape that reveals distinct areas within macaque inferior temporal cortex. *Science*, *288*, 2054–2056.
- Janssen, P., Vogels, R., & Orban, G. A. (2000b). Three-dimensional shape coding in inferior temporal cortex. *Neuron*, *27*, 385–397.
- Jenkins, B. (1982). Redundancy in the perception of bilateral symmetry in dot textures. *Perception & Psychophysics*, *32*, 171–177.
- Jenkins, B. (1983). Component processes in the perception of bilaterally symmetric dot textures. *Perception & Psychophysics*, *34*, 433–440.
- Jiang, Y., Boehler, C. N., Nönnig, N., Düzel, E., Hopf, J.-M., Heinze, H.-J., & Schoenfeld, M. A. (2008). Binding 3-D object perception in the human visual cortex. *Journal of Cognitive Neuroscience*, *20*, 553–562.
- Joung, W., & Latimer, C. (2003). Tilt aftereffects generated by symmetrical dot patterns with two or four axes of symmetry. *Spatial Vision*, *16*, 155–182.



- Joung, W., van der Zwan, R., & Latimer, C. R. (2000). Tilt aftereffects generated by bilaterally symmetrical patterns. *Spatial Vision*, *13*, 107–128.
- Julesz, B. (1960). Binocular depth perception of computer generated patterns. *Bell Systems Technical Journal*, *39*, 1125.
- Julesz, B. (1966). Binocular disappearance of monocular symmetry. *Science*, *153*, 657–658.
- Julesz, B. (1971). *Foundations of cyclopean perception*. Chicago, IL: University of Chicago Press.
- Julesz, B., & Chang, J. J. (1979). Symmetry perception and spatial-frequency channels. *Perception*, *8*, 711–718.
- Kanizsa, G. (1985). Seeing and thinking. *Acta Psychologica*, *59*, 23–33.
- Khuu, S. K., & Hayes, A. (2005). Glass-pattern detection is tuned for stereo-depth. *Vision Research*, *45*, 2461–2469.
- Klink, P. C., van Ee, R., Nijs, M. M., Brouwer, G. J., Noest, A. J., & van Wezel, R. J. A. (2008). Early interactions between neuronal adaptation and voluntary control determine perceptual choices in bistable vision. *Journal of Vision*, *8*, 16.1–1618.
- Koffka, K. (1935). *Principles of Gestalt Psychology*. London: Routledge & Kegan Paul.
- Koning, A., & van Lier, R. (2003). Object-based connectedness facilitates matching. *Perception & Psychophysics*, *65*, 1094–1102.
- Koning, A., & van Lier, R. (2004). Mental rotation depends on the number of objects rather than on the number of image fragments. *Acta Psychologica*, *117*, 65–77.
- Koning, A., & Wagemans, J. (2009). Detection of symmetry and repetition in one and two objects. Structures versus strategies. *Experimental Psychology*, *56*, 5–17.
- Kontsevich, L. L. (1996). *Human symmetry perception and its computational analysis*, chap. Symmetry as a depth cue, (pp. 331–348). Zeist, The Netherlands: VSP.
- Kornmeier, J., & Bach, M. (2005). The Necker cube—an ambiguous figure disambiguated in early visual processing. *Vision Research*, *45*, 955–960.
- Kourtzi, Z., & Kanwisher, N. (2001). Representation of perceived object shape in the human lateral occipital complex. *Science*, *293*, 1506–1509.
- Kourtzi, Z., Krekelberg, B., & van Wezel, R. J. A. (2008). Linking form and motion in the primate brain. *Trends in Cognitive Sciences*, *12*, 230–236.
- Kovesi, P. (1997). Symmetry and asymmetry from local phase. In *AI'97, Tenth Australian Joint Conference on Artificial Intelligence*, (pp. 185–190).

- Kovesi, P. (1999). Image features from phase congruency. *Videre: A Journal of Computer Vision Research*, 1.
- Kwee, I. L., Fujii, Y., Matsuzawa, H., & Nakada, T. (1999). Perceptual processing of stereopsis in humans: high-field (3.0-tesla) functional MRI study. *Neurology*, 53, 1599–1601.
- Köhler, W. (1920). *Die physischen Gestalten in Ruhe und im stationären Zustand [Static and stationary physical shapes]*. Braunschweig, Germany: Vieweg.
- Labonté, F., Shapira, Y., & Cohen, P. (1993). A perceptually plausible model for global symmetry detection. In *Proceedings of the Fourth International Conference on Computer Vision*, (pp. 258–263).
- Lamme, V. A., & Roelfsema, P. R. (2000). The distinct modes of vision offered by feedforward and recurrent processing. *Trends in Neuroscience*, 23, 571–579.
- Latimer, C., Joung, W., & Stevens, C. (1994). Modelling symmetry detection with back-propagation networks. *Spatial Vision*, 8, 415–431.
- Lee, T. S., Mumford, D., Romero, R., & Lamme, V. A. (1998). The role of the primary visual cortex in higher level vision. *Vision Research*, 38, 2429–2454.
- Leeuwenberg, E., der Helm, P. V., & Lier, R. V. (1994). From geons to structure. A note on object representation. *Perception*, 23, 505–515.
- Leeuwenberg, E. L. (1969). Quantitative specification of information in sequential patterns. *Psychological Review*, 76, 216–220.
- Leeuwenberg, E. L. (1971). A perceptual coding language for visual and auditory patterns. *American Journal of Psychology*, 84, 307–349.
- Leeuwenberg, E. L. J., & Buffart, H. F. J. M. (1984). The perception of foreground and background as derived from structural information theory. *Acta Psychologica*, 55, 249–272.
- Li, H. C., & Kingdom, F. A. (1998). Does segregation by colour/luminance facilitate the detection of structure-from-motion in noise? *Perception*, 27, 769–784.
- Li, H. C., & Kingdom, F. A. (1999). Feature specific segmentation in perceived structure-from-motion. *Vision Research*, 39, 881–886.
- Li, H. C., & Kingdom, F. A. (2001). Motion-surface labeling by orientation, spatial frequency and luminance polarity in 3-D structure-from-motion. *Vision Research*, 41, 3873–3882.
- Li, Y., Pizlo, Z., & Steinman, R. M. (2009). A computational model that recovers the 3D shape of an object from a single 2D retinal representation. *Vision Research*, 49, 979–991.
- Locher, P., & Wagemans, J. (1993). The effects of element type and spatial grouping on symmetry detection. *Perception*, 22, 565–587.

- Locher, P. J., & Smets, G. (1992). The influence of stimulus dimensionality and viewing orientation on detection of symmetry in dot patterns. *Bulletin of the Psychonomic Society*, *30*, 43–46.
- Mach, E. (1886). *Beiträge zur Analyse der Empfindungen [Contributions to the analysis of sensations]*. Jena, Germany: Gustav Fisher.
- Malach, R., Reppas, J. B., Benson, R. R., Kwong, K. K., Jiang, H., Kennedy, W. A., Ledden, P. J., Brady, T. J., Rosen, B. R., & Tootell, R. B. (1995). Object-related activity revealed by functional magnetic resonance imaging in human occipital cortex. *Proceedings of the National Academy of Sciences of the United States of America*, *92*, 8135–8139.
- Mancini, S., Sally, S. L., & Gurnsey, R. (2005). Detection of symmetry and anti-symmetry. *Vision Research*, *45*, 2145–2160.
- Marr, D. (1982). *Vision: A Computational Approach*. San Francisco: Freeman.
- Marr, D., & Nishihara, H. K. (1978). Representation and recognition of the spatial organization of three-dimensional shapes. *Proc R Soc Lond B Biol Sci*, *200*, 269–294.
- Martinez-Trujillo, J. C., Tsotsos, J. K., Simine, E., Pomplun, M., Wildes, R., Treue, S., Heinze, H.-J., & Hopf, J.-M. (2005). Selectivity for speed gradients in human area MT/V5. *Neuroreport*, *16*, 435–438.
- McClelland, J. L., & Rumelhart, D. E. (1981). An interactive activation model of context effects in letter perception: Part 1. An account of basic findings. *Psychological Review*, *88*, 375–407.
- Mendola, J. D., Dale, A. M., Fischl, B., Lui, A. K., & Tootell, R. B. H. (1999). The representation of illusory and real contours in human cortical visual areas revealed by functional magnetic resonance imaging. *The Journal of Neuroscience*, *19*, 8560–8572.
- Merboldt, K.-J., Baudewig, J., Treue, S., & Frahm, J. (2002). Functional MRI of self-controlled stereoscopic depth perception. *Neuroreport*, *13*, 1721–1725.
- Mitsumoto, H., Tamura, S., Okazaki, K., Kajimi, N., & Fukui, Y. (1992). 3D reconstruction using mirror images based on a plane symmetry recovering method. *IEEE Transactions on Pattern Analysis and Machine Intelligence*, *14*, 941–946.
- Morales, D., & Pashler, H. (1999). No role for colour in symmetry perception. *Nature*, *399*, 115–116.
- Murray, S. O., Olshausen, B. A., & Woods, D. L. (2003). Processing shape, motion and three-dimensional shape-from-motion in the human cortex. *Cerebral Cortex*, *13*, 508–516.
- Møller, A. P., & Thornhill, R. (1998). Bilateral symmetry and sexual selection: a meta-analysis. *The American Naturalist*, *151*, 174–192.

- Negawa, T., Mizuno, S., Hahashi, T., Kuwata, H., Tomida, M., Hoshi, H., Era, S., & Kuwata, K. (2002). M pathway and areas 44 and 45 are involved in stereoscopic recognition based on binocular disparity. *Japanese Journal of Physiology*, *52*, 191–198.
- Neri, P. (2004). A stereoscopic look at visual cortex. *Journal of Neurophysiology*, *93*, 1823–1826.
- Neri, P., Bridge, H., & Heeger, D. J. (2004). Stereoscopic processing of absolute and relative disparity in human visual cortex. *Journal of Neurophysiology*, *92*, 1880–1891.
- Niimi, R., Watanabe, K., & Yokosawa, K. (2005). The role of visible persistence for perception of visual bilateral symmetry. *Japanese Psychological Research*, *47*, 262–270.
- Niimi, R., & Yokosawa, K. (2008). Determining the orientation of depth-rotated familiar objects. *Psychonomic Bulletin & Review*, *15*, 208–214.
- Norcia, A. M., Candy, T. R., Pettet, M. W., Vildavski, V. Y., & Tyler, C. W. (2002). Temporal dynamics of the human response to symmetry. *Journal of Vision*, *2*, 132–139.
- Nucci, M., & Wagemans, J. (2007). Goodness of regularity in dot patterns: global symmetry, local symmetry, and their interactions. *Perception*, *36*, 1305–1319.
- Oka, S., Victor, J. D., Conte, M. M., & Yanagida, T. (2007). VEPs elicited by local correlations and global symmetry: characteristics and interactions. *Vision Research*, *47*, 2212–2222.
- Orban, G. A., Sunaert, S., Todd, J. T., Hecke, P. V., & Marchal, G. (1999). Human cortical regions involved in extracting depth from motion. *Neuron*, *24*, 929–940.
- Osorio, D. (1996). Symmetry detection by categorization of spatial phase, a model. *Proceedings of the Royal Society of London B*, *263*, 105–110.
- Palmer, S. E. (1983). *Human and machine vision*, chap. The psychology of perceptual organization: A transformational approach, (pp. 269–339). New York: Academic Press.
- Palmer, S. E. (1991). *The Perception of Structure: Essays in Honor of Wendell R. Garner*, chap. On goodness, Gestalt, groups, and Garner: Local symmetry subgroups as a theory of figural goodness. Washington, DC, USA: American Psychological Association.
- Palmer, S. E. (Ed.) (1999). *Vision Science: Photons to Phenomenology*. MIT Press.
- Palmer, S. E. (2002). Perceptual grouping: It's later than you think. *Current Directions in Psychological Science*, *11*, 101–106.
- Palmer, S. E., Brooks, J. L., & Nelson, R. (2003). When does grouping happen? *Acta Psychologica*, *114*, 311–330.
- Palmer, S. E., Gardner, J. S., & Wickens, T. D. (2008). Aesthetic issues in spatial composition: effects of position and direction on framing single objects. *Spatial Vision*, *21*, 421–449.

- Palmer, S. E., & Hemenway, K. (1978). Orientation and symmetry: effects of multiple, rotational, and near symmetries. *Journal of Experimental Psychology: Human Perception and Performance*, 4, 691–702.
- Paradis, A. L., Cornilleau-Pérès, V., Droulez, J., Moortele, P. F. V. D., Lobel, E., Berthoz, A., Bihan, D. L., & Poline, J. B. (2000). Visual perception of motion and 3-D structure from motion: an fMRI study. *Cerebral Cortex*, 10, 772–783.
- Parker, A. J., Krug, K., & Cumming, B. G. (2002). Neuronal activity and its links with the perception of multi-stable figures. *Philosophical Transactions Royal Society London B: Biological Sciences*, 357, 1053–1062.
- Pashler, H. (1990). Coordinate frame for symmetry detection and object recognition. *Journal of Experimental Psychology: Human Perception and Performance*, 16, 150–163.
- Poggio, T., & Vetter, T. (1992). Recognition and structure from one 2D model view: Observations on prototypes, object classes and symmetries. Tech. rep., Massachusetts Institute of Technology Laboratory.
- Ptito, M., Zatorre, R. J., Petrides, M., Frey, S., Alivisatos, B., & Evans, A. C. (1993). Localization and lateralization of stereoscopic processing in the human brain. *Neuroreport*, 4, 1155–1158.
- Pylyshyn, Z. W. (1973). What the mind's eye tells the mind's brain: a critique of mental imagery. *Psychological Bulletin*, 80, 1–24.
- Qian, N., & Andersen, R. A. (1994). Transparent motion perception as detection of unbalanced motion signals. II. Physiology. *The Journal of Neuroscience*, 14, 7367–7380.
- Raemaekers, M., van der Schaaf, M. E., van Ee, R., & van Wezel, R. J. A. (2009). Widespread fMRI activity differences between perceptual states in visual rivalry are correlated with differences in observer biases. *Brain Research*, 1252, 161–171.
- Rainville, S. J. M., & Kingdom, F. A. A. (1999). Spatial-scale contribution to the detection of mirror symmetry in fractal noise. *Journal of the Optical Society of America A*, 16, 2112–2123.
- Rainville, S. J. M., & Kingdom, F. A. A. (2000). The functional role of oriented spatial filters in the perception of mirror symmetry—psychophysics and modeling. *Vision Research*, 40, 2621–2644.
- Rainville, S. J. M., & Kingdom, F. A. A. (2002). Scale invariance is driven by stimulus density. *Vision Research*, 42, 351–367.
- Rhodes, G., Peters, M., Lee, K., Morrone, M. C., & Burr, D. (2005). Higher-level mechanisms detect facial symmetry. *Proceedings of the Royal Society B: Biological Sciences*, 272, 1379–1384.

- Ringach, D. L., Hawken, M., & Shapley, R. (1997). Dynamics of orientation tuning in macaque primary visual cortex. *Nature*, *387*, 281–284.
- Ritter, M. (1980). Perception of depth: Different processing times for simple and relative positional disparity. *Psychological Research*, *41*, 285–295.
- Rosen, J. (2009). Commentary: Symmetry at the foundation of science and nature. *Symmetry*, *1*, 3–9.
- Rothwell, C. A., Forsyth, D., Zisserman, A., & Mundy, J. L. (1993). Extracting projective structure from single perspective views of 3D point sets. In *Views of 3-D Point Sets Proc. of 4:th ICCV*, (pp. 573–582).
- Royer, F. L. (1981). Detection of symmetry. *Journal of Experimental Psychology: Human Perception and Performance*, *7*, 1186–1210.
- Saarinen, J. (1988). Detection of mirror symmetry in random dot patterns at different eccentricities. *Vision Research*, *28*, 755–759.
- Saarinen, J., & Levi, D. M. (2000). Perception of mirror symmetry reveals long-range interactions between orientation-selective cortical filters. *Neuroreport*, *11*, 2133–2138.
- Sally, S., & Gurnsey, R. (2001). Symmetry detection across the visual field. *Spatial Vision*, *14*, 217–234.
- Sasaki, Y., Vanduffel, W., Knutsen, T., Tyler, C., & Tootell, R. (2005). Symmetry activates extrastriate visual cortex in human and nonhuman primates. *Proceedings of the National Academy of Sciences of the United States of America*, *102*, 3159–3163.
- Saunders, J. A., & Backus, B. T. (2006). Perception of surface slant from oriented textures. *Journal of Vision*, *6*, 882–897.
- Sawada, T., & Pizlo, Z. (2008). Detection of skewed symmetry. *Journal of Vision*, *8*, 14.1–1418.
- Scheib, J. E., Gangestad, S. W., & Thornhill, R. (1999). Facial attractiveness, symmetry and cues of good genes. *Proceedings of the Royal Society B: Biological Sciences*, *266*, 1913–1917.
- Schulz, M. F., & Sanocki, T. (2003). Time course of perceptual grouping by color. *Psychological Science*, *14*, 26–30.
- Sekuler, A. B., & Palmer, S. E. (1992). Perception of partly occluded objects: A microgenetic analysis. *Journal of Experimental Psychology: General*, *121*, 95–111.
- Shapley, R., Hawken, M., & Ringach, D. L. (2003). Dynamics of orientation selectivity in the primary visual cortex and the importance of cortical inhibition. *Neuron*, *38*, 689–699.
- Shepard, R. N., & Metzler, J. (1971). Mental rotation of three-dimensional objects. *Science*, *171*, 701–703.

- Swets, J. A. (1964). *Signal detection and recognition by human observers: contemporary readings*. New York: Wiley.
- Tapiovaara, M. (1990). Ideal observer and absolute efficiency of detecting mirror symmetry in random images. *Journal of the Optical Society of America A*, 7, 2245–2253.
- Todd, J. T. (2004). The visual perception of 3D shape. *Trends in Cognitive Sciences*, 8, 115–121.
- Todd, J. T., & Norman, J. F. (1991). The visual perception of smoothly curved surfaces from minimal apparent motion sequences. *Perception & Psychophysics*, 50, 509–523.
- Tong, F., Nakayama, K., Vaughan, J. T., & Kanwisher, N. (1998). Binocular rivalry and visual awareness in human extrastriate cortex. *Neuron*, 21, 753–759.
- Treder, M. S., & van der Helm, P. A. (2007). Symmetry versus repetition in cyclopean vision: a microgenetic analysis. *Vision Research*, 47, 2956–2967.
- Treue, S., & Andersen, R. A. (1996). Neural responses to velocity gradients in macaque cortical area MT. *Visual Neuroscience*, 13, 797–804.
- Treue, S., Andersen, R. A., Ando, H., & Hildreth, E. C. (1995). Structure-from-motion: perceptual evidence for surface interpolation. *Vision Research*, 35, 139–148.
- Treue, S., Husain, M., & Andersen, R. A. (1991). Human perception of structure from motion. *Vision Research*, 31, 59–75.
- Troscianko, T. (1987). Perception of random-dot symmetry and apparent movement at and near isoluminance. *Vision Research*, 27, 547–554.
- Tyler, C. W. (1994). Theoretical issues in symmetry perception. *Spatial Vision*, 8, 383–391.
- Tyler, C. W. (1996). *Human symmetry perception and its computational analysis*. Zeist, The Netherlands: VSP.
- Tyler, C. W., Baseler, H. A., Kontsevich, L. L., Likova, L. T., Wade, A. R., & Wandell, B. A. (2005). Predominantly extra-retinotopic cortical response to pattern symmetry. *Neuroimage*, 24, 306–314.
- Tyler, C. W., & Hardage, L. (1996). *Human symmetry perception and its computational analysis*, chap. Mirror symmetry detection: Predominance of second-order pattern processing throughout the visual field, (pp. 157–172). Zeist, The Netherlands: VSP.
- Ullman, S. (1984). Maximizing rigidity: the incremental recovery of a 3-D structure from rigid and non-rigid motion. *Perception*, 13, 255–274.
- Ungerleider, L. G., & Mishkin, M. (1982). *Analysis of Visual Behavior*, chap. Two cortical visual systems, (pp. 549–586). Cambridge, MA: MIT Press.

- Valois, K. K. D. (1977). Spatial frequency adaptation can enhance contrast sensitivity. *Vision Research*, *17*, 1057–1065.
- Valois, R. L. D., Morgan, H., & Snodderly, D. M. (1974). Psychophysical studies of monkey vision. 3. spatial luminance contrast sensitivity tests of macaque and human observers. *Vision Research*, *14*, 75–81.
- Valois, R. L. D., Thorell, L. G., & Albrecht, D. G. (1985). Periodicity of striate-cortex-cell receptive fields. *Journal of the Optical Society of America A*, *2*, 1115–1123.
- Valois, R. L. D., & Valois, K. K. D. (1988). *Spatial vision*. New York: Oxford University Press.
- van der Helm, P. A. (2000). Simplicity versus likelihood in visual perception: from surprisals to precisals. *Psychological Bulletin*, *126*, 770–800.
- van der Helm, P. A., & Leeuwenberg, E. L. (1996). Goodness of visual regularities: a non-transformational approach. *Psychological Review*, *103*, 429–456.
- van der Helm, P. A., & Leeuwenberg, E. L. J. (1991). Accessibility, a criterion for regularity and hierarchy in visual pattern codes. *Journal of Mathematical Psychology*, *35*, 151–213.
- van der Helm, P. A., & Leeuwenberg, E. L. J. (1999). A better approach to goodness: Reply to Wagemans (1999). *Psychological Review*, *106*, 622–630.
- van der Helm, P. A., & Leeuwenberg, E. L. J. (2004). Holographic goodness is not that bad: Reply to Olivers, Chater, and Watson (2004). *Psychological Review*, *111*, 261–273.
- van der Helm, P. A., van Lier, R., & Wagemans, J. (2003). Special issue on "Visual Gestalt Formation". *Acta Psychologica*, *114*, 211–213.
- van der Vloed, G. (2005). *The structure of visual regularities*. Ph.D. thesis, University of Nijmegen, The Netherlands.
- van der Vloed, G., Csathó, Á., & van der Helm, P. A. (2005). Symmetry and repetition in perspective. *Acta Psychologica*, *120*, 74–92.
- van der Zwan, R., Leo, E., Joung, W., Latimer, C., & Wenderoth, P. (1998). Evidence that both area V1 and extrastriate visual cortex contribute to symmetry perception. *Current Biology*, *8*, 889–892.
- van Lier, R., van der Helm, P., & Leeuwenberg, E. (1995). Competing global and local completions in visual occlusion. *Journal of Experimental Psychology: Human Perception and Performance*, *21*, 571–583.
- van Lier, R., & Wagemans, J. (1998). Effects of physical connectivity on the representational unity of multi-part configurations. *Cognition*, *69*, B1–B9.
- Vanduffel, W., Fize, D., Peuskens, H., Denys, K., Sunaert, S., Todd, J. T., & Orban, G. A. (2002a). Extracting 3D from motion: differences in human and monkey intraparietal cortex. *Science*, *298*, 413–415.



- Vanduffel, W., Tootell, R. B. H., Schoups, A. A., & Orban, G. A. (2002b). The organization of orientation selectivity throughout macaque visual cortex. *Cerebral Cortex*, *12*, 647–662.
- Vetter, T., Poggio, T., & Bülthoff, H. H. (1994). The importance of symmetry and virtual views in three-dimensional object recognition. *Current Biology*, *4*, 18–23.
- von Fersen, L., Manos, C. S., Goldowsky, B., & Roitblat, H. (1992). *Marine mammal sensory systems*, chap. Dolphin detection and conceptualization of symmetry, (pp. 753–762). New York: Plenum.
- Wagemans, J. (1995). Detection of visual symmetries. *Spatial Vision*, *9*, 9–32.
- Wagemans, J., Gool, L. V., & d'Ydewalle, G. (1991). Detection of symmetry in tachistoscopically presented dot patterns: effects of multiple axes and skewing. *Perception & Psychophysics*, *50*, 413–427.
- Wagemans, J., Gool, L. V., Swinnen, V., & Horebeek, J. V. (1993). Higher-order structure in regularity detection. *Vision Research*, *33*, 1067–1088.
- Wagemans, J., van Gool, L., & d'Ydewalle, G. (1992). Orientational effects and component processes in symmetry detection. *The Quarterly Journal of Experimental Psychology*, *44A*, 475–508.
- Wallach, . O. D. N., H. (1953). The kinetic depth effect. *Journal of Experimental Psychology*, *45*, 205–217.
- Wannig, A., Rodríguez, V., & Freiwald, W. A. (2007). Attention to surfaces modulates motion processing in extrastriate area MT. *Neuron*, *54*, 639–651.
- Wenderoth, P. (1994). The salience of vertical symmetry. *Perception*, *23*, 221–236.
- Wenderoth, P. (1995). The role of pattern outline in bilateral symmetry detection with briefly flashed dot patterns. *Spatial Vision*, *9*, 57–77.
- Wenderoth, P. (1996). The effects of the contrast polarity of dot-pair partners on the detection of bilateral symmetry. *Perception*, *25*, 757–771.
- Wenderoth, P. (1997). The effects on bilateral-symmetry detection of multiple symmetry, near symmetry, and axis orientation. *Perception*, *26*, 891–904.
- Wenderoth, P. (2000). Monocular symmetry is neither necessary nor sufficient for the dichoptic perception of bilateral symmetry. *Vision Research*, *40*, 2097–2100.
- Wenderoth, P., & Welsh, S. (1998a). The effects of cuing on the detection of bilateral symmetry. *Quarterly Journal of Experimental Psychology A*, *51*, 883–903.
- Wenderoth, P., & Welsh, S. (1998b). Effects of pattern orientation and number of symmetry axes on the detection of mirror symmetry in dot and solid patterns. *Perception*, *27*, 965–976.

- Wertheimer, M. (1912). Experimentelle Studien über das Sehen von Bewegung. *Zeitschrift für Psychologie*, *12*, 161–265.
- Wertheimer, M. (1923). Untersuchungen zur Lehre von der Gestalt [On Gestalt theory]. *Psychologische Forschung*, *4*, 301–350.
- Wickens, T. D. (2002). *Elementary signal detection theory*. New York: Oxford University Press.
- Wilkinson, D. T., & Halligan, P. W. (2002). The effects of stimulus symmetry on landmark judgments in left and right visual fields. *Neuropsychologia*, *40*, 1045–1058.
- Wilkinson, F., Wilson, H. R., & Habak, C. (1998). Detection and recognition of radial frequency patterns. *Vision Research*, *38*, 3555–3568.
- Wilson, H. R., & Wilkinson, F. (2002). Symmetry perception: a novel approach for biological shapes. *Vision Research*, *42*, 589–597.
- Wolfe, J. M., & Friedman-Hill, S. R. (1992). On the role of symmetry in visual search. *Psychological Science*, *3*, 194–198.
- Xiao, D. K., Marcar, V. L., Raiguel, S. E., & Orban, G. A. (1997). Selectivity of macaque MT/V5 neurons for surface orientation in depth specified by motion. *European Journal of Neuroscience*, *9*, 956–964.
- Yakushijin, R., & Ishiguchi, A. (1999). The effect of a noise plane on discrimination of mirror symmetry in a different plane. *Journal of Experimental Psychology: Human Perception and Performance*, *25*, 162–173.
- Zabrodsky, H., & Algom, D. (1994). Continuous symmetry: a model for human figural perception. *Spatial Vision*, *8*, 455–467.
- Zabrodsky, H., & Weinshall, D. (1997). Using bilateral symmetry to improve 3D reconstruction from image sequences. *Computer Vision and Image Understanding*, *67*, 48–57.
- Zhang, L., & Gerbino, W. (1992). Symmetry in opposite-contrast dot patterns. *Perception*, *21* (Supp. 2), 95a.
- Zimmer, A. C. (1984). Foundations for the measurement of phenomenal symmetry. *Gestalt Theory*, *6*, 118–157.



---

## Samenvatting

---

Het gemak met dat we door onze visuele omgeving navigeren en met haar interageren logenstraft de complexiteit van het zien. Om vanuit de 2D projectie op het netvlies de visuele wereld te reconstrueren, maakt het visuele systeem gebruik van talrijke visuele processen die parallel opereren en verschillende kenmerken van het visuele input, zoals kleur, beweging, en diepte, verwerken. Één van deze visuele processen is *symmetrie detectie*, d.w.z., de detectie van spiegelsymmetrische arrangements van stimulus elementen. Deze proefschrift behandelt de rol van symmetrie detectie in het ensemble van visuele processen. Om deze reden wordt symmetrie detectie niet alleen als een geïsoleerd proces onderzocht, maar ook in interactie met andere visuele processen.

Het eerste empirische hoofdstuk (hoofdstuk 2) onderzoekt of, en zo ja, hoe, de assen in een multiple symmetrie met elkaar interageren. De hoofdbevinding is dat de detectie van een symmetrie gestoord kan worden door een tweede symmetrie, als de symmetrieassen niet-orthogonal t.o.v. elkaar staan, en gefaciliteerd kan worden als ze orthogonaal t.o.v. elkaar staan. Een vergelijkbare aard van interactie is de wederzijdse remming van oriëntatie sensitieve visuele neuronnen. Daarom wordt voorgesteld dat er een mechanisme van wederzijdse remming betrokken is bij de waarneming van multiple symmetrie.

Hoofdstuk 3 laat zien dat zowel symmetrie als ook herhaling (een andere vorm van visuele regelmaat) als verzamelbegrippen gebruikt werden die ook structuren bevatten die géén rol in perceptuele organisatie spelen. In een contour-matching taak wordt gevonden dat taak-irrelevante symmetrische of herhaalde contouren de detectie van een regelmaat kunnen faciliteren, maar alleen als de paren van contouren overeenkomstige contour polariteiten hebben en niet als ze tegenovergestelde contour polariteiten hebben (waarin concave vertices in één contour overeenkomen met convexe vertices in een andere contour, en andersom).

In hoofdstuk 4 wordt de interactie tussen de verwerking van symmetrie en herhaling en de verwerking van stereoscopische diepte kenmerken onderzocht. De resultaten laten zien dat symmetrie detectie van een retinotopische referentiekader over kan gaan naar een stereoscopische referentiekader, gegeven dat symmetrie-paren op dezelfde diepte-laag terecht komen.

In hoofdstuk 5 wordt de interactie tussen symmetrieverwerking en bewegingsverwerking onderzocht. Er wordt aangetoond dat zodra de elementen van een roterende cylinder symmetrisch geplaatst zijn, er nieuwe perceptuele interpretaties gezien kunnen worden. Het feit dat zowel op symmetrie gebaseerde interpretaties als ook op beweging gebaseerde interpretaties op een alternerende waargenomen kunnen worden suggereert dat er een aanhoudende interactie tussen symmetrieverwerking en bewegingsverwerking tijdens perceptuele organisatie is.

Bij elkaar documenteren deze studies symmetrie in (inter)actie. Symmetrieverwerking is snel, veelzijdig en interactief. Het heeft invloed op, en wordt beïnvloedt door, andere visuele processen zoals stereowaarneming en bewegingswaarneming.

---

## Summary

---

The ease with which we navigate through and interact with our visual environment belies the intricacy of vision. To reconstruct the visual world from its impoverished 2D projection on the retina, the visual system recruits numerous visual processes running in parallel to process the different features of visual input, such as color, motion, and depth. One of these visual processes is *symmetry detection*, that is, the detection of mirror-symmetric arrangements of stimulus parts. This thesis focuses on the role symmetry detection plays in the ensemble of visual processes. To this end, the present work addresses symmetry detection not only as an isolated process, but also in interaction with other visual processes.

The first empirical chapter (Chapter 2) investigates whether, and if so, how, the constituent axes in a multiple symmetry interact. The main finding is that the detection of a symmetry can be hampered by a second symmetry if their relative orientation is non-orthogonal, and can be facilitated if their relative orientation is orthogonal. This kind of interaction is reminiscent of the inhibition of surrounding orientations in orientation-sensitive visual neurons. Therefore, it is proposed that a mechanism of surround inhibition might be involved in the perception of multiple symmetry.

Chapter 3 shows that both symmetry and repetition (another form of visual regularity) have been used as umbrella terms to also include structures that do not play a role in perceptual organization. In a contour-matching task, it was found that task-irrelevant symmetric or repeated contours can facilitate the detection of regularity, but only if pairs of contours have matched contour polarities and not if they have opposite contour polarities (wherein concave vertices in one contour map to convex vertices in the other contour, and vice versa).

Chapter 4 investigates the interaction between the processing of symmetry and repetition and the processing of stereoscopic depth cues. The results show that symmetry processing can shift from a retinotopic to a

stereoscopic frame of reference if symmetry pairs are placed on the same depth plane.

Chapter 5 investigates the interaction between symmetry processing and motion processing. It is shown that if the elements constituting a rotating cylinder are symmetrically positioned, novel stimulus interpretations can be perceived. The fact that both symmetry-based interpretations and motion-based interpretations can be perceived in an alternating fashion suggests that there is an ongoing interaction between symmetry processing and motion processing.

Together, these studies document symmetry in (inter)action. Symmetry processing is shown to be quick, versatile, and interactive. It is affected by the presence of a symmetry with a different orientation. Furthermore, it affects, and is affected by, other kinds of visual processes such as stereovision and motion processing.

---

# Zusammenfassung

---

Die Leichtigkeit, mit der wir uns durch unsere visuelle Umgebung bewegen und mit ihr interagieren, straft die Komplexität menschlichen Sehens Lügen. Damit das Kunststück gelingt, aus einer verkümmerten 2D Projektion auf der Netzhaut die visuelle Welt zu rekonstruieren, macht das visuelle System Gebrauch von zahlreichen visuellen Prozessen, die gleichzeitig operieren und unterschiedliche visuelle Merkmale verarbeiten, wie etwa Farbe, Bewegung und räumliche Tiefe. Einer dieser visuellen Prozesse ist *Symmetriedetektion*, das heißt, die Detektion von spiegelsymmetrischen Anordnungen von Stimuluselementen. Das Hauptaugenmerk der vorliegenden Dissertation liegt auf der Rolle, die Symmetriedetektion in dem Ensemble von visuellen Prozessen einnimmt. Zu diesem Zwecke wird Symmetriedetektion nicht nur als isolierter Prozess betrachtet, sondern auch in Interaktion mit anderen visuellen Prozessen.

Das erste empirische Kapitel (Kapitel 2) widmet sich der Frage, ob, und wenn ja, wie, die Achsen in einer multiplen Symmetrie miteinander interagieren. Die Hauptidee ist, dass die Detektion einer Symmetrie durch die Anwesenheit einer zweiten Symmetrie erschwert wird, wenn die beiden Symmetrieachsen nicht-orthogonal zueinander stehen, und erleichtert wird, wenn sie orthogonal zueinander stehen. Eine vergleichbare Art von Wechselbeziehung existiert in der visuellen Kortex, in Form von gegenseitiger Inhibition von orientierungssensiblen Neuronen. Ein analoges Modell wird für die Inhibition nicht-orthogonaler Symmetrieachsen entwickelt und validiert.

Kapitel 3 veranschaulicht, dass sowohl Symmetrie als auch Wiederholung (eine weitere Spielart von visuellen Regelmäßigkeiten) als Sammelbegriffe benutzt wurden und als solche Strukturen enthielten, die in perzeptueller Organisation keine Rolle spielen. In einer Kontur-matching Aufgabe wurde gefunden, dass aufgabenirrelevante symmetrische oder wiederholte Konturen die Detektion von Regelmäßigkeit erleichtern können, aber nur, wenn



Paare von Konturen identische Kontur-Polaritäten besitzen, und nicht, wenn sie gegensätzliche Kontur-Polaritäten besitzen (wobei konkave Vertices in einer Kontur konvexen Vertices in der anderen Kontur entsprechen, und umgekehrt).

Kapitel 4 erforscht die Interaktion zwischen der Prozessierung von Symmetrie und Wiederholung und der Prozessierung von stereoskopischen Hinweisreizen. Dabei wird gezeigt, dass die Prozessierung von Symmetrie von einem retinotopischen Referenzrahmen zu einem stereoskopischen Referenzrahmen übergehen kann, wenn Symmetriepaare auf der gleichen stereoskopischen Ebene liegen.

Kapitel 5 widmet sich der Interaktion zwischen Symmetrie-Prozessierung und der Prozessierung von Bewegung. Es wird gezeigt, dass, wenn die Elemente eines rotierenden Zylinders symmetrisch angeordnet sind, neurartige Stimulus Interpretationen wahrgenommen werden können. Die Tatsache, dass sowohl symmetriebasierte als auch bewegungsbasierte Interpretationen alternierend wahrnehmbar sind, legt nahe, dass es eine kontinuierliche Interaktion zwischen der Prozessierung von Symmetrie und der Prozessierung von Bewegung gibt.

Zusammenfassend zeigen diese Studien Symmetrie in (Inter)aktion. Sie dokumentieren die Schnelligkeit, Vielseitigkeit und Interaktivität von Symmetriewahrnehmung. Symmetriewahrnehmung wird von der Anwesenheit einer Symmetrie einer anderen Orientierung beeinflusst. Darüber hinaus übt Symmetriewahrnehmung Einfluss auf andere Arten von visuellen Prozessen, wie Stereosehen und Bewegungssehen, aus, und wird umgekehrt auch durch sie beeinflusst.

---

## Dankwoord

---

“Your friend and humble narrator of this thesis is in debt to numerous people, each of whom has contributed to this thesis with their ideas, insights, and support throughout the years.”

Peter, jij hebt zonder twijfel, afgezien van mijn aandeel, de grootste bijdrage aan dit proefschrift geleverd. Ik wil je danken voor de vruchtbare samenwerking en je easy-going omgang met mij. Vooral van de gemeenschappelijke schrijf-acties heb ik altijd genoten en er kwam altijd iets heel constructiefs uit. Ik wens je het beste voor de toekomst, veel succes en vooral gezondheid. Ruud, je hebt me door een misschien korte maar desondanks cruciale fase begeleid. Dank je voor jouw gestructureerde aanpak, de ‘Holländische Gründlichkeit’ en je aanvoelingsvermogen. Gert, ook al is het een tijdje geleden dat je mijn stagebegeleider was: Jouw tips, trucjes en mijn talrijke permutaties van jouw Delphi code waren een onvervangbare hulp voor mij, en jouw openheid en gezelligheid maakten het begin @NICI voor mij heel soepel. Charles, ook al hadden we geen intensief contact, jij was er altijd als jouw raad nodig was, en ik heb veel van je ervaring en wijsheid geprofitteerd.

PPP-people, perceptie collega's Rob, Arno, Tessa, Sven en Vinod, bedankt voor de constructieve en leuke tijd. Ondanks de latente Titanic-sfeer in onze groep de afgelopen jaren was de interactie met jullie altijd positief; jullie zijn niet alleen excellente wetenschappers maar ook heel erg gezellige mensen, dat heb ik tijdens onze kroegtouren en stadsexcursies kunnen verifiëren. Ik wil verder alle mensen op het NICI (aka DCC) danken, vooral de junioren, Janneke, Makiko, Majken, Edita, Celine, Loes, Sabine, Stan, Jurian, Markus, Christine, Sebo, Sybrine, Alex, Rebecca, om er maar een paar te noemen. Dank aan de Nijmegen climbers, vooral Annika (Heippä!), Peter, Cinzia, Ellen en Martin, niet alleen voor de leuke klimexcursies maar ook voor de heel gezellige avonden. Mathieu, je had de pech dat jouw kamer naast onze kamer was, het was té makkelijk voor mij langs te komen en

jouw tijd te roven, bedankt voor je geduld en help met al die wiskundige issues. De ERG groep, dank niet alleen voor de excellente technische steun maar vooral ook voor het aardige gezelschap.

Mark, roomie, zenuwpees en aardige collega, met jou was het nooit saai op onze kamer. Je hebt mijn Nederlands op een acceptabel niveau gebracht (ja, doch?) en je hebt me veel over Nederlandse cultuur geleerd - geen slagroom op stroopwafels bijvoorbeeld. Naast je humor was ik verrast over je sterk analytisch vermogen. Mijn ingenieuze ideeën wist je vaak binnen seconden als triviaal af te doen. Ook naast het werk hebben we vele leuke dingen samen gedaan die ik nooit zal vergeten - overlange David Lynch films kijken, met de fiets voor krokodillen vluchten, en tussen een high-way en een drukke rijksweg in een kleine swimmingpool frisbee spelen. Of je nu stand-up comedian wordt, wetenschapper blijft, een nostalgische muziekwinkel opent, ik heb geen twijfel dat je er veel van zult maken!

Dank ook aan de 'Duitse gang', vooral Michael, Daniel, Christian, Birgit, voor het aardige gezelschap en een stukje Heimat in Nijmegen, für Parkour-Spritztouren, literarische Abende und Jazz-sessions im Musikkeller.

Danke auch an die Berlin-BCI Leute, für den herzlichen Empfang im Januar 2009 und im Sommer, sowie für den Freiraum, letzte Hand an diese Doktorarbeit zu legen. Mit euch ist's schön in unserem Großraum-wohnzimmer-Büro, und ich freue mich auf die kommenden Jahre.

Evgenia, ich bin dir in vielen Dingen zu Dank verpflichtet, im Rahmen dieser Dissertation vor allem auch für den tatkräftigen Design-Einsatz beim Einband!

Zuletzt möchte ich meiner Familie danken, vor allem meiner Schwester Loren und meinen Eltern (auch unseren Hunden, die die trübste Laune im Nu auflösen). Ihr habt mich ganze 30 Jahre ertragen und getragen, an mich geglaubt, mich motiviert und unterstützt, dafür bin ich euch aus tiefstem Herzen dankbar, schön, dass es euch gibt!

---

# Publications

---

## Journal publications

Treder, M. S., & Meulenbroek, R. G. J. (in press). Integration of structure-from-motion and symmetry during surface perception. *Journal of Vision*.

van der Helm, P. A., & Treder, M. S. (2009). Detection of (anti)symmetry and (anti)repetition: Perceptual mechanisms versus cognitive strategies. *Vision Research*, 49, 2754–2763.

Treder, M. S., & van der Helm, P. A. (2007). Symmetry and repetition in cyclopean vision: a microgenetic analysis. *Vision Research*, 47, 2956–2967.

Treder, M. S., & van der Helm, P. A. (2007). There is no symmetry like orthogonal symmetry. *Journal of Vision*, 7, VSS Abstract.

Treder, M. S., & van der Helm, P. A. (2006). Breaking up symmetry in depth. *Perception*, 35, ECVF Abstract Supplement.

Treder, M. S., van der Vloed, G., & van der Helm, P. A. (2005). Signal-to-noise ratio as a crucial determinant of vertical symmetry detection. *Perception*, 34, ECVF Abstract Supplement.

## Publications in progress

Treder, M. S., van der Vloed, G., & van der Helm, P. A. Interactions between the constituent single symmetries in multiple symmetry. *submitted*

Blankertz, B., Lemm, S., Treder, M., Haufe, S., & Müller, K.-R. Analysis and Single-Trial Classification of ERP Components — a Tutorial. *submitted*

Treder, M. S., & Blankertz, B. (C)overt attention and speller design in an ERP-based brain-computer interface. *in preparation*

Venthur, B., Scholler, S., Dähne, S., Treder, M. S., Kramarek, M. T., Müller, K.-R., & Blankertz, B. Pyff—A Pythonic Framework for Feedback Applications in Neuroscience. *in preparation*

## Talks & poster presentations

Haufe, S. Treder, M. S., Sagebaum, M., Gugler, M. F., Ewald, A., Curio, G., & Blankertz, B. Event-Related Potentials preceding Emergency Braking Situations during Simulated Driving. *Poster presented at the TOBI Workshop 2010, Graz, Austria (February 2010).*

Blankertz, B., Haufe, S., & Treder, M. S. Effective Classification and Interpretability of ERP Components using Shrinkage Linear Discriminant Analysis. *Poster presented at the TOBI Workshop 2010, Graz, Austria (February 2010).*

Treder, M. S., Venthur, B., & Blankertz, B. (C)overt attention and P300-speller design. *Poster presented at the BBCI workshop 2009 – Advances in Neurotechnology, Berlin, Germany (July 2009).*

Treder, M. S., & van der Helm, P. A. Visual regularity versus antiregularity in object perception. *Talk given at the 11th Winter Conference of the Dutch Psychonomic Society, Egmond, The Netherlands (December 2007).*

Treder, M. S., & van der Helm, P. A. There is no symmetry like orthogonal symmetry. *Talk given at the 7th annual meeting of the Vision Sciences Society, Sarasota, FL, USA (May 2007).*

Treder, M. S., & van der Helm, P. A. Breaking up symmetry in depth. *Poster presented at the 29th European Conference on Visual Perception, St. Petersburg, Russia (August 2006), and at the Dag van de perceptie, Soesterberg, The Netherlands (October 2006).*

Treder, M. S., van der Vloed, G., & van der Helm, P. A. Signal-to-noise ratio as a crucial determinant of vertical symmetry detection. *Poster presented at the 28th European Conference on Visual Perception, A Coruna, Spain (August 2005), and at the Approaches to Emotion and Attention workshop in Doorwerth, The Netherlands (October 2005).*

---

## Curriculum vitae

---

Matthias Treder was born in Lauenburg, Pomerania (Poland), on the 31st of March 1979. He grew up Duisburg, an industrial city in the Ruhr area, Germany. After primary school, he entered the Abtei-Gymnasium in the district of Hamborn. In 1994, his family yearned for the less greyish/more greenish countryside and moved to Goch, a town 60 km northwest from Duisburg, close to the Dutch border. In 1998, Matthias finished school at the Städtisches Gymnasium Goch with the Abitur, which made him eligible to enter university. The same year, after finishing a crash course in Dutch language and passing the exam, he enrolled at closeby Radboud Universiteit Nijmegen, at that time called Katholieke Universiteit Nijmegen, in Nijmegen, the Netherlands. At the Faculty of Social Sciences, he studied *Psychology* and, after his his second year, specialised in *functieleer* (cognitive psychology). During this phase, he followed a course on visual perception held by Peter van der Helm and got interested in the topic. After a semester abroad at UCL in London, United Kingdom, he started the study of *informatica* (computer science) at Radboud University, at the same time preparing his Psychology internship at the Nijmegen Institute for Cognition and Information (NICI). During his internship, he investigated Weber's law in human symmetry perception, under supervision of Peter van der Helm and Gert van der Vloed. This work smoothly faded into his subsequent PhD project *The role of visual regularities in perceptual organization* at the NICI, supervised by Peter van der Helm, starting in March 2005. After having had the opportunity to work at the Berlin BCI (BBCI) group at the Machine Learning Laboratory in Berlin, Germany, in early 2009, he successfully applied for a position in the group. In August 2009, he took office and moved to the district of Moabit in West Berlin. He is currently doing research on brain-computer interfacing, neuroergonomy, EEG-based driver assistance systems and, as time permits, symmetry perception.



---

# Series Donders Institute for Brain, Cognition and Behaviour

---

1. van Aalderen-Smeets, S. I. (2007). *Neural dynamics of visual selection*. Maastricht University, Maastricht, The Netherlands.
2. Schoffelen, J. M. (2007). *Neuronal communication through coherence in the human motor system*. Radboud University Nijmegen, Nijmegen, The Netherlands.
3. de Lange, F. P. (2008). *Neural mechanisms of motor imagery*. Radboud University Nijmegen, Nijmegen, The Netherlands.
4. Grol, M. J. (2008). *Parieto-frontal circuitry in visuomotor control*. University Utrecht, Utrecht, The Netherlands.
5. Bauer, M. (2008). *Functional roles of rhythmic neuronal activity in the human visual and somatosensory system*. Radboud University Nijmegen, Nijmegen, The Netherlands.
6. Mazaheri, A. (2008). *The Influence of Ongoing Oscillatory Brain Activity on Evoked Responses and Behaviour*. Radboud University Nijmegen, Nijmegen, The Netherlands.
7. Hooijmans, C. R. (2008). *Impact of nutritional lipids and vascular factors in Alzheimer's Disease*. Radboud University Nijmegen, Nijmegen, The Netherlands.
8. Gaszner, B. (2008). *Plastic responses to stress by the rodent urocortineric Edinger-Westphal nucleus*. Radboud University Nijmegen, Nijmegen, The Netherlands.
9. Willems, R. M. (2009). *Neural reflections of meaning in gesture, language and action*. Radboud University Nijmegen, Nijmegen, The Netherlands.
10. Van Pelt, S. (2009). *Dynamic neural representations of human visuomotor space*. Radboud University Nijmegen, Nijmegen, The Netherlands.
11. Lommertzen, J. (2009). *Visuomotor coupling at different levels of complexity*. Radboud University Nijmegen, Nijmegen, The Netherlands.
12. Poljac, E. (2009). *Dynamics of cognitive control in task switching: Looking beyond the switch cost*. Radboud University Nijmegen, Nijmegen, The Netherlands.
13. Poser, B. A. (2009). *Techniques for BOLD and blood volume weighted fMRI*. Radboud University Nijmegen, Nijmegen, The Netherlands.
14. Baggio, G. (2009). *Semantics and the electrophysiology of meaning. Tense, aspect, event structure*. Radboud University Nijmegen, Nijmegen, The Netherlands.
15. van Wingen, G. A. (2009). *Biological determinants of amygdala functioning*. Radboud University Nijmegen Medical Centre, Nijmegen, The Netherlands.



16. Bakker, M. (2009). *Supraspinal control of walking: lessons from motor imagery*. Radboud University Nijmegen Medical Centre, Nijmegen, The Netherlands.
17. Aarts, E. (2009). *Resisting temptation: the role of the anterior cingulate cortex in adjusting cognitive control*. Radboud University Nijmegen, Nijmegen, The Netherlands.
18. Prinz, S. (2009). *Waterbath stunning of chickens – Effects of electrical parameters on the electroencephalogram and physical reflexes of broilers*. Radboud University Nijmegen, Nijmegen, The Netherlands.
19. Knippenberg, J. M. J. (2009). *The N150 of the Auditory Evoked Potential from the rat amygdala: In search for its functional significance*. Radboud University Nijmegen, Nijmegen, The Netherlands.
20. Dumont, G. J. H. (2009). *Cognitive and physiological effects of 3,4-methylenedioxymethamphetamine (MDMA or 'ecstasy') in combination with alcohol or cannabis in humans*. Radboud University Nijmegen, Nijmegen, The Netherlands.
21. Pijnacker, J. (2010). *Defeasible inference in autism: a behavioral and electrophysiological approach*. Radboud Universiteit Nijmegen, The Netherlands.
22. de Vrijer, M. (2010). *Multisensory integration in spatial orientation*. Radboud University Nijmegen, Nijmegen, The Netherlands.
23. Vergeer, M. (2010). *Perceptual visibility and appearance: Effects of color and form*. Radboud University Nijmegen, Nijmegen, The Netherlands.
24. Levy, J. (2010). *In Cerebro Unveiling Unconscious Mechanisms during Reading*. Radboud University Nijmegen, Nijmegen, The Netherlands.
25. Treder, M. S. (2010). *Symmetry in (inter)action*. Radboud University Nijmegen, Nijmegen, The Netherlands.